Natural Resources Canada / Ressources naturelles Canada

GEOLOGICAL SURVEY OF CANADA
OPEN FILE 8047

Integrated analysis of vitrinite reflectance, Rock-Eval 6, gas chromatography, and gas chromatography-mass spectrometry data for the Reindeer D-27 and Tununuk K-10 wells, Beaufort-Mackenzie Basin, northern Canada

D.R. Issler, C. Jiang, J. Reyes and M. Obermajer

2016

Canada

GEOLOGICAL SURVEY OF CANADA
OPEN FILE 8047

Integrated analysis of vitrinite reflectance, Rock-Eval 6, gas chromatography, and gas chromatography-mass spectrometry data for the Reindeer D-27 and Tununuk K-10 wells, Beaufort-Mackenzie Basin, northern Canada

D.R. Issler, C. Jiang, J. Reyes and M. Obermajer

2016

doi:10.4095/297905

This publication is available for free download through GEOSCAN (http://geoscan.nrcan.gc.ca/).

Recommended citation
Issler, D.R., Jiang, C., Reyes, J., and Obermajer, M., 2016. Integrated analysis of vitrinite reflectance, Rock-Eval 6, gas chromatography, and gas chromatography-mass spectrometry data for the Reindeer D-27 and Tununuk K-10 wells, Beaufort-Mackenzie Basin, northern Canada; Geological Survey of Canada, Open File 8047, 94 p. doi:10.4095/297905

Publications in this series have not been edited; they are released as submitted by the author.

TABLE OF CONTENTS

LIST OF FIGURES

LIST OF TABLES

ABSTRACT

Core and cuttings samples were selected from the Reindeer D-27 and Tununuk K-10 wells for detailed Rock-Eval/TOC, vitrinite reflectance, gas chromatography, and gas chromatography-mass spectrometry analysis as part of a regional thermal maturity study of the Beaufort-Mackenzie Basin in Arctic Canada. These deep and extensively cored wells, located at the southern end of Richards Island in the thrusted eastern margin of the Taglu Fault Zone (Tununuk High), provide a useful reference for interpreting new and legacy Rock-Eval data for cuttings samples that are known to be susceptible to contamination. Organic petrological observations and elevated Rock-Eval Tmax values indicate that recycled organic matter is common in the Iperk, Richards and Taglu sequences of the Reindeer D-27 well, and the Iperk, Aklak, Fish River and Arctic Red successions of the Tununuk K-10 well. Samples from both wells show evidence of contamination based on anomalous Rock-Eval pyrograms (*e.g.* multi-modal, asymmetric) and anomalous Rock-Eval parameters such Tmax, S1 and PI. For the Reindeer D-27 well, oil staining, hydrocarbon fluid inclusions, exudatinite (early and locally generated waxy oil from terrestrial organic matter) and bitumen have been observed in samples from the Taglu, Aklak and Arctic Red successions and these are associated with elevated PI and reduced Tmax values. Oil staining and bitumen have been observed in some samples from the Tununuk K-10 well also. Tmax values are low and decrease with increasing TOC content in the abundant, immature to marginally mature coal-rich samples of the Taglu Sequence in the Reindeer D-27 well. Some post-drilling contamination of samples is indicated by the presence of the plasticizer, dibutylphthalate (from plastic sample vials), in extracts of cuttings samples from the Reindeer D-27 well. Although such contamination can contribute to anomalous Rock-Eval parameters, the observed elevated S1 values and reduced Tmax values for cuttings samples relative to core samples for both wells suggests that drilling mud additives are the main source of contamination.

Measured mean random reflectance for indigenous vitrinite varies from 0.37 %Ro (Richards Sequence) to 0.79 %Ro (Arctic Red Formation) for the Reindeer D-27 well and 0.39 %Ro (Aklak Sequence) to 1.30 %Ro (Arctic Red Formation) for the Tununuk K-10 well. The unconformably overlying Iperk Sequence in both wells is thermally immature and dominated by recycled vitrinite. Rock-Eval, apatite fission track, and biomarker (sterane and terpane) isomer ratio data provide independent confirmation of organic maturity levels. In accordance with previous published studies, petrological, Rock-Eval and organic geochemical data indicate that the Cretaceous Smoking Hills/Boundary Creek and Arctic Red Formations are dominated by marine (Type II) organic matter whereas the overlying mainly Cenozoic, deltaic sediments contain abundant terrestrially-derived organic matter (Type III). Thermal modelling, constrained using maturity and biomarker data, suggests that marine Cretaceous rocks in both wells entered the oil window at 135°C and reached peak generation at approximately 145°C during late Eocene-Oligocene time. The distribution of n-alkanes and alkyl naphthalenes in extracts of Taglu cuttings samples suggests that oil migrated from the Arctic Red Formation into the overlying Taglu and probably Aklak sequences in the Reindeer D-27 well. Good results are achieved using the new basin%Ro kinetic model for vitrinite reflectance with constant geothermal gradients equal to present values of 25.2°C/km and 28.6°C/km, and with pre-Iperk eroded thicknesses of 2200 m and 2300 m, for the Reindeer D-27 and Tununuk K-10 wells, respectively. The popular EASY%Ro kinetic model gives poorer results that may indicate a systematic miscalibration of vitrinite reflectance with respect to temperature for this model.

INTRODUCTION

The Geological Survey of Canada (GSC) is involved in a multi-disciplinary study of petroleum systems of the Beaufort-Mackenzie Basin under phase 2 of the Earth Sciences Sector Geo-Mapping for Energy and Minerals (GEM) Program. As part of this research, new organic maturity and geochemical data are being acquired for selected petroleum exploration wells to help constrain quantitative models of thermal history and petroleum generation for this basin. Detailed studies of key wells are necessary to supplement and aid in the interpretation and synthesis of a large body of legacy organic maturity and related data that has accumulated for this basin over the last 40 years (Issler *et al.*, 2012b). Organic maturity measurements and interpretations can be affected significantly by geological factors (*e.g.* recycling of organic matter from eroded older successions and oil migration) and drilling-related contamination (*e.g.* organic additives in drilling mud and recirculation of well cuttings or caving that leads to mixing of samples from different stratigraphic intervals). Therefore, an integrated, multi-parameter approach is used to assess thermal maturity to ensure data quality.

Quality control measures include using independent optical (observed vitrinite reflectance), bulk analytical (Rock-Eval pyrolysis), and organic geochemical (gas chromatography-mass spectrometry) methods to assess thermal maturity and source rock properties. Bulk analysis methods such as Rock-Eval pyrolysis are more susceptible to sample contamination than microscope-based methods that can measure different organic components separately within a sample. Gas chromatography-mass spectrometry provides valuable data on the chemical composition of solvent-soluble organic matter in samples that can help identify sources of contamination as well as support and enhance interpretations based on organic petrology and pyrolysis techniques. The two study wells, Reindeer D-27 and Tununuk K-10, were chosen because they are deep wells with numerous cored intervals. The better quality core samples were used where possible because they avoid some of the drilling-related contamination associated with drill cuttings samples.

Apatite fission track (AFT) thermochronology is an inorganic method for paleotemperature reconstruction that avoids the problems associated with organic contamination. Apatite is a common heavy mineral component of sandstones and AFT data are available for the Reindeer D-27 well. Fission tracks are linear regions of crystal damage that form over geological time by the spontaneous fission decay of ^{238}U within apatite crystals (*e.g.* Wagner and Van den Haute, 1992; Gallagher *et al.*, 1998; Gleadow *et al.*, 2002). They form with an initial length of approximately 16 μm but with increasing burial temperature, thermal annealing reduces AFT lengths and ages in a systematic manner. The characteristic patterns of AFT age and length reduction observed for Beaufort-Mackenzie Basin well samples allow for an independent assessment of the quality of the thermal maturity data.

Stasiuk *et al.* (2005, 2009) and Issler *et al.* (2012a) have published three GSC open file reports on thermal maturity for selected Beaufort-Mackenzie wells. This publication is the fourth in a series of five planned GSC open file reports examining the thermal maturity of core and cuttings samples from wells in the Beaufort-Mackenzie Basin. The fifth publication in the series will present an integrated interpretation of a large suite of new and legacy vitrinite reflectance data for the Beaufort-Mackenzie Basin. A preliminary analysis of some of this data is presented in Issler *et al*. (2012b).

WELL LOCATIONS AND STRATIGRAPHY

Figure 1 shows the location of the Tununuk High (grey shading), a regional tectonic element characterised by folded and uplifted Tertiary strata. The Tununuk High occurs within the much larger SW-NE trending Kugmallit Trough, a syncline containing thick accumulations of Upper Jurassic to Lower Cretaceous syn-rift strata (Lane and Dietrich, 1995; Dixon, 1996). The Kugmallit Trough is bounded to the southeast by the Jurassic-Cretaceous syn-rift normal faults of the SW-NE trending Eskimo Lakes Fault Zone and to the northwest by the SW-NE trending Tertiary normal faults of the Taglu Fault Zone which also forms the northwest margin of the Tununuk High (Lane and Dietrich, 1995; Dixon, 1996). The Tununuk K-10 well is located on the Tununuk High whereas the Reindeer D-27 well is at its northeast margin immediately northeast of the Reindeer F-36 gas discovery well (National Energy Board, 1998; Figure 1). Both wells are part of the thrusted eastern margin of the Taglu Fault Zone. The Reindeer D-27 well was spudded in 1965 and was the third well to be drilled in the Beaufort-Mackenzie region. Two prior wells (Nicholson G-56 and N-45) were drilled in 1962 in the physiographic region known as the Anderson Plain southeast of Tuktoyaktuk Peninsula and they penetrated approximately 860 m of Cretaceous syn- and post-rift strata. The Tununuk K-10 well was the fourth well to be drilled in the area and it was spudded in 1968. Currently, there are approximately 280 wells in the onshore and offshore parts of the Beaufort-Mackenzie basin.

Figure 2 shows the Mesozoic-Cenozoic stratigraphy for the Beaufort-Mackenzie Basin. The Reindeer D-27 well was the first deep well in the area (3850 m) and it encountered a thick succession of Cenozoic post-rift strata (3260 m) overlying syn-rift strata of the Albian Arctic Red Formation. There is a major unconformity within the Cenozoic succession of the Reindeer D-27 well where Pliocene-Pleistocene strata of the Iperk Sequence overlie Eocene and Paleocene strata of the Richards, Taglu and Aklak sequences (> 30 million year gap in time). To the southwest, the Tununuk K-10 well encountered a thinner (approximately 2600 m) and older Upper Cretaceous-Cenozoic post-rift succession before terminating in syn-rift sediments of the Arctic Red Formation at approximately 3750 m. Pliocene?-Quaternary strata overlie the Eocene Taglu Sequence at Tununuk K-10 and this represents > 40 million years of missing geological record. A large number of cores are available for the Taglu, Aklak and Arctic Red successions in the Reindeer D-27 well. The Tununuk K-10 well also has core which is mainly from the Arctic Red Formation.

METHODS

Vitrinite Reflectance

Vitrinite reflectance is a widely used thermal maturity parameter for evaluating the thermal history and petroleum potential of sedimentary basins (*e.g.* Mukhopadhyay and Dow, 1994; Taylor et al., 1998). The method is based on measuring the percentage of incident light reflected from polished vitrinite macerals obtained from sedimentary rocks. It is well established that vitrinite reflectance increases with increasing burial temperature and this forms the basis for temperature-dependent kinetic models that calculate vitrinite reflectance values as a function of basin thermal history (EASY%Ro (Sweeney and Burnham, 1990) and the recently recalibrated version, basin%Ro (Nielsen *et al*., 2015)). Random per cent reflectance in oil (%Ro) was measured for various macerals in whole rock cuttings and conventional core samples that were prepared according to the standard procedures used by the organic petrology laboratory at the GSC Calgary office (*e.g.* Stasiuk *et al*., 2009; Issler *et al*., 2012a).

Rock-Eval Pyrolysis

Rock-Eval pyrolysis is a bulk analytical technique for characterizing the quality, quantity and thermal maturity of organic matter (OM) in sedimentary rocks (Figure 3). Lafargue *et al*. (1998) and Behar *et al*. (2001) provide details on the Rock-Eval pyrolysis method for the newest version of the instrument (Rock-Eval 6 apparatus) that is used at GSC Calgary. The method involves programmed heating of a sample in an inert atmosphere (nitrogen) to yield hydrocarbons (HCs; S1 and S2 curves) plus oxidized carbon from organic (S3; 300-400°C) and mineral sources (400-650°C) followed by sample heating in an oxidation oven to obtain total organic carbon (TOC) and mineral carbon (MINC) in weight % (wt %). Figure 3 shows an example of pyrolysis curves for a sample standard and summarizes key Rock-Eval parameters and the type of information that can be obtained from Rock-Eval analysis. An initial isothermal heating phase (300°C) volatilizes existing free hydrocarbons within a sample (S1 curve) and subsequent ramped linear heating (300-650°C) generates new hydrocarbons by thermal cracking of sedimentary organic matter (S2 curve) (Figure 3).

Well whole rock core and washed cuttings samples were analysed at the Geological Survey of Canada using a Rock-Eval 6 instrument according to the procedures outlined in Issler *et al*. (2012a). Rock-Eval 6 pyrolysis yields a large number of parameters and results have been expressed using the older Rock-Eval 2 format for ease of interpretation. The temperature at peak generation on the S2 pyrolysis curve (Tpeak; Figure 3) is converted to the relative temperature, Tmax (in °C), which is an accepted thermal maturity parameter based on the older Rock-Eval 2 technology. The amount of pyrolysable organic carbon (PC in wt %) is determined by combining the S1, S2 and temperature-dependent CO_2 (S3) and CO pyrolysis contributions according to a specific formula (Behar *et al*., 2001).

Peters (1986) discussed factors that can affect Rock-Eval parameters and presented guidelines for interpreting Rock-Eval 2 data. S1, S2 and Tmax values can be unreliable for TOC values < 0.5 wt % and Tmax values can be unreliable for S2 values <0.2-0.5 mg HC/g rock depending on the type of organic matter and rock matrix (Peters, 1986; Riediger *et al*., 2004; Obermajer *et al*., 2007). Multi-modal S2 peaks and PI values > 0.2 can indicate natural or drilling-related contamination for immature samples. Issler *et al*. (2012a) discuss how Rock-Eval parameters have been affected by geological and drilling-related contamination of samples from three Beaufort-Mackenzie wells.

Gas Chromatography and Gas Chromatography-Mass Spectrometry

Organic geochemistry analysis was undertaken to help constrain interpretations based on vitrinite reflectance and Rock-Eval analysis. The composition of sample solvent-soluble organic matter can provide important information on source input, depositional environment, and thermal maturity that is relevant to assessing petroleum potential and sample contamination.

Residual cuttings samples from the Reindeer D-27 well were selected for solvent extraction based on their Rock-Eval results. After solvent removal by rotary evaporation of the extract mixtures to about 5mL each, gas chromatography (GC) analysis was carried out on the whole extracts using a Varian 3800 FID gas chromatograph to obtain a GC fingerprint of the total hydrocarbon components of each sample. Gas chromatography-mass spectrometry (GC-MS) analysis of the total hydrocarbon fraction of the extracted cuttings samples was done using a Varian 3800 GC coupled to a Varian 1200L Triple Quadrupole Mass Spectrometer. There was insufficient residual core material for further analysis so new core samples were collected from the Reindeer D-27 and Tununuk K-10 wells for Rock-Eval, GC and GC-MS analysis. After Rock-Eval analysis, the core samples were subjected to solvent extraction followed by open column chromatography separation of the extracts to obtain the saturated, aromatic, resin and asphaltenes (SARA) fractions, then GC and GC-MS analysis of the saturated and aromatic fractions. Issler *et al.* (2012a) provides more details on the sample preparation and analysis procedures used at GSC Calgary.

RESULTS AND INTERPRETATIONS

Vitrinite Reflectance

Tables 1 and 2 contain vitrinite reflectance results for the two study wells. Tabulated information includes the GSC sample curation and organic petrology lab pellet numbers, measured sample depth (in feet (original) and metres) with respect to Kelly Bushing elevation, true vertical depth (from well history borehole deviation survey) in metres with respect to Kelly Bushing and ground level elevations, stratigraphic unit, sample type (core or cuttings), comments on sample measurements, and mean random percent vitrinite reflectance in oil plus the standard deviation and number of measurements. Only measurements for interpreted primary (indigenous) vitrinite are shown in Tables 1 and 2. Bitumen and caved or recycled vitrinite were also measured to aid interpretation but these results are not included here.

Reindeer D-27 organic maturity trend

Most of the %Ro measurements for the Reindeer D-27 well were done on core samples, especially through the Aklak and Arctic Red successions (Table 1). Cuttings samples were used to supplement core measurements in the Taglu Sequence and for the Iperk and Richards sequences where core is not available. Recycled vitrinite exists in both cuttings and core samples, and dominates the Iperk, Richards and upper part of the Taglu sequences (Table 1). Core samples were collected for AFT and %Ro analysis in 1992 and the %Ro measurements of Maria Tomica, formerly of the GSC organic petrology laboratory, are included in the last part of Table 1 for comparison with the newer data. Oil staining is known to suppress vitrinite reflectance values and this has been observed in other wells in the Beaufort-Mackenzie region (*e.g.* Stasiuk *et al*., 2009; Issler *et al*., 2012a). Oil staining is common in samples from the Taglu Sequence and it occurs in Aklak and Arctic Red samples as well and it may be associated with minor %Ro suppression (Table 1). Any %Ro suppression due to oil staining must be very minor because the oil-stained samples conform closely to the %Ro-depth trend (Figure 4).

The data in Table 1 are plotted with respect to estimated true vertical depth in Figure 4. Measured organic maturity increases from 0.37 %Ro at the top of the Richards Sequence to 0.79 %Ro in the Arctic Red Formation near the base of the well. Measured %Ro decreases from 0.33 at the top of the Iperk Sequence to 0.28 near its base. The inverse %Ro-depth trend reflects the dominance of recycled organic matter that is common for the Iperk Sequence across the study region. The %Ro values corresponding to the AFT core samples (blue solid squares; Figure 4) show good agreement with the newer %Ro data. %Ro-depth data for the Richards and older successions were fit using an exponential equation. Calculated vitrinite reflectance varies from 0.38 %Ro at the top of the Richards Sequence (317 mKB) to 0.81 %Ro in the Arctic Red Formation at the base of the well (3854 mKB; Figure 4).

Seismic, well log and thermal maturity data indicate that there has been substantial erosion prior to the deposition of the Iperk Sequence. Extrapolation of the exponential trend in Figure 4 to an initial surface value of 0.2 %Ro gives an estimated erosion magnitude of approximately 2940 m (312 m thickness of the post-erosion Iperk sequence was added to obtain the estimate because post-erosion reburial reduces the calculated amount of eroded section). The extrapolation of shale compaction data as described by Issler (1992) yields 1270 m of pre-Iperk erosion for the Reindeer D-27 well. The %Ro-depth gradient converts to a paleogeothermal gradient of 18.3°C/km based on Middleton's (1982) method. This is less than the present value of approximately 25°C/km (Hu *et al*., 2014) derived from well temperature data (Hu *et al*., 2010). Although it is possible that the paleogeothermal gradient was lower than the present value, this difference may also be the result of an inaccurate calibration of %Ro with temperature for the Middleton (1982) model. For example, the Nielsen *et al.* (2015) basin%Ro model predicts a significantly different relationship between %Ro and temperature than the widely used EASY%Ro model of Sweeney and Burnham (1990).

Reindeer D-27 thermal/burial history model results

A first-order, steady-state thermal/burial history model (Feinstein *et al*., 1996) is used to investigate the effect of geothermal gradient and maximum burial thickness on calculated %Ro values for the Reindeer D-27 well. A simple burial history model using a paleosurface temperature of 10ºC (decreasing to -8.5°C at present to reflect present permafrost thickness), a constant geothermal gradient of 25.2ºC/km (present value), an eroded thickness of 2200 m (maximum burial depth and temperature of 5737 m and 155ºC, respectively, for the deepest layer), and the basin%Ro model (Nielsen *et al*., 2015) yields a good fit to the Reindeer D-27 %Ro-depth data (Figure 5). Given the quality of the well temperature data, it is possible that the present geothermal gradient for the Reindeer D-27 well is underestimated. A slightly better fit to the %Ro data can be achieved using a geothermal gradient of 27°C/km and an eroded thickness of 1900 m (maximum burial depth and temperature of 5437 m and 157ºC, respectively).

The Easy%Ro model (Sweeney and Burnham, 1990) can provide a good fit to the Reindeer D-27 %Ro data but a lower geothermal gradient (paleogeothermal gradient of 18ºC/km) and a larger eroded thickness (2940 m) (maximum burial depth and temperature of 6480 m and 128ºC, respectively, for the deepest layer) are required. It is possible that rapid deltaic sedimentation suppressed the paleogeothermal gradient. However, compared with the basin%Ro results, the implied 30% reduction in paleogeothermal gradient (relative to the present value) and the significant increase in the amount of erosion (nearly 3 km) are better explained by systematic errors with the EASY%Ro model as suggested by Nielsen *et al*. (2015). Overall, the EASY%Ro model misfits the Reindeer D-27 %Ro data if the present geothermal gradient is used for thermal history reconstruction. For example, the EASY%Ro model provides a good fit to %Ro data in the Arctic Red Formation and the lower part of the Aklak Sequence but predicts lower than observed thermal maturity in the upper part of the section if the present geothermal gradient and an eroded thickness of 1270 m (shale compaction estimate) are used to model the Reindeer D-27 thermal history. Thermal maturity gradients are more variable than compaction gradients in the study region, implying more variable erosion than is inferred from shale compaction. This may be caused by thermal and depositional processes that are not included in a simple burial model that assumes constant temperature and maturity gradients.

Reindeer D-27 apatite fission track thermal annealing

AFT thermochronological data provide an independent check on the quality of the thermal maturity data. Unlike vitrinite reflectance which is a cumulative thermal history indicator in which %Ro values increase with increasing temperature, fission tracks undergo thermal annealing that reduces AFT ages and lengths with increasing temperature. At temperatures greater than the total AFT annealing temperature, all pre-existing tracks are erased and no new tracks accumulate until the apatite-bearing rock cools below the total annealing temperature. Figure 6 shows the variation in AFT ages and mean lengths with %Ro for two AFT populations from the Ellice O-14 well (Figure 1) that have different annealing kinetics related to mineral composition (blue curves). Kinetic population 1 is the least track retentive (most easily annealed) and has a fluorapatite composition. Kinetic population 2 is more track retentive (higher total annealing temperature) and has higher concentrations of Cl, Fe and other cations that increase the total AFT annealing temperature relative to fluorapatite (Carlson *et al*., 1999; Ketcham *et al*., 1999; Barbarand *et al*., 2003). Kinetic population 1 shows a more consistent decrease in AFT age with increasing %Ro than kinetic population 2. Some variability in AFT age is expected because the apatite is detrital and carries an initial age older than the stratigraphic age of the unit from which it was obtained (reflecting the cooling history of the sediment source area). The Ellice O-14 AFT data are considered to be representative of AFT age and length trends for exhumed Tertiary strata on the southern basin margin. These data have been modelled successfully (Issler and Grist, 2008) and results will be published elsewhere.

AFT samples from the Reindeer D-27 well have two AFT kinetic populations of similar composition and annealing behaviour as those from the Ellice O-14 well. AFT ages and mean lengths for these two kinetic populations in core samples from the Reindeer D-27 well are plotted with respect to %Ro in Figure 6 (red curves). The mean AFT lengths of the Reindeer samples are relatively long (12-13.2 μm; Figure 6b) and this implies moderate amounts of AFT annealing. AFT age and length parameters for the Reindeer D-27 samples overlap with the upper range of values for the Ellice O-14 samples. Qualitatively, the observed modest amount of AFT annealing is consistent with the measured range in maturity (0.43-0.57 %Ro) for the Reindeer D-

27 well. Integrated thermal modelling of AFT and %Ro data for the Reindeer D-27 well and other Beaufort-Mackenzie wells is part of an ongoing study that will be published elsewhere.

Tununuk K-10 organic maturity trend

Most of the %Ro measurements (>70 %) for the Tununuk K-10 well were done on cuttings samples except for samples from the Arctic Red Formation which was cored extensively (Table 2). Similar to the Reindeer D-27 well, recycled vitrinite occurs throughout the well, particularly in the Iperk, Aklak and Arctic Red successions. In general, the Tununuk K-10 samples had less indigenous vitrinite than the Reindeer D-27 samples. Approximately 80 % (26) of the Tununuk K-10 %Ro samples had < 30 measurements per sample (Table 2) whereas 78 % (32) of the Reindeer D-27 %Ro samples had 30 or more measurements per sample (Table 1). Samples from the Smoking Hills/Boundary Creek succession and upper part of the Arctic Red Formation contain anomalously low %Ro values that may be associated with a change in organic facies from terrestrial (Type III) to marine (Type II) organic matter (Table 2; Figure 7; see below). Reduced %Ro values have been observed in the Upper Cretaceous bituminous shales (Smoking Hills and Boundary Creek formations) for other wells in the area (Stasiuk *et al*., 2009; Issler *et al*., 2012a). The reduction in %Ro values appears rather large when a single exponential function is used to fit the %Ro-depth data (solid black curve, Figure 7). However, if two functions are used (red dashed curves, Figure 7), then the reduction in %Ro values appears to be minor. This second interpretation appears to be a better approximation based on modelling results in the section below.

The Tununuk K-10 well is in the eastern margin of the Beaufort Foldbelt where seismic correlations are difficult due to structural complications. Significant tectonic wedging is evident with the potential for thrust faults and associated anomalous stratigraphy and maturity trends (J. Dietrich, personal communication, 2009). Carbonate-filled microfractures were noted in core samples from the Arctic Red Formation (Table 2). Cores collected between 3441-3543 mKB (11290-11625 ft) are highly fractured and brecciated with some calcite- and quartz-filled fractures that could indicate proximity to a fault (Dixon, 2002). However, existing biostratigraphic and log data are consistent with a continuous Arctic Red succession at the bottom of the well. Figure 7 shows a plot of %Ro versus true vertical depth for the Tununuk K-10 well. Measured organic maturity increases from 0.39 %Ro in the Aklak Sequence to 1.30 %Ro in the Arctic Red Formation near the base of the well. Maturity varies between 0.27 to 0.35 %Ro in the Quaternary-Iperk succession and, like the Reindeer D-27 well, it shows the influence of organic matter recycling. The Quaternary-Iperk succession rests unconformably on a thin Eocene Taglu Sequence and extensive erosion has resulted in a maturity discontinuity across this unconformity.

An exponential fit to the $\%Ro_R$-depth data for the Aklak to Arctic Red interval (excluding anomalously low %Ro values in blue; Figure 7) gives calculated vitrinite reflectance values of 0.44 %Ro at the top of the Taglu Sequence (243 mKB) and 1.21 %Ro in the Arctic Red Formation at the base of the well (3752 mKB). The %Ro-depth gradient in Figure 7 gives a paleogeothermal gradient of 24.4°C/km based on Middleton's (1982) method whereas the present geothermal gradient derived from well temperature data (Hu *et a*l., 2010) is approximately 28.6°C/km (Hu *et al*., 2014). Extrapolation of the exponential %Ro-depth trend to an initial surface value of 0.2 %Ro gives an estimated pre-Iperk erosion magnitude of 2740 m (thickness of Quaternary-Iperk succession added to extrapolated value). These paleogeothermal gradient and erosion estimates could have significant error if the %Ro data are better described using two empirical functions (Figure 7). Shale compaction data give approximately 1180 m of pre-Iperk erosion for the Tununuk K-10 well which is less than the 1270 m estimate for the Reindeer D-27 well. The Tununuk K-10 compaction-based erosion estimate is poorly constrained because only a few data points are available. Stratigraphic and maturity data suggest that there should have been more pre-Iperk erosion at the Tununuk K-10 well than at the Reindeer D-27 well, especially because the K-10 well is situated on the Tununuk High and should have experienced more deformation-related uplift and erosion.

Tununuk K-10 thermal/burial history model results

A simple burial history model using a paleosurface temperature of 10ºC (decreasing to -2.6°C at present to reflect present permafrost thickness), a constant geothermal gradient of 28.6ºC/km (present value), an eroded thickness of 2300 m (maximum burial depth and temperature of 5810 m and 176ºC, respectively, for the deepest sedimentary layer), and the basin%Ro model (Nielsen *et al*., 2015) yields a reasonable fit to the Tununuk K-10 %Ro-depth data (Figure 8). The present geothermal gradient at Tununuk K-10 is based on "fair" quality well temperature data (Hu *et al*., 2014) and is more likely to underestimate than overestimate geothermal gradient, given the typical problems with correcting log bottomhole temperature data (*e.g.* Hu *et al*., 2010). The closest wells are Reindeer A-41 and Tununuk F-30 (Figure 1) with calculated geothermal gradients of 35ºC/km and 25.1ºC/km (Hu *et al*., 2014), respectively. A slightly better fit to the %Ro data can be obtained with the basin%Ro model using a geothermal gradient of 25.1°C/km and an eroded thickness of 3100 m (maximum burial depth and temperature of 6610 m and 176ºC, respectively, for the deepest layer). However, it is unclear that this is a better model, given all the sources of uncertainty in the analysis, and the fact that the high amount of recycled vitrinite may be affecting some %Ro measurements in the Aklak and Fish River sequences.

Even with significant changes to the geothermal gradient and erosion estimates, the EASY%Ro model provides a poorer fit to the Tununuk K-10 %Ro data than the basin%Ro model. A burial history model with a paleogeothermal gradient of 24.4ºC/km and an eroded thickness of 2740 m (derived from an exponential fit to the %Ro data as described above) (maximum burial depth and temperature of 6250 m and 162ºC, respectively, for the deepest layer) can adequately fit the %Ro data in the upper and lower parts of the well but it overestimates %Ro values by approximately 0.1 to 0.2 % for the Smoking Hills/Boundary Creek and upper Arctic Red samples (blue symbols in Figures 7 and 8). A worse fit to the data is obtained if the present geothermal gradient is used with the EASY%Ro model (1800 m of erosion is needed to match the %Ro values at the base of the well). %Ro values are underestimated by 0.1-0.3 %Ro for the entire well if the present geothermal gradient and compaction-derived eroded thickness of 1180 m are used (maximum burial depth and temperature of 4690 m and 145ºC, respectively, for the deepest layer). This further confirms that the shale compaction erosion estimate for this well is poorly based.

Rock-Eval Pyrolysis

Rock-Eval pyrolysis was done first and results were used to screen samples for subsequent organic petrology based on TOC values. Rock-Eval 6 results for the Reindeer D-27 and Tununuk K-10 wells are shown in Tables 3 and 4, respectively. Data are presented in Rock-Eval 2 format with additional columns for mineral carbon, organic matter type and calculated %Ro-equivalent values. Tmax values were converted to vitrinite reflectance equivalent values using polynomial equations fitted to tabulated data for Type II (marine-derived) and III (terrestrially-derived) organic matter (MATOIL™, 1990; see Issler *et al*. (2005) for Type III equation). Sample depths are given in both feet and metres in the data tables. Depth values highlighted in yellow correspond to samples with vitrinite reflectance data. Both wells contain samples with disturbed pyrograms that are most likely caused by contamination. Colour coding is used to distinguish between normal or minimally disturbed pyrograms (green) and anomalous (disturbed) pyrograms (purple) (*e.g.* multi-modal, asymmetric, etc.). Average Tmax values were calculated for each rock formation using all sample measurements and data from samples with the least disturbed pyrograms (green). PI values of 0.2 or greater and TOC values > 5 wt % are highlighted in orange and yellow, respectively (Tables 3 and 4).

Reindeer D-27 Rock-Eval log and drilling mud additives

Selected Rock-Eval parameters for the Reindeer D-27 well (Table 3) are plotted as a function of depth in Figure 9. Although there is an overall increase in Tmax with increasing depth, it is apparent that there are problems with data quality, particularly at depths less than 6660 feet (2030 m) where there are large variations in Tmax, PI and TOC values (Figure 9). This is confirmed by the analysis of sample pyrograms that show anomalous features (abnormally low Tmax, multimodal S2 peaks, asymmetric S2 curves with left and right shoulders; see comments in Table 3) that commonly are associated with sample contamination from drilling mud additives and migrated oil or bitumen (Peters, 1986). Although the cuttings samples were washed, there is still potential for drilling contamination based on the type of organic mud additives described in the well history report. Additives that could affect Rock-Eval pyrograms include Carbonox (lignitic humic acid powder used as a mud thinner and dispersant), Q Broxin (ferrochrome lignosulphonate used as a mud thinner) and Cellex (Hi Viscosity and Regular) (sodium carboxymethyl cellulose used as a filtrate reducer). For example, lignosulphonates give low Tmax (330-380°C) and high TOC (16-30 wt %) values but usually they can be washed out of samples (Robertson Group, 1989). In general, organic mud additives tend to decrease Tmax and can increase S1, S2, HI, PI and TOC values, depending on their composition (Peters, 1986).

Rock-Eval characteristics of each stratigraphic unit in the Reindeer D-27 well

The upper part of the Iperk Sequence was air-drilled down to 665 feet (202.7 m) and then a dense mud was used below this depth to control sloughing of unconsolidated sands beneath the ice-bonded permafrost zone. There is no record of organic mud additives being used during drilling of the Iperk Sequence (mainly Aquagel (Na montmorillonite), Baroid ($BaSO_4$), caustic soda (NaOH), and unspecified weight material were used in the drilling mud below 665 feet). Nevertheless, samples from the Iperk Sequence have anomalously high PI values (0.2-0.5), some low Tmax values (< 420°C) and anomalous pyrograms (78 %) that are probably related to the presence of thermally immature biological material that has not yet transformed into kerogen (Figure 9; Table 3). Some samples have very low S2 (< 0.5 mg/g rock) and TOC (<0.5 wt %) values that make Rock-Eval parameters unreliable. The least disturbed pyrograms yield an average Tmax of 421.3±1.1°C which is consistent with the expected low organic maturity of the Iperk Sequence (Table 3). Organic petrological observations indicate that recycled organic matter is abundant and this may be associated with higher Tmax values (>423°C). Indigenous organic matter consists mainly of brown-fluorescing lignitic macerals with bright yellow-fluorescing liptinite inclusions.

Samples from the underlying Richards Sequence generally have very low TOC (mainly 0.2-0.5 wt %) and S2 values (mainly 0.1-0.5 mg/g rock) and high PI values (mainly 0.2-0.4) with > 90 % anomalous pyrograms (Figure 9; Table 3). There are also anomalously low (< 420°C) and high (>430°C) Tmax values that are probably associated with contamination and organic recycling. The average Tmax value for the two least disturbed pyrograms is 422.0±1.4°C (Table 3) which gives a lower organic maturity (0.23 %Ro equivalent value) than measured optically (0.37-0.38 %Ro; Table 1; Figure 4). Hi Viscosity Cellex was added to the mud system during drilling of the interval, 1184–1472 feet (360.9-448.7 m). Although this may have contributed to drilling-related sample contamination, most of the Rock-Eval parameters are unreliable due to the very low TOC and S2 values.

Samples from the Taglu Sequence are dominated by coal with exudatinite (waxy oil derived from liptinite), hydrocarbon fluid inclusions, and lots of oil staining as observed petrographically and as noted in the cuttings samples descriptions of the well history report. TOC values can be very high with many samples in the range of 10-50 wt% and there are some high PI values (0.2-0.38) (Table 3; Figure 9). Approximately 38 % of the pyrograms show obvious disturbance (asymmetric and multi-modal S2 curves) but even the least disturbed pyrograms show some irregularities (Table 3). Tmax is highly variable and generally suppressed through this immature to marginally mature (0.39-0.51 %Ro; Table 1) coal-rich succession (Figure 9). Although Carbonox was added to the mud system and may contribute to Tmax suppression, there is a significant amount of geological “contamination” related to the presence of oil and coal. The average Tmax value for the least disturbed pyrograms is 417.4±6.6°C (75 samples) (Table 3). If samples with TOC values >5 wt % are excluded, the average Tmax increases to 422.1±5.3°C (30 samples) (Table 3). In the lower part of the Taglu succession (>4823 feet or >1470 m), some pyrograms may be affected by caved coal based on cuttings descriptions in the well history report.

Tmax shows less variability and a general increase in depth through the Aklak Sequence (Figure 9). Samples from the upper part of the Aklak Sequence have high PI values, slightly elevated HI values and some low Tmax values that are probably related to oil staining based on cuttings and core descriptions in the well history report (Figure 9; Table 3). After core #5 (5310-5370 feet or 1618.5-1636.8 m) was recovered, coarse sand lenses in the last 17.5 feet (5.3 m) exsolved gas, bled a light yellow brown oil film and showed fluorescence. Fluorescence and light spotty oil staining were reported for part of core #7 (6094-6116 feet or 1857.5-1864.2 m). There is another interval of high PI values below 8580 feet (2615.2 m) and trace hydrocarbon fluid inclusions are observed in samples from this interval (Figure 9; Table 3). Approximately 29 % of the pyrograms show significant disturbance but all pyrograms show some degree of irregularity and

Tmax appears to be suppressed for most samples (Table 3). The average Tmax value for the least disturbed pyrograms is 428.5±2.9°C (Table 3). This gives a %Ro equivalent value of 0.48 which is less than the measured range of 0.51-0.69 %Ro (Table 1). Carbonox was used in the mud system during drilling of the upper part of the Aklak Sequence (down to 5797 feet or 1767 m) and below a depth of 8200 feet (2499 m). Rock-Eval parameters could be affected by drilling-related contamination but geological contamination (oil staining, exudatinite, hydrocarbon inclusions) is also a significant factor.

Samples from the Arctic Red Formation have a relatively narrow range of Tmax values that show a general increase with depth (Figure 9). Almost all pyrograms are normal to minimally disturbed (small left shoulder on S2) and yield an average Tmax value of 436.8±2.0°C (67 samples; Table 3). This gives %Ro equivalent values of 0.65 and 0.74 for Type II and Type III organic matter, respectively. The latter value is closer to the measured vitrinite reflectance range (0.69-0.79 %Ro; Table 1) but the dominance of alginite (*Leiosphaeridia* and *Prasinophyte*) with minor sporinite and cutinite suggests mainly Type II organic matter with some terrestrial input. Most of the minimally disturbed pyrograms are associated with a zone of high PI values (0.21-0.39) below 11530 feet (3514.3 m) (Figure 9; Table 3). An oil-stained core sample at 12462 feet (3798.4 m) has an anomalous pyrogram (bimodal S2) with a suppressed Tmax (295°C), and high S1 (8.94 mg/g rock), PI (0.63) and HI (221) values (Table 3; Figure 9). Solid bitumen was observed in all the Arctic Red core samples and the well history report includes descriptions of gas kicks and oil staining. Carbonox and some Cellex were added to the mud system during the drilling of this interval and therefore drilling-related sample contamination is possible.

Reindeer D-27 organic matter type, thermal maturity and well cuttings contamination

Plots of HI versus OI (Espitalié *et al*., 1977) can provide information on sample organic matter type and thermal maturity but they must be interpreted with caution because both parameters are sensitive to contamination. HI versus Tmax plots (Espitalié *et al*., 1984) can be used to examine organic maturation pathways when OI values are unreliable (*e.g.* anomalously high due to contributions from mineral carbon or other factors; Peters, 1986).

Figure 10 shows plots of HI versus OI and HI versus Tmax for samples from the Reindeer D-27 well. The data are scattered with some elevated HI and OI values but most points plot in the field indicating immature to mature, Type III organic matter. Sample contamination has affected HI and OI values, mainly in the upper part of the well (Iperk, Richards and, to a lesser extent, Taglu sequences). There is a zone of elevated HI values in the Iperk Sequence (150-255; 34 % of samples) that coincides with high PI values (Figure 9; Table 3) and > 60 % of the samples have anomalously high OI values (200-1772; Table 3). For the Richards Sequence, most samples have HI values < 100 but 65 % of the OI values are in the range, 200-525 (Table 3). For the Taglu Sequence, < 20% of the samples have high OI values (150-600) and HI values are < 165 with 58 % of the samples having HI values < 100. Some HI values > 115 are associated with oil staining (Table 3). Almost all of the Aklak samples have OI and HI values < 150. Samples from the Arctic Red Formation tend to have lower OI values (< 50; 78 % of samples) consistent with a mixture of Type II and III organic matter. HI values are < 144 except for an oil stained core sample (HI=221; Table 3) that plots along the Type II evolution curve in Figure 10. The increase in S2/S3 ratio in the Arctic Red Formation (effectively HI/OI) implies a change in organic matter type (Figure 9).

As discussed above, Tmax values are variable due to the presence of recycled organic matter and contamination that has distorted sample pyrograms, particularly in the upper part of the well. The lower half of the well shows a more consistent maturity trend with Tmax values up to 440°C near the base of the well (Figure 9; Table 3). The highest Tmax value (445°C) in Figure 10 is from a low TOC sample from the Richards Sequence.

Rock-Eval organic maturity determinations for the Reindeer D-27 well can be visually assessed with respect to optically measured maturity by plotting %Ro values (Table 1; Figure 4) and Tmax values converted to %Ro-equivalent values (Table 3) versus depth (Figure 11). Figure 11a shows %Ro-equivalent data (blue x symbols for cuttings and solid green diamonds for cores) for all Tmax values yielding %Ro-equivalent values > 0.2% whereas Figure 11b shows only %Ro-equivalent data for samples with the least disturbed pyrograms in Table 3. The wide variation in %Ro-equivalent values for the Iperk, Richards and upper part of the Taglu sequences (Figure 11a) is consistent with petrological observations of organic matter recycling (Table 1) and contamination that has distorted sample pyrograms (Table 3). It is interesting to note that %Ro-equivalent data for core samples (solid green diamonds) in the lower part of the well show good agreement with optically measured %Ro values whereas cutting samples yield much lower %Ro-equivalent values (Figure 11b). Although geological factors (coal, oil staining, recycling) have affected both core and cuttings data, the difference between core and cuttings Tmax values suggests that drilling contamination (Carbonox?) has suppressed Tmax values. %Ro-equivalent values for Arctic Red samples were calculated assuming Type II organic matter whereas organic petrologic observations indicate a mixture of Type II and III organic matter. If Type III organic matter is assumed for this formation, cuttings Tmax %Ro-equivalent data show closer agreement with %Ro measurements but core Tmax values overestimate organic maturity.

Tununuk K-10 Rock-Eval log and drilling mud additives

Figure 12 shows a plot of selected Rock-Eval parameters (Table 4) versus depth for the Tununuk K-10 well. Sample contamination is apparent throughout the well, particularly in the Upper Cretaceous-Cenozoic deltaic successions (Fish River, Aklak, Taglu and Iperk sequences) which have variable Tmax, PI, TOC and HI values (Figure 12). Extensive sample contamination is confirmed by the large number of anomalous sample pyrograms (see comments in Table 4). In general, the Tununuk K-10 well has a higher percentage of anomalous pyrograms than the Reindeer D-27 well. More mud additives were used to drill the Tununuk K-10 well than the Reindeer D-27 well. The daily drilling reports in the well history file list a number of organic mud additives that could potentially affect Rock-Eval parameters. These include: Quick Vis (mud viscosifier made of hydroxyethyl cellulose), Peltex (ferrochrome lignosulphonate mud thinner and dispersant), Kelzan XC (xanthum gum mud viscosifier), CMC (carboxymethyl cellulose mud filtrate reducer), Dakolite (lignite emulsifier), Dowicide (sodium pentachlorophenate bactericide), Trimulso (blend of anionic surfactants used as an oil in water emulsifier), D Foam (petroleum hydrocarbons and polysiloxanes used as a defoamer), diesel (lubricant), and walnut shells and sawdust (lost circulation material).

In general, Dowicide and Kelzan XC were added to the mud system through most of the well. Peltex was introduced below approximately 2800 feet (> 850 m; lower part of Aklak Sequence) and then was added regularly to the mud system down to the base of the well. Quick Vis was used during drilling of the Aklak Sequence between 1647-2891 feet (502-881 m), and sawdust and Trimulso were added at 2891 feet (881 m). Most of the mud additives were used during drilling of the Arctic Red Formation. Dakolite was used over the interval, 10,692-10,951 (3259-3338 m). Quick Vis was used at the following depths: 8864 feet (2702 m), 9848 feet (3001.7 m), 10,221 feet (3115.4 m), 10,338 feet (3151 m), 10583 feet (3226 m) and 10,692 feet (3259 m). CMC was added to the mud system at 10,692 feet (3259 m), 11595 feet (3534 m), 11723-11791 (3573-3594 m) and 12037-12087 feet (3669-3684 m). Diesel was added at 8524 feet (2598 m), 11723 feet (3573 m), 12037 feet (3669 m) and 12118-12183 feet (3694-3713 m). Nutshells were added at 11,009 feet (3355.5 m). Very little D Foam was used in drilling the well.

Rock-Eval characteristics of each stratigraphic unit in the Tununuk K-10 well

More than 60 % of sample pyrograms in the Iperk Sequence are anomalous (Table 4). The upper part of the Iperk Sequence has high S1, TOC, PI and HI values and low Tmax values with asymmetric and bimodal S2 curves (Figure 12; Table 4). The lower part of the sequence appears to be dominated by recycled organic matter with high Tmax values yielding %Ro-equivalent values of 0.5-0.66 (Table 4). The least disturbed pyrograms give an average Tmax of 432.3±1.6°C (Table 4), reflecting the dominance of recycled organic matter in this thermally immature succession. The underlying Taglu Sequence has suppressed Tmax values and some high PI values (Figure 12), and 90 % of the sample pyrograms are anomalous (Table 4). A single normal pyrogram has a Tmax of 423°C. Many of the samples from the Aklak Sequence have anomalous pyrograms (>70 %; Table 4) with high PI values and suppressed Tmax values as well high Tmax values associated with petrologically observed recycled organic matter (Table 2). The least affected sample pyrograms give an average Tmax of 427.4±10.2°C (Table 4) (equivalent %Ro = 0.44) which is at the low end of the measured organic maturity range (0.39-0.59 %Ro; Table 2). This average Tmax is not very meaningful given the large standard deviation. The well history report describes some gas yield, oil staining and fluorescence within the Aklak interval. Oil staining is noted at 2120-2150 feet (646-655 m) but no cuttings samples are available between 2000-2650 feet (610-808 m) (Figure 12; Table 4). Most of the sample pyrograms for the Fish River Sequence are anomalous (85 %; Table 4) with many suppressed Tmax values and high PI values; some higher Tmax values are associated with recycled organic matter (Figure 12). The average Tmax for the least disturbed pyrograms is 435.7±3.0°C (Table 4; %Ro equivalent = 0.71) which is slightly higher than the optically measured maturity range (0.59-0.67 %Ro; Table 2). Sporadic oil staining was mentioned in the well history report for this interval. It is likely that drilling related contamination is the main factor affecting Rock-Eval parameters for the Upper Cretaceous-Cenozoic deltaic sequences with some possible contribution from oil staining.

There is a shift to higher S2/S3 (HI/OI) ratios for the Smoking Hills/Boundary Creek and Arctic Red successions (Figure 12) coincident with an observed change in organic matter character. These units have framboidal pyrite and alginite (*Tasmanites*, *Leiosphaeridia*, and *Prasinophyte*) consistent with a marine depositional environment. Tmax is variable but shows a general increase with depth through these intervals (Figure 12). The Boundary Creek/Smoking Hills interval has the lowest number of anomalous pyrograms (27 %) compared with other stratigraphic intervals in the well whereas 75 % of the Arctic Red pyrograms are anomalous (Table 4). Average Tmax values for the least disturbed pyrograms are 432.1±4.9°C and 440.0±2.7°C for the Smoking Hills/Boundary Creek and Arctic Red successions, respectively. Solid bitumen was observed for samples from these stratigraphic intervals and the well history report contains descriptions of oil staining, dead oil and fluorescence. Some of the low Tmax and high S1, S2, PI and HI values below 3500 m may be related to diesel contamination (Figure 12).

Tununuk K-10 organic matter type, thermal maturity and well cuttings contamination

Figure 13 shows plots of HI versus OI and HI versus Tmax for the Tununuk K-10 well. From the above discussion, HI and OI values will be affected to some degree by sample contamination given the large number of anomalous pyrograms and the associated variable Tmax values. Most of the samples plot in the field for immature to mature, Type III organic matter (Figure 13). OI values show a narrower range of variation in comparison to samples from the Reindeer D-27 well (Figure 10; Table 3). Fourteen samples (11 from the Aklak Sequence) have OI values in the range, 200-360, whereas all other OI values are less than 200 (Figure 13, Table 4). Most samples with HI values > 200 and OI values > 100 are from a suspected drilling-contaminated interval in the Iperk Sequence. Samples with higher HI (>150) and lower OI (<60) values are mainly from the Arctic Red and Smoking Hills/Boundary Creek successions. The higher HI values in part may reflect an increase in Type II organic matter but they are also associated with diesel contamination near the base of the Arctic Red Formation (Figure 12). Contamination is also indicated by the high HI values associated with low Tmax values (< 400°C; Figure 13).

Figure 14 shows plots of measured %Ro values (Table 2; Figure 7) and %Ro-equivalent values calculated from Tmax (Table 4) versus depth for the Tununuk K-10 well. All samples with %Ro-equivalent data > 0.2 are shown in Figure 14a (blue x symbols for cuttings and solid green diamonds for core) whereas Figure 14b shows only %Ro-equivalent data for samples with the least disturbed pyrograms. High %Ro-equivalent values from Tmax for the Iperk, Aklak, Fish River and Arctic Red successions are consistent with the amount of recycled organic matter determined by organic petrology (Figure 14a). Core and cuttings samples have anomalous pyrograms suggesting that geological (oil staining, bitumen) and drilling related contamination have affected Rock-Eval parameters. There is good agreement between %Ro-equivalent values and measured %Ro values for core and cuttings samples from the Smoking Hills/Boundary Creek and upper Arctic Red intervals (Figure 14b). Tmax and %Ro values appear to be suppressed within these intervals when the data are compared with a single exponential fit to the measured %Ro data (black curve, Figure 14b). A reduction in %Ro value may be associated with a change in organic matter type as observed petrographically and suggested by Rock-Eval data. However, the degree of suppression is much less than inferred from this figure and it is relatively minor (approximately 0.05 %Ro) based on the thermal modelling results above (Figure 8).

Organic Geochemistry of the Cuttings Samples from Reindeer D-27 Well

Seven cuttings samples from the Taglu and Aklak sequences and Arctic Red Formation of the Reindeer D-27 well were selected for solvent extraction and subsequent GC and GC-MS analysis (Table 5) on the basis of their Rock-Eval results. The choice of samples was limited by the availability of sufficient residual sample material because many of the original samples that were collected for organic petrology and Rock-Eval pyrolysis were consumed for these analyses. Therefore, only a tiny amount of solvent extractable organic matter was obtained from each sample and this was deemed to be insufficient for traditional open column fractionation which yields saturated, aromatic, resin, and asphaltene fractions and related SARA data. As a result, fractionation of the extracts using C18-SPE columns was performed to remove polar fractions and generate a total hydrocarbon fraction for each sample for GC-MS analysis.

Rock-Eval pyrograms for seven Reindeer D-27 cuttings samples

Figure 15 shows Rock-Eval pyrograms for the seven samples listed in Table 5. Although some of the samples from the Taglu Sequence have irregular pyrograms (Table 3), and some oil staining has been observed for this stratigraphic interval (Tables 1 and 3), the three Taglu samples (X11364, X11365 and X11366) in Figure 15 have normal pyrograms that are typical for coal-rich samples with broad, unimodal S2 peaks, high TOC values (17-35 wt%), and relatively low Tmax values (412-420°C) (Tables 3 and 5). The two Aklak samples are from the upper and lower parts of the Aklak Sequence where there are continuous zones with high PI values (>0.2), irregular pyrograms, and reported occurrences of hydrocarbons (Table 3 and Figure 9). The shallower Aklak sample (X11367) shows a large S1 peak and a bimodal S2 curve with an anomalously low Tmax (304°C) (Figure 15). Similar pyrograms are observed in other Beaufort-Mackenzie wells that are known to contain migrated oil (*e.g.* Issler *et al*., 2012a). The S1 curve has not returned to baseline and volatile hydrocarbons are contributing to the first peak on the S2 curve. The deeper Aklak sample (X11368) shows a less disturbed pyrogram with a large S1 peak and a left shoulder on the S2 curve. The two samples from the thermally mature Arctic Red Formation (X11369 and X11370) have normal pyrograms with a large S1curve and unimodal S2 curves with small left shoulders.

Contamination from plastic containers

Up to this point, cuttings sample contamination has been discussed in terms of drilling mud additives or geological contamination by oil staining. In this section, evidence is presented for sample contamination resulting from sample processing and storage.

Figure 16 shows the GC traces of the solvent extracts for the Reindeer D-27 cuttings samples. The two peaks labelled with * are likely impurities from the solvent used for soxhlet extraction, and they have been identified as cyclohexane and 3-methylhexane by their GC retention time. Other than these two peaks, the peak labelled with # and eluting around 53 minutes is the major component of the GC-amenable fraction of the solvent extracts. The mass spectrum of this compound obtained from full scan GC-MS analysis of the total hydrocarbon fraction indicates it to be the plasticizer, dibutylphthalate (Figure 17). As phthalate esters are used extensively in the manufacturing of a wide range of plastics and can be readily leached from plastic material by contact with solvents, plasticizers are a very common type of contaminant in geological samples, especially cuttings. The Reindeer D-27 cuttings samples are small in quantity (*i.e.* 1.5 to 3.8 g) and have been in constant contact with plastic materials (*e.g.* sample containers). This has inevitably resulted in their uptake of plastic material that may be partly responsible for the irregular Rock-Eval pyrograms (*e.g.* left shoulder on S2 peaks or broader S2 peaks) observed for some samples. The amount of plastic material contamination in the powdered cuttings samples is likely to be very significant considering the dominance of plasticizer on the GC traces.

Hydrocarbon composition by GC analysis

Due to the limited amount of sample (1.5 to 3.8 g) available for solvent extraction, the GC traces of the total extracts are overwhelmed by contaminants (*e.g.* plasticizer and solvent impurities), and display poor distributions of petroleum hydrocarbons. The three samples (X11368 to X11370) from the deeper sections (2761.49 m, 3550.92 m and 3706.37 m) of the Reindeer D-27 well show hydrocarbon distributions that are similar to a normal crude oil and mature source rock, with normal alkanes being the dominant components over other aliphatic and aromatic hydrocarbons (Figure 16). Normal alkanes are barely recognizable for the cuttings samples from the top section of the well. Despite this, a calculation of pristine-to-phytane (Pr/Ph) ratio has been attempted and results are presented in Table 5. The Pr/Ph ratio for all the samples is in the range of 1.0 to 2.3, suggesting a shaly source for the similar range of hydrocarbons in the samples.

Hydrocarbon composition by GC-MS analysis

Hydrocarbon components other than n-alkanes are very abundant in the top three samples (X11364 to X11366) from the Taglu Sequence that are either coal or a mix of coal and shale (Figure 16). Full scan GC-MS analysis of coal sample X11365 from 1133.86 m depth indicates that its major hydrocarbon components are the bicyclic and tricyclic diterpenoid compounds including isopimarane, 19-norisopimarane, cadalene, retene and simonellite (Figures 17 and 18). These diterpenoids are typical higher plant biomarkers derived from gymnosperms (conifers), some of which have been reported from crude oils and Tertiary Taglu source rocks from the Beaufort-Mackenzie basin (Peters *et al*., 2005; Snowdon *et al*., 2004).

To further investigate the hydrocarbon composition of the cuttings samples, GC-MS analysis in selected ion monitoring (SIM) mode was performed on the total hydrocarbon fractions obtained by C18-SPE column separation of solvent extracts from the cuttings samples. The m/z 85 mass chromatograms showing the distribution of acyclic alkanes for the cuttings samples are displayed in Figure 19. It is obvious that normal alkanes (n-alkanes) are the dominant components. The coal or coal containing cuttings samples from the Taglu Sequence (X11364 to X11366) have a bimodal distribution with the front one being at nC_{15} and the rear one around nC_{23} to nC_{25}. In addition, all the Taglu samples display an apparent odd-to-even predominance (OEP) in the nC_{23} to nC_{35} range of n-alkanes. This is in agreement with their organic immaturity as indicated by their Rock-Eval Tmax values and vitrinite reflectance data (Tables 1 and 3). As with the diterpenoid compounds discussed above, the relatively higher abundance of C_{23} to C_{33} high molecular weight (MW) n-alkanes is also the result of abundant higher plant input to these Tertiary coal or coal containing samples.

The carbon number preference or OEP in the distribution of n-alkanes does not exist in the deeper samples from Aklak Sequence (X11367 and X11368 from 1722.12m and 2761.49m) and Arctic Red Formation (X11369 and X11370 from 3550.92m and 3706.37m) (Figure 19). This is primarily due to their increased maturity and partially due to decreased higher plant input to the sediments in the deeper sections, especially the Arctic Red Formation. The unimodal and non-OEP n-alkane composition in the Arctic Red samples shows that source rocks in this interval have entered the oil window which is consistent with the Rock-Eval Tmax and vitrinite reflectance results (Tables 1 and 3).

Sample X11367 from 1722.12m of Aklak Sequence has a unimodal distribution of n-alkanes around C_{22} which is different from the other samples. Rock-Eval analysis produced a bimodal S2 peak (Figure 15) and an abnormally low Tmax value (304°C) for this sample, suggesting possible heavy hydrocarbon impregnation. However this is not clear from its hydrocarbon composition (Figure 19). Lighter hydrocarbons are missing at the front end of the distribution (possibly due to evaporative loss?). According to the Reindeer D-27 well history report, oil has been observed in Aklak core (1631.4-1636.8 m and 1857.4-1861.9 m) and cuttings samples (1636.8-1642.9 m, 1661.2-1664.2 m and 1743.5-1746.5 m) at depths above and below sample X11367 and some of these intervals coincide with high Rock-Eval PI values (Table 3 and Figure 9). Unfortunately, sterane and hopane biomarkers cannot be detected from GC-MS analysis of the total hydrocarbon fractions in the cuttings samples (except the coal or coaly samples) due to their low concentrations and the small amount of extracts available. In samples X11364 and X11365, the major biomarker compound is C_{31} (R) hopane (Figure 17), consistent with the immaturity of these samples.

Oil migration/impregnation in the Taglu Sequence?

The Taglu samples have a bimodal distribution of n-alkanes around C_{15} and C_{23}-C_{25} at the present condition (Figure 19). Considering the evaporative loss of volatile components during drilling, transportation, storage and lab preparation, the Taglu Sequence seems to have a high abundance of the hydrocarbon fraction below C_{20} that has a composition (*e.g.* Pr/Ph, Pr/nC_{17} and Ph/nC_{18}) which is not compatible with the abundant higher plant input during deposition and the low maturation level experienced by the host (coaly source) rock. For immature coal and coaly samples, they mostly show a higher abundance of pristine and phytane over nC_{17} and nC_{18} alkanes respectively, and higher Pr/Ph than the 1.0 to 2.3 range shown by these Taglu samples. As diesel has not been used during drilling of the well, and the alkane distribution pattern in the C_{15} to C_{20} range for the Taglu cuttings samples does not display any feature of diesel, this suggests that the low MW hydrocarbons in the Taglu sequence are unlikely generated *in situ* but rather have likely been sourced from deeper formations/sequences in the oil generation window. This is consistent with numerous observations of oil staining in Taglu samples (Tables 1 and 3).

The distribution of alkyl naphthalenes, types of 2-ring aromatic hydrocarbons that are commonly present in crude oils and source rocks, lends another line of evidence to the above proposed impregnation of Taglu Sequence by crude oil generated in the deeper mature source rocks. The coaly cuttings samples from the Taglu Sequence have a distribution pattern of methyl-, dimethyl- and trimethyl-naphthalenes similar to that from the deeper Arctic Red Formation samples; the Aklak Sequence sample (X11368) shows an even closer match with the Arctic Red samples (Figure 20). The high abundance of 1,2,5-trimethylnaphthalene relative to other trimethyl naphthalenes (m/z 170) in coal sample X11365 compared with the coaly shales above and below also suggests that a large proportion of $<C_{20}$ hydrocarbons are sourced externally, probably from deeper and more mature source rocks. Due to the poor quality of the cuttings samples, the

proposed impregnation of the Taglu Sequence by migrated oil at the Reindeer D-27 well location needs to be verified by further investigation utilizing higher quality (preferably core) samples.

Organic Geochemistry of Core Samples from Reindeer D-27 and Tununuk K-10 Wells

To better characterize the thermal maturation, hydrocarbon generation potential, source input and depositional environment of the Tertiary and Cretaceous sections intersected at the Reindeer D-27 and Tununuk K-10 wells, an additional twelve core samples (Table 6) have been collected from shale or coal intervals in these two wells for Rock-Eval and organic geochemical analysis. New core samples were required because most of the original core samples were consumed during the initial phase of analysis. As discussed above, higher quality core samples avoid some of the drilling contamination and caving problems that can be associated with cuttings samples. The resultant better quality analytical data allows for an improved source rock evaluation.

Rock-Eval results for additional core samples

The additional core samples have been analyzed on Rock-Eval 6 instruments under the same conditions as the cuttings samples. The results are summarized in Table 6 and Rock-Eval pyrograms for each of the twelve core samples are shown in Figure 21. Except sample X11570 from the Taglu coal interval of Reindeer D-27, samples from the shale intervals cored at both wells generally display a TOC content less than 2.5% and HI values below 200, indicating poor hydrocarbon generating potential at the present. This is especially true for the Tertiary successions, considering they are immature to marginally mature. The pyrograms are typical for the Type III organic matter of the coal and shale successions of the Taglu and Aklak sequences, and the more marine sediments of the Arctic Red Formation. The more asymmetric shape of the S2 curves for the two deepest Arctic Red samples (X11512 and X11513) is most likely related to their high maturity (Figure 21). Compared with cuttings samples from similar depths, the core samples have slightly lower S1 values (Figure 22), probably due to contamination of cuttings by drilling mud additives. Nevertheless the TOC and S2 values for both cores and cuttings are in similar ranges (Figure 23 and 24).

It has been discussed above that the Tmax-converted %Ro-equivalent values from cuttings samples are generally lower than the petrographically measured percent vitrinite reflectance, especially for the contaminated samples. The Rock-Eval maturity parameter, Tmax, generated on the core samples has been plotted against depth for both wells in Figure 25, together with data obtained on cuttings samples. It appears that the core samples generally have a higher Rock-Eval Tmax than the corresponding cuttings samples, suggesting that Tmax values from core samples may provide a better estimate of thermal maturity than the cuttings. Figure 26 shows a strong positive correlation between the Rock-Eval Tmax from the core samples (Table 6) and the measured %Ro at similar depths in both wells (Tables 1 and 2).

Thermal maturation and petroleum generation

Figures 27 and 28 present the mass chromatograms m/z 217 for the distributions of steranes and m/z 191 for the distributions of terpanes for selected core samples from the Reindeer D-27 and Tununuk K-10 wells, respectively. It is clear that the abundances of thermally more stable isomers of steranes and terpanes relative to their less stable counterparts increase with increasing depth for both wells. For example, the thermally less stable 20R chiral isomers of C_{27} to C_{29} steranes and 22R chiral isomers of C_{31} to C_{35} homohopanes predominate over their thermally more stable 20S and 22S counterparts, respectively, in the top Aklak samples, whereas the S chiral isomers become relatively more abundant in the deeper samples regardless of their age. As a result, the 20S/(20S+20R) ratio of C_{29} $\alpha\alpha\alpha$ steranes and 22S/(22S+22R) ratio of C_{32} hopanes increase with burial in the top sections of both wells (Table 7). In addition, the thermally more stable diasteranes become more dominant on the m/z 217 mass chromatograms in the deeper samples than the shallower ones for both wells (Figures 27 and 28). The m/z 217 mass chromatograms of samples from the bottom sections of both wells are dominated by diasteranes, with the less stable regular steranes being minor, suggesting that organic matter in the bottom Arctic Red samples of both wells has experienced severe thermal cracking. The high maturation level is also evident from the dominance C_{19} to C_{21} short chain tricyclic terpanes over other tricyclic terpanes and hopanes on the m/z 191 mass chromatograms of samples deeper than 3600m at Reindeer D-27 and 3350m at Tununuk K-10.

Previous studies show that significant hydrocarbon generation starts when the 22R to 22S isomerisation of C_{31} and C_{32} hopanes just reach equilibria (approximately 0.57-0.62) and when the 20S/(20S+20R) of C_{29} $\alpha\alpha\alpha$ steranes is around 0.25 (Peters *et al*., 2005). Peak oil generation occurs approximately when the 20R to 20S isomerisation of C_{29} steranes reaches equilibrium with the 20S/(20S+20R) value being around 0.55. Based on these two isomerisation ratios, rocks at a current depth of 3150 m (0.69 %Ro; Table 1) near the base of the Aklak Sequence reached the top of the oil generation window whereas rocks at 3600 m (0.77 %Ro; Figure 4 and Table 1) in the Arctic Red Formation attained peak oil generation conditions in the Reindeer D-27 well (Table 7). These results and the results of thermal modelling constrained using %Ro data (Figure 5) suggest that source rocks at Reindeer D-27 entered the oil generation window at a paleodepth of approximately 5000 m (approximately 135°C) and reached peak oil generation at a paleodepth of 5400-5500 m (approximately 145-150°C). For Tununuk K-10 well, the analyzed Aklak core sample from 898.53 m is obviously immature; however, source rocks at this location seem to have already reached peak oil generation in the 2535 to 3708m Smoking Hills/Boundary Creek and Arctic Red sections where core samples were collected for this study (Table 7). Thermal modelling results (Figure 8) suggest that source rocks in the Tununuk K-10 well reached the oil generation window at a paleodepth of approximately 4400 m (135°C) and peak petroleum generation at approximately 4600 m (140-145°C). The hydrocarbon generation history derived from the biomarker maturity parameters seems to be in agreement with the maturation history based on Rock-Eval Tmax and measured vitrinite reflectance.

Either based on biomarkers, Rock-Eval Tmax or measured vitrinite reflectance, the thermal maturation level of source rocks at Tununuk K-10 is indicated to be higher than that of the source rocks of corresponding depth/age at Reindeer D-27 well. This likely suggests a higher paleothermal gradient at Tununuk K-10 than Reindeer D-27 which is supported by thermal modelling (Figures 5 and 8) and consistent with present thermal conditions (Hu *et al*., 2014).

Source rock depositional environment and organic input

Cadalene, retene, simoneillite and tetramethyl tetralins are types of aromatic compounds mainly formed from resinite diterpenoid structures in gymnosperm (*i.e.* conifers) higher plants during diagenesis (van Aarssen *et al*., 2000; Peters *et al*., 2005). These compounds are among the major aromatic components in some of the Tertiary Taglu and Aklak shales and coals, but are barely detectable in the Cretaceous Smoking Hills/Boundary Creek and Artic Red shale core samples (Figure 29). The relative abundances of these compounds (compared with phenanthrene and naphthalenes) are much lower in the Cretaceous samples than in the Tertiary samples (Table 7). In addition, some of the Tertiary shale and coal samples also contain tricyclic diterpanes including isopimaranes, abietanes, and phyllocladanes. This is likely a result of the deltaic depositional environment for the Tertiary sediments where a significant portion of the organic input is from the terrestrial vegetation containing resinite precursors (Snowdon, 1980; Snowdon and Powell, 1982). On the other hand, the low abundance of the diterpenoid-related biomarkers in the Cretaceous shales seems to suggest that terrestrial input was insignificant during their deposition in an inferred marine depositional environment.

The Tertiary coal and shale samples also have a much higher relative abundance of perylene compared with the Cretaceous Smoking Hills/Boundary Creek and Arctic Red shale samples. Perylene is a major peak on the total ion chromatograms (TICs) of aromatic fractions and dominates over benzo(e)pyrene, a polycyclic aromatic hydrocarbon (PAH) of same molecular weight as perylene but with a pyrogenic origin (Figure 29). Its concentration relative to other PAHs such phenanthrene, benzofluoranthenes and benzopyrenes are orders of magnitude higher in the Tertiary deltaic sediments than in the Cretaceous shale samples (Table 7). Despite being a PAH as well, perylene has been proposed to be of diagenetic origin, and is likely related to terrestrial input in a reducing environment including wood-degrading fungi, insects and plant pigments in which precursor structures of perylene have been detected (Aizenshtat, 1973; Silliman *et al*., 2000; Jiang *et al*., 2000; Grice *et al*., 2009). Thus the abundant occurrence of perylene in the Taglu and Aklak core samples is a reflection of their deltaic depositional environments where organic inputs are dominated by higher plants bodies and the associated fungi, bacteria and insects that degrade them. As with the scarcity of diterpenoid compounds, the low concentration of perylene in the Cretaceous shale extracts also indicates a limited terrestrial influence on their deposition.

DISCUSSION

Anomalous Rock-Eval pyrograms (*e.g.* multi-modal S2 curves, asymmetric S2 curves with shoulders, etc.) and anomalous values for Rock-Eval parameters such as Tmax and PI (Tables 3 and 4 and Figures 9 and 12) are common and observed for both cuttings and core samples from the Reindeer D-27 and Tununuk K-10 wells. However, the factors causing these anomalies (drilling or storage-related contamination of samples or geological factors) may be different for the two sample types. In general, core samples from both wells have lower S1 (Figure 22) and higher Tmax (Figure 25) values than cuttings samples whereas TOC (Figure 23) and S2 (Figure 24) values are similar for both types of sample. Furthermore, some of the core Tmax-derived organic maturity values are in close agreement with measured %Ro values for inferred indigenous vitrinite macerals whereas many of the cuttings Tmax-based estimates are systematically too low, particularly for the Reindeer D-27 well (Figures 11, 14 and 26). This strongly suggests that cuttings samples are affected by drilling-related contamination through the addition of organic-based mud additives (recorded in the well history mud reports) that preferentially increase S1 (and derived PI) values and decrease Tmax values. This preferential suppression of cuttings Tmax values suggests that drilling contamination has had a larger effect on Reindeer D-27 Rock-Eval parameters than inferred from a simple analysis of the shape of pyrograms (Figure 11). GC and GC-MS analysis of extracts from seven Reindeer D-27 cuttings samples shows that the powdered samples are contaminated by the plasticizer, dibutylphthalate (Figures 16 and 17), derived from the plastic sample vials and this can affect Rock-Eval parameters in the same way as organic mud additives, depending on the size of the samples.

Geological factors such as the presence of oil and bitumen (observed petrographically and noted in well history sample descriptions; Tables 1, 3 and 4) have a similar effect on Rock-Eval parameters as organic mud additives (increased S1, reduced Tmax, distorted pyrograms, etc.) and affect both core and cuttings samples. Recycled organic matter is common in the Iperk, Richards and Taglu sequences of the Reindeer D-27 well (Table 1), and in the Iperk and Aklak sequences, and lower part of the Arctic Red Formation in the Tununuk K-10 well (Table 2), and is associated with anomalously high Tmax values in core and cuttings samples (Figures 11 and 14). Coal-rich samples are abundant in the Taglu Sequence of the Reindeer D-27 well and they have broad, unimodal S2 peaks (Figure 15) and are associated with high TOC (typically 5-50 wt %) and reduced Tmax (generally < 420°C) values (Table 3; Figure 9). In general, Tmax decreases with increasing TOC for the coal samples.

Between 60-90 % of sample pyrograms for the Tununuk K-10 well are anomalous (excluding samples from the Smoking Hills/Boundary Creek succession where >70 % of pyrograms show minimal disturbance) (Table 4). Although oil staining and bitumen were observed in some samples, a significant number of organic mud additives were used for the Tununuk K-10 well, suggesting that drilling contamination may be the main factor affecting Rock-Eval parameters along with organic matter recycling. In general, samples from the Reindeer D-27 well contain more indigenous organic matter and have fewer anomalous pyrograms. The number of anomalous pyrograms appears to decrease with depth: Iperk and Richards sequences (80-90 %), Taglu Sequence (38 %), Aklak Sequence (29 %) and Arctic Red Formation (1 %) (Table 3). Oil staining, exudatinite, hydrocarbon fluid inclusions and bitumen are observed in samples from the Taglu, Aklak and Arctic Red successions and these could distort sample pyrograms and contribute to higher PI values and reduced Tmax values (in addition to mud additives and coal). The distribution of low molecular weight n-alkanes (Figure 19) and alkyl naphthalenes (Figure 20) in extracts of Taglu cuttings samples from the Reindeer D-27 well suggest that petroleum has migrated from the Arctic Red Formation into the overlying Taglu (and probably Aklak) Sequence.

In spite of significant sample contamination, integrated analysis of multi-parameter petrological, geochemical and anhydrous pyrolysis data has yielded reliable and consistent new data on the thermal maturity and nature of organic matter in the Cenozoic and Cretaceous successions of the Reindeer D-27 and Tununuk K-10 wells. The most reliable estimates of organic maturity for these wells are from vitrinite reflectance measurements (Figures 4 and 7) because indigenous vitrinite macerals were analysed selectively, thus minimizing the perturbing effects of geological (recycling, oil staining) and drilling contamination (caving and mixing of cuttings). The abundance of core samples greatly enhances the quality and reliability of the interpretations by providing key depth control points for interpreting cuttings samples that may contain mixed material from variable depth intervals. Rock-Eval Tmax data provide independent confirmation of organic maturity levels for samples with minimal contamination (especially core samples). There is good agreement between Tmax and %Ro values for core samples from the Aklak and Arctic Red successions in the Reindeer D-27 well (Figure 11), and for core and cuttings samples from the Smoking Hills/Boundary Creek and upper Arctic Red successions in the Tununuk K-10 well (Figure 14). Apatite fission track age and length parameters for core samples from the Reindeer D-27 well show variable partial annealing that is consistent with measured %Ro values for the organically immature Taglu and Aklak sequences (Figure 6). Biomarker ratios (sterane and terpane isomers) (Figures 27 and 28; Table 7) for core extracts provide independent information for the top of the oil generation window and peak oil generation in the deeper, organically mature sections of both wells in accordance with %Ro and Tmax data. In addition, hydrocarbon compositions of extracts show qualitative agreement with the level of maturity based on %Ro and Tmax data. The overall agreement among the multiple paleotemperature indicators gives us a high degree of confidence in the thermal maturity results.

Simple thermal/burial models that use assumed pre-Iperk erosion magnitudes of 2200 m and 2300 m, and time invariant geothermal gradients equal to the present values of 25.2°C/km and 28.6°C/km for the Reindeer D-27 and Tununuk K-10 wells, respectively, provide good fits to the observed organic maturity data using the new basin%Ro kinetic model for vitrinite reflectance (Figures 5 and 8). The older vitrinite reflectance models of Middleton (1982) and Sweeney and Burnham (1990; EASY%Ro) require significantly lower geothermal gradients and larger erosion estimates to fit the Reindeer D-27 data. The higher maturity Tununuk K-10 data cannot be fit using the popular EASY%Ro model no matter how the geothermal gradient and erosion magnitude are adjusted. The simplest explanation is that the calibration between temperature and vitrinite reflectance is incorrect for these older models.

Consistent with previous work, petrographic observations, Rock-Eval data (Figures 9, 10, 12 and 13), and biomarker geochemistry (Figures 17, 18 and 29; Table 7) show that organic matter in the Cenozoic Taglu and Aklak sequences is dominated by higher plant (gymnosperm) input in a deltaic depositional environment with generally poor source rock character. Conversely, the Cretaceous Smoking Hills/Boundary Creek and Arctic Red formations have low amounts of terrestrial organic matter in accordance with deposition under marine conditions that may be more conducive to source rock development. Thermal modelling (constrained using biomarker and %Ro data) suggests that source rocks would have started to generate oil at approximately 135°C at paleodepths of approximately 5000 m and 4400 m, and reached peak oil generation at approximately 145°C at paleodepths of 5400-5500 m and 4600 m, for the Reindeer D-27 and Tununuk K-10 wells, respectively, probably during late Eocene-Oligocene time. Oils generated in the marine Cretaceous rocks probably migrated through the overlying deltaic successions, consistent with petrographic, Rock-Eval and geochemical evidence for migrated oil. Due to extensive erosion and the unknown attributes of the source rocks, the timing of oil generation is uncertain but ongoing apatite fission track thermochronology studies will provide useful limits on the time of maximum temperature. Overall, maturity models suggest that the Reindeer D-27 and Tununuk K-10 successions reached similar maximum burial depths but maximum paleotemperatures were higher at Tununuk K-10 (176ºC) than at Reindeer D-27 (155°C) due to a higher geothermal gradient.

CONCLUSIONS

Vitrinite reflectance, Rock-Eval, and organic geochemical analyses for cuttings and core samples from the Reindeer D-27 and Tununuk K-10 wells contribute new data for regional thermal maturity and petroleum system studies and provide valuable reference data for interpreting new and legacy Rock-Eval data for exploration wells in the Beaufort-Mackenzie Basin. Cuttings and core samples from both wells have anomalous Rock-Eval pyrograms and parameters that can be attributed to sample contamination (organic drilling mud additives and plasticizer from sample vials) and geological factors (organic recycling, oil staining and coal). The most significant factor for both wells is drilling contamination that preferentially affects cuttings samples by increasing their S1 values and reducing their Tmax values relative to core samples. Coal samples, which occur in abundance in the Taglu Sequence of the Reindeer D-27 well, have anomalously low Tmax values whereas organic recycling is common in both wells and associated with anomalously high Tmax values. Oil staining occurs in zones with high Rock-Eval PI values within the Taglu and Aklak sequences of the Reindeer D-27 well and, based on geochemical analyses, this may represent oil that has migrated from mature, marine rocks of the underlying Arctic Red Formation. Integration of vitrinite reflectance, Rock-Eval, biomarker, and apatite fission track data yields consistent and reliable thermal maturity data for the Cretaceous and Cenozoic successions in the two study wells. Thermal modelling suggests that marine Cretaceous rocks in both wells entered the oil generation window at temperatures >135°C during late Eocene-Oligocene time. The new basin%Ro kinetic model for vitrinite reflectance gives good fits to the %Ro data for both wells using time-invariant geothermal gradients equal to the present values. The widely-used EASY%Ro model systematically misfits the data, suggesting a miscalibration between temperature and vitrinite reflectance for this model.

ACKNOWLEDGEMENTS

The first author (DI) did most of the writing, data integration and thermal modelling, and he is responsible for any errors or omissions in the report. CJ planned and coordinated the GC and GC-MS analyses and interpreted the data. JR did the organic petrology and vitrinite reflectance analysis, and MO assisted with the manipulation and plotting of the Rock-Eval data. We thank the National Energy Board of Canada for granting us permission to collect well samples from their core and sample repository at the Geological Survey of Canada in Calgary. Sarah Saad collected, prepared and curated the initial set of well cuttings and core samples and Ross Stewart did the Rock-Eval 6 analysis using the equipment at GSC Calgary. Marina Milovic and Rachel Robinson of the organic geochemistry laboratory at GSC Calgary prepared the sample extracts and performed the GC and GC-MS analyses. This study was funded by Natural Resources Canada through the Earth Sciences Sector Geomapping for Energy and Minerals (GEM) program. We thank Dr. Roger Macqueen for reviewing the manuscript and making numerous suggestions to improve the clarity of the writing and presentation.

REFERENCES

Aizenshtat, Z. 1973. Perylene and its geochemical significance. Geochimica et Cosmochimica Acta, v. 37, p. 559-567.

Barbarand, J., Carter, A., Wood, I. and Hurford, T. 2003. Compositional and structural control of fission-track annealing in apatite. Chemical Geology, v. 198, p. 107-137.

Behar, F., Beaumont, V. and De B. Penteado, H.L. 2001. Rock-Eval 6 Technology: Performances and Developments. Oil & Gas Science and Technology – Revue de l'Institut Français du Pétrole, v. 56, no. 2, p. 111-134.

Carlson, W.D., Donelick, R.A. and Ketcham, R.A. 1999. Variability of apatite fission-track annealing kinetics: I. Experimental results. American Mineralogist, v. 84, p. 1213-1223.

Dixon, J., editor, 1996. Geological Atlas of the Beaufort-Mackenzie Area. Geological Survey of Canada, Miscellaneous Report 59, 173p.

Dixon, J. 2002. Description of some cores from the Beaufort-Mackenzie area, Northwest Territories. Geological Survey of Canada, Open File 4194, 1 CD-ROM, doi:10.4095/213099.

Espitalié, J., Madec, M., Tissot, B., Mennig, J.J. and Leplat, P. 1977. Source rock characterization method for petroleum exploration. Proceedings of the 9th Annual Offshore Technology Conference, v. 3, p. 439-448.

Espitalié, J., Marquis, F. and Barsony, I. 1984. Geochemical Logging. *In*: Analytical Pyrolysis – Techniques and Applications. K.J. Voorhees (ed.). Boston, Butterworth, p. 276-304.

Feinstein, S., Issler, D.R., Snowdon, L.R. and Williams, G. K. 1996. Characterization of major unconformities by paleothermometric and paleobarometric methods: application to the Mackenzie Plain, Northwest Territories, Canada. Bulletin of Canadian Petroleum Geology, v. 44, no. 1, p. 55-71.

Gallagher, K., Brown, R. and Johnson, C. 1998. Fission track analysis and its applications to geological problems. Annual Reviews of Earth and Planetary Science, v. 26, p. 519-572.

Gleadow, A.J.W., Belton, D.X., Kohn, B.P. and Brown, R.W. 2002. Fission track dating of phosphate minerals and the thermochronology of apatite. *In*: Phosphates; Geochemical, Geobiological and Materials Importance. M. J. Kohn, J. Rakovan and J.M. Hughes (eds.). Reviews in Mineralogy and Geochemistry, v. 48, p. 579-630.

Grice, K., Lu, H., Atahan, P., Asif, M., Hallmann, C., Greenwood, P., Maslen, E., Tulipani, S., Williford, K. and Dodson J. 2009. New insights into the origin of perylene in geological samples. Geochimica et Cosmochimica Acta, v. 73, p. 6531-6543.

Hu, K., Issler, D.R. and Jessop, A.M. 2010. Well temperature data compilation, correction and quality assessment for the Beaufort-Mackenzie Basin. Geological Survey of Canada, Open File 6057, 17 p., doi:10.4095/262755.

Hu, K., Chen, Z. and Issler, D.R. 2014. Determination of geothermal gradient from borehole temperature and permafrost base for exploration wells in the Beaufort-Mackenzie Basin. Geological Survey of Canada, Open File 6957, 23 p., doi:10.4095/293872.

Issler, D.R. 1992. A new approach to shale compaction and stratigraphic restoration, Beaufort-Mackenzie Basin and Mackenzie Corridor, northern Canada. American Association of Petroleum Geologists Bulletin, v. 76, no. 8, p. 1170-1189.

Issler, D.R., Grist, A.M. and Stasiuk, L.D. 2005. Post-Early Devonian thermal constraints on hydrocarbon source rock maturation in the Keele Tectonic Zone, Tulita area, NWT,

Canada, from multi-kinetic apatite fission track thermochronology, vitrinite reflectance and shale compaction. Bulletin of Canadian Petroleum Geology, v. 53, no. 4, p. 405-431.
Issler, D.R. and Grist, A.M. 2008. Integrated thermal history analysis of the Beaufort-Mackenzie basin using multi-kinetic apatite fission track thermochronology. Geochimica et Cosmochimica Acta, v. 72, no. 12S, p. A413 (Special Supplement, Awards Ceremony Speeches and Abstracts of the 18th Annual V.M. Goldschmidt Conference, Vancouver, Canada, July 13-18, 2008).
Issler, D.R., Obermajer, M., Reyes, J. and Li, M. 2012a. Integrated analysis of vitrinite reflectance, Rock-Eval 6, gas chromatography, and gas chromatography-mass spectrometry data for the Mallik A-06, Parsons N-10 and Kugaluk N-02 wells, Beaufort-Mackenzie Basin, northern Canada. Geological Survey of Canada, Open File 6978, 78 p. doi:10.4095/289672.
Issler, D.R., Reyes, J., Chen, Z., Hu, K., Negulic, E., Grist, A., Stasiuk, L., and Goodarzi, F. 2012b. Thermal History Analysis of the Beaufort-Mackenzie Basin, Arctic Canada. In: New Understandings of the Petroleum Systems of Continental Margins of the World, Papers presented at the 32nd Annual Gulf Coast Section, Society of Economic Paleontologists and Mineralogists Foundation Bob F. Perkins Research Conference, v. 32, p. 609-641. (DVD)
Jiang, C., Alexander, R., Kagi, R. I. and Murray, A. P. 2000. Origin of perylene in ancient sediments and its geological significance. Organic Geochemistry, v. 31, p. 1545-1559.
Ketcham, R.A., Donelick, R.A. and Carlson, W.D. 1999. Variability of apatite fission-track annealing kinetics: III. Extrapolation to geological time scales. American Mineralogist, v. 84, p. 1235-1255.
Lafargue, E., Marquis, F. and Pillot, D. 1998. Rock-Eval 6 Applications in Hydrocarbon Exploration, Production and Soil Contamination Studies. Oil & Gas Science and Technology – Revue de l'Institut Français du Pétrole, v. 53, no. 4, p. 421-437.
Lane, L.S. and Dietrich, J.R. 1995. Tertiary structural evolution of the Beaufort Sea – Mackenzie Delta region, Arctic Canada. Bulletin of Canadian Petroleum Geology, v. 43, no. 3, p. 293-314.
MATOIL^{TM} 1990. A quantitative model of hydrocarbon generation for the personal computer. Bureau d'Etudes Industrielles et de Coopération de l'Institut Français du Pétrole. Rueil-Malmaison, France.
Middleton, M.F. 1982. Tectonic history from vitrinite reflectance. Geophysical Journal of the Royal Astronomical Society, v. 68, p. 121-132.
Mukhopadhyay, P.K. and Dow, W.G. (editors) 1994. Vitrinite Reflectance as a Maturity Parameter - Applications and Limitations. American Chemical Society Symposium Series 570, Washington, D.C., 294 p.
National Energy Board 1998. Probabilistic estimate of hydrocarbon volumes in the Mackenzie Delta and Beaufort Sea discoveries. National Energy Board Report, Catalogue No. NE23-78/1998E, Calgary, 8 p.
Nielsen, S.B., Clausen, O.R. and McGregor, E. 2015. basin%Ro: A vitrinite reflectance model derived from basin and laboratory data. Basin Research (first published online October 24, 2015) doi:10.1111/bre.12160 (to appear in v. 28 in 2016).
Obermajer, M., Stewart, K. R. and Dewing, K. 2007. Geological and geochemical data from the Canadian Arctic Islands, Part II: Rock-Eval/TOC Data. Geological Survey of Canada, Open File 5459, 27 p., 1 CD-ROM, doi:10.4095/223457.

Peters, K.E. 1986. Guidelines for evaluating petroleum source rock using programmed pyrolysis. American Association of Petroleum Geologists Bulletin, v. 70, no. 3, p. 318-329.

Peters, K. E., Walters, C. C. and Moldowan, J. M. 2005. The Biomarker Guide, v. 2, Biomarkers and Isotopes in Petroleum Systems and Earth History. Second Edition, Cambridge, U.K., Cambridge University Press.

Riediger, C., Carrelli, G.G. and Zonneveld, J.-P. 2004. Hydrocarbon source rock characterization and thermal maturity of the Upper Triassic Baldonnel and Pardonet formations, northeastern British Columbia, Canada. Bulletin of Canadian Petroleum Geology, v. 52, no. 4, p. 277-301.

Robertson Group 1989. A Manual of the Geochemical and Palynological Properties of Selected Mud Additives. Publication by The Roberston Group plc, 209 p.

Silliman, J. E., Meyers, P. A., Ostrom, P. H., Ostrom, N. W. and Eadie, B. J. 2000. Insights into the origin of perylene from isotopic analysis of sediments from Saanich Inlet, British Columbia. Organic Geochemistry, v. 31, p. 1133-1142.

Snowdon, L. R. 1980. Resinite-a potential petroleum source in the Upper Cretaceous/Tertiary of the Beaufort-Mackenzie basin. *In*: Facts and Principles of World Petroleum Occurrence. A.D. Miall (ed.). Canadian Society of Petroleum Geologists, Memoir 6, p. 421-446.

Snowdon, L. R. and Powell, T. G. 1982. Immature oil and condensate: modification of hydrocarbon generation model for Tertiary organic matter. American Association of Petroleum Geologists Bulletin, v. 66, p. 775-788.

Snowdon, L. R., Stasiuk, L. D., Robinson, R., Dixon, J., Dietrich, J. and McNeil D. H. 2004. Organic geochemistry and organic petrology of a potential source rock of early Eocene age in the Beaufort-Mackenzie Basin. Organic Geochemistry, v. 35, p. 1039-1052.

Stasiuk, L.D., Issler, D.R., Tomica, M. and Potter, J. 2005. Re-evaluation of thermal maturation - vitrinite reflectance profiles for Cretaceous and Tertiary strata, Beaufort-Mackenzie basin, Northwest Territories (Adlartok P-09, Amerk O-09, Edlok N–56, Ikhil K-35, Sarpik B-35, Hansen G-07 and Havik B-41). Geological Survey of Canada, Open File 4665, 1 CD-ROM, doi:10.4095/220350.

Stasiuk, L.D., Issler, D.R., Dixon, J. and McNeil, D.H. 2009. Thermal maturity of Cretaceous and Tertiary strata in the Itiginkpak F-29, Napartok M-01, Kurk M-15, Tuk B-02 and Tuk M-18 wells, Beaufort-Mackenzie Basin, Northwest Territories. Geological Survey of Canada, Open File 5639, 35 p., 1 CD-ROM, doi:10.4095/248085.

Sweeney, J.J. and Burnham, A.K. 1990. Evaluation of a simple model of vitrinite reflectance based on chemical kinetics. American Association of Petroleum Geologists Bulletin, v. 74, p. 1559-1570.

Taylor, G.H., Teichmüller, M., Davis, A., Diessel, C.F.K., Littke, R. and Robert, P. 1998. Organic Petrology. Berlin, Gebrüder Borntraeger, 704 p.

Van Aarssen, B. G. K., Alexander R. and Kagi, R. I. 2000. Higher plant biomarkers reflect palaeovegetation changes during Jurassic time. Geochimica et Cosmochimica Acta, v. 64, p. 1417-1424.

Wagner, G.A. and Van den Haute, P. 1992. Fission track dating. Dordrecht, Klewer Academic Publishers, 285 p.

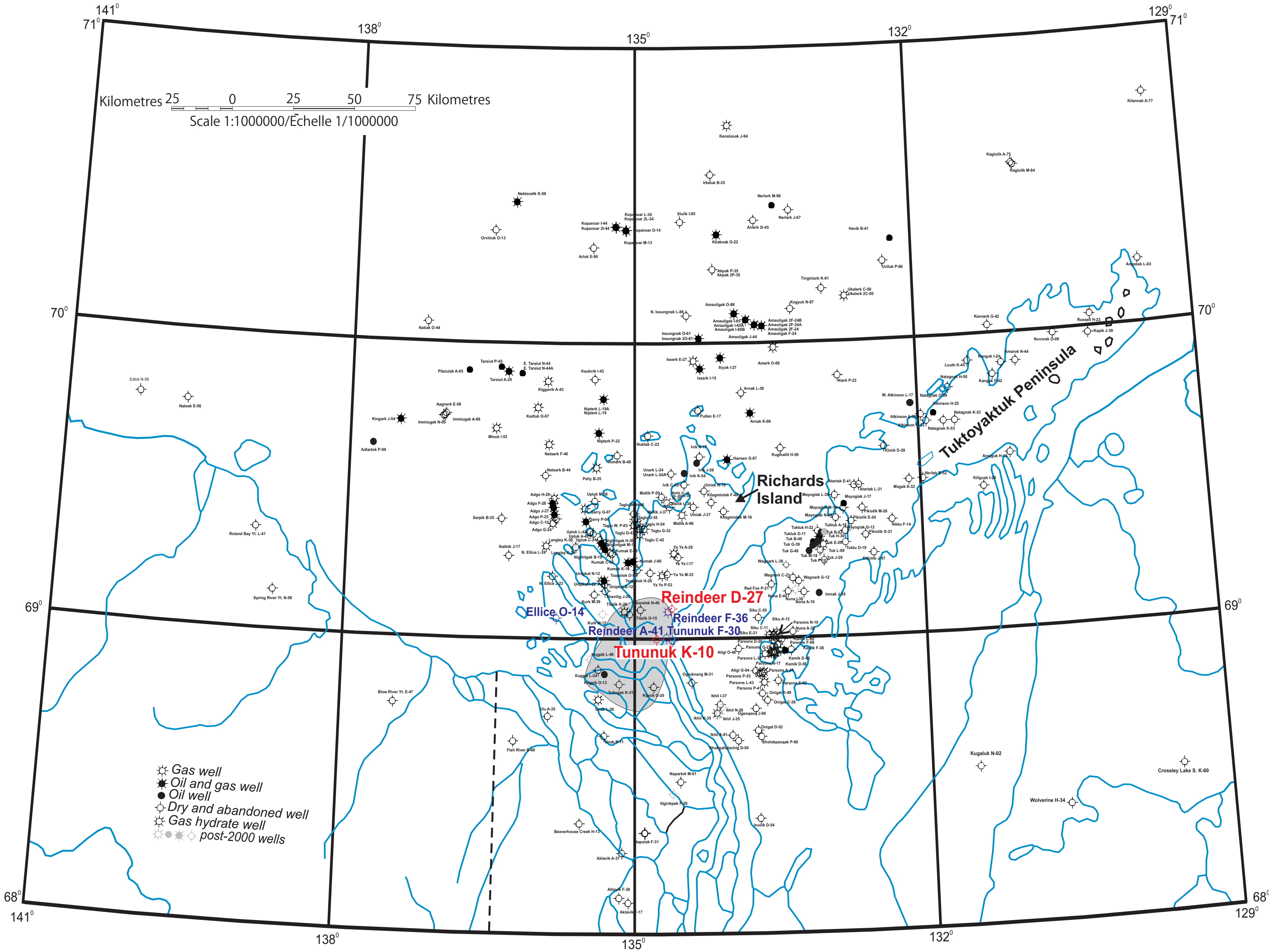

Figure 1. Location map for the two study wells (in red) with vitrinite reflectance, Rock-Eval, GC, and GC-MS data, Beaufort-Mackenzie Basin, NWT. Light grey shaded region outlines the Tununuk High, an area of folded Tertiary strata. Other wells mentioned in the text are shown in blue.

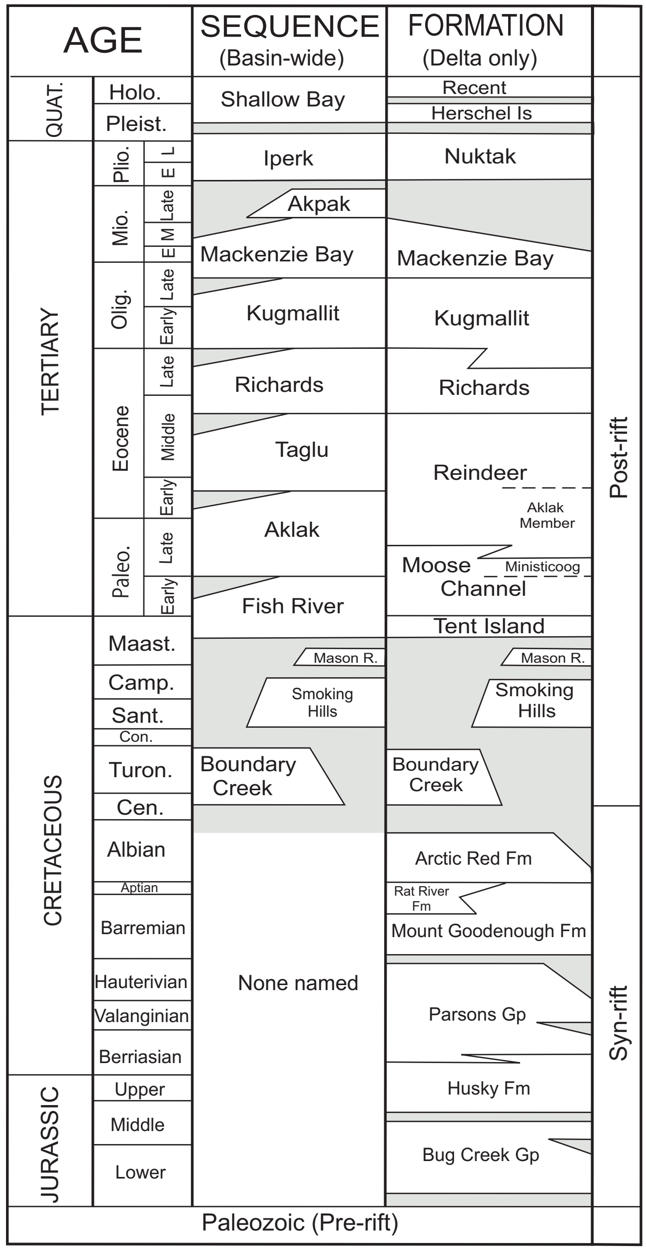

Figure 2. Stratigraphy of the Beaufort-Mackenzie region (modified after J. Dixon, personal communication, 2009).

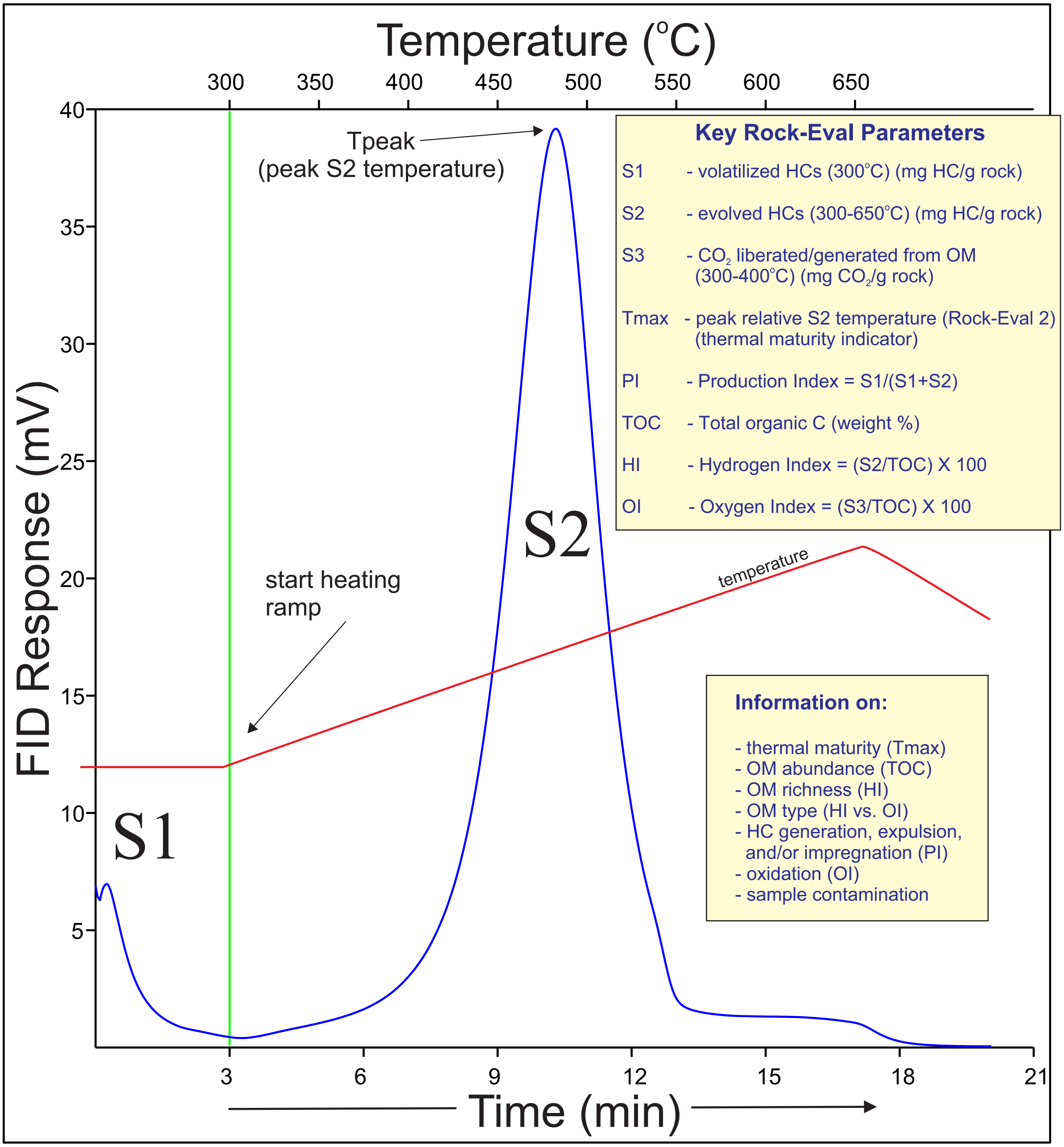

Figure 3. Rock-Eval 6 pyrogram showing the S1 and S2 curves for a sample standard (S3 not shown). Hydrocarbons are measured using a flame ionization detector (FID).

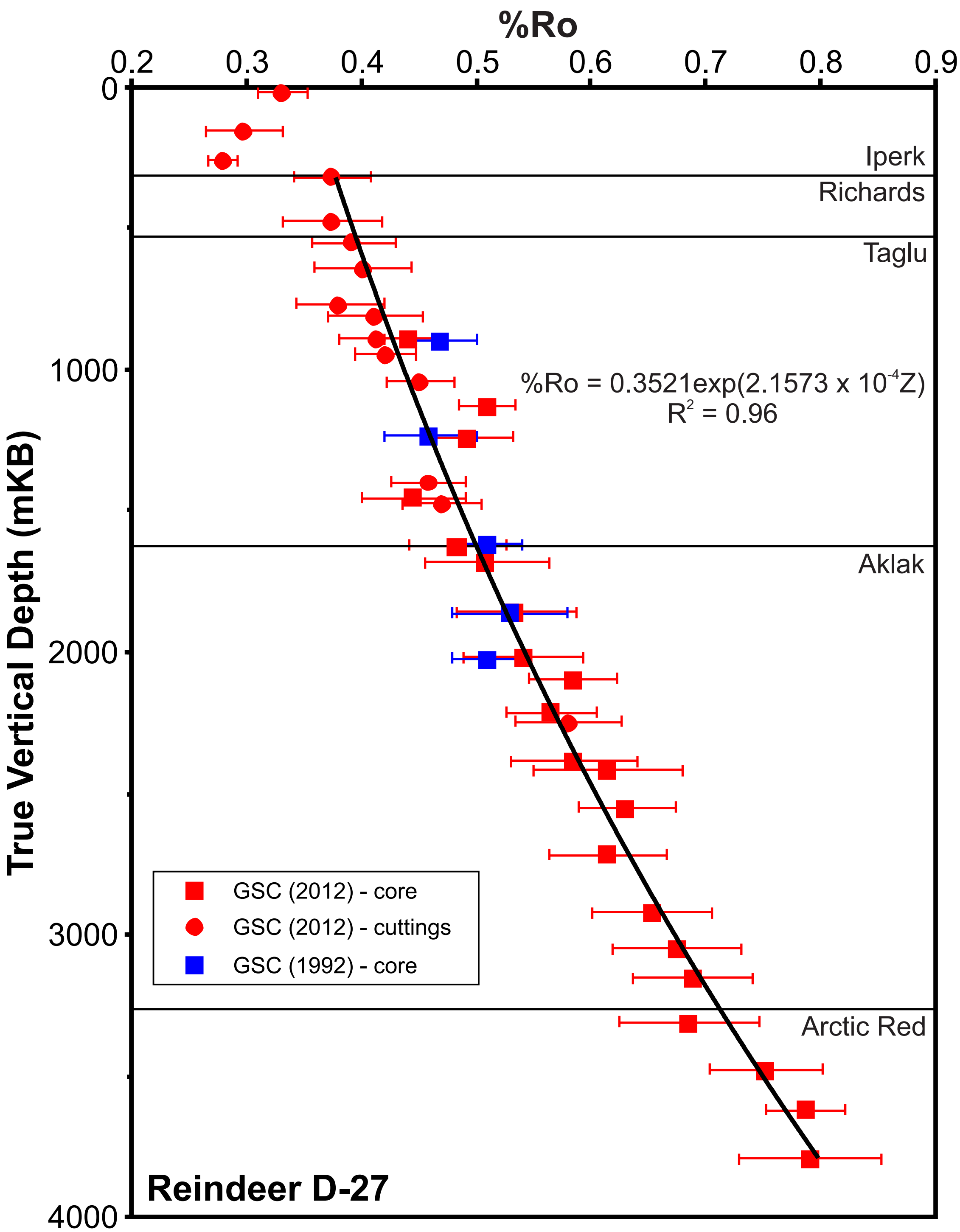

Figure 4. Random percent vitrinite reflectance in oil (%Ro) for samples from the Reindeer D-27 well. Measured depths were corrected to true vertical depth with respect to Kelly Bushing elevation using the borehole deviation survey in the well history report.

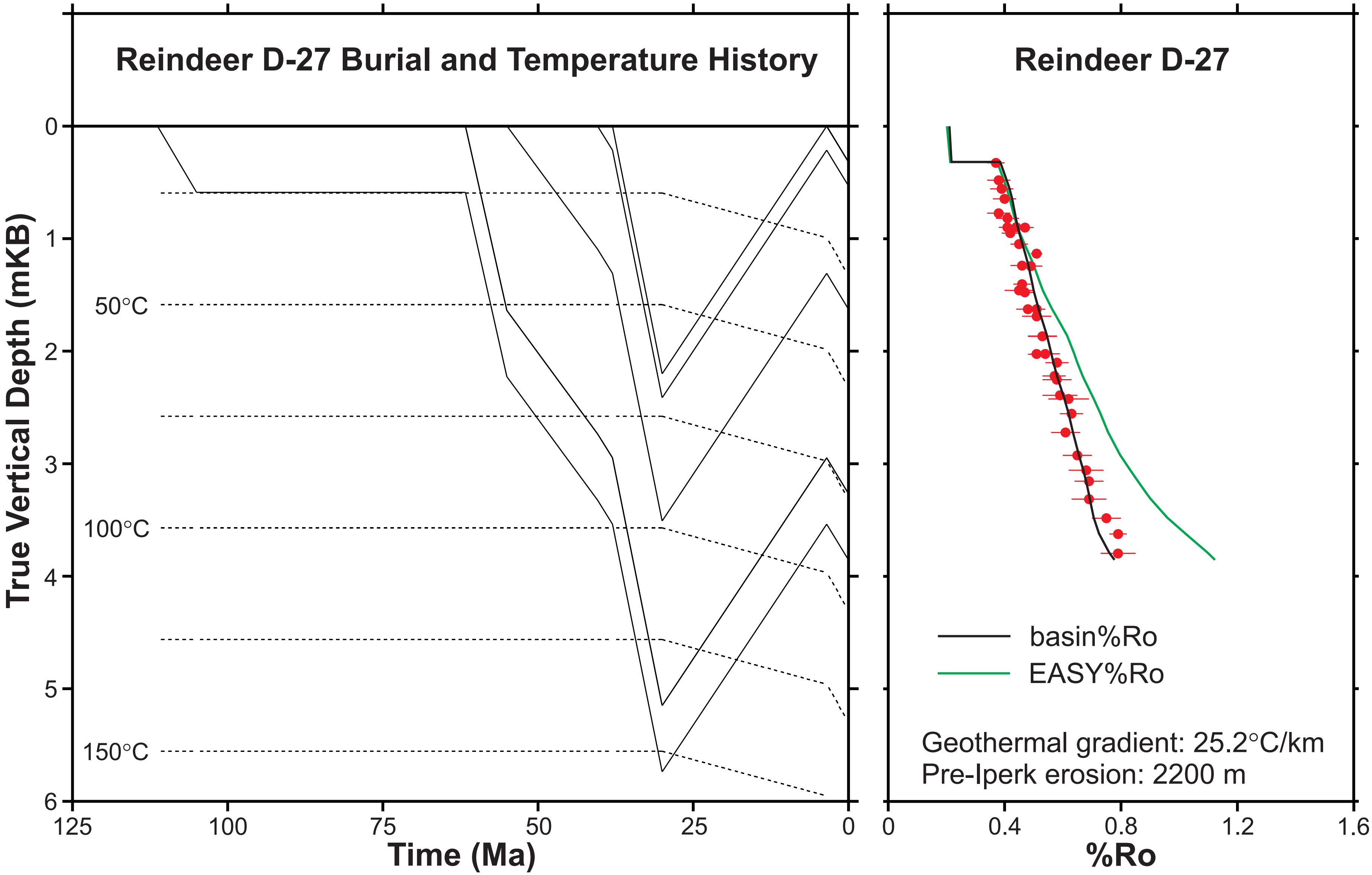

Figure 5. Left panel shows a simple thermal and burial history model for the Reindeer D-27 well assuming a constant geothermal gradient equal to the present value and 2200 m of pre-Iperk Sequence erosion. Right panel shows a comparison of observed and calculated %Ro values (using basin%Ro) derived from the thermal history reconstruction. EASY%Ro misfits the data if the present geothermal gradient is used.

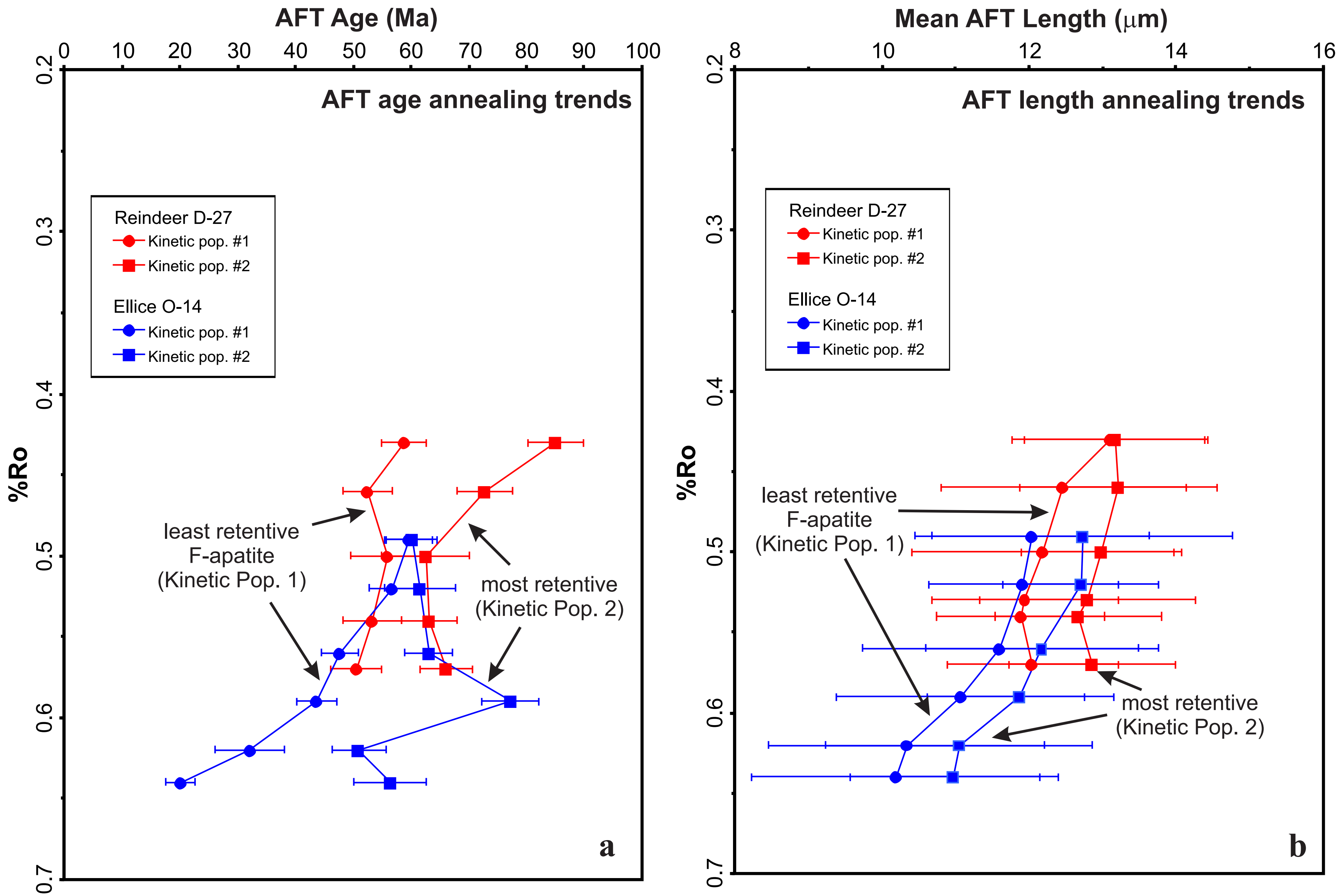

Figure 6. Comparison of apatite fission track (AFT) thermal annealing trends with vitrinite reflectance (%Ro). AFT age (a) and mean AFT length (b) versus %Ro for the Reindeer D-27 and Ellice O-14 wells. Both wells contain samples with two apatite populations with different annealing kinetics. See text for more details.

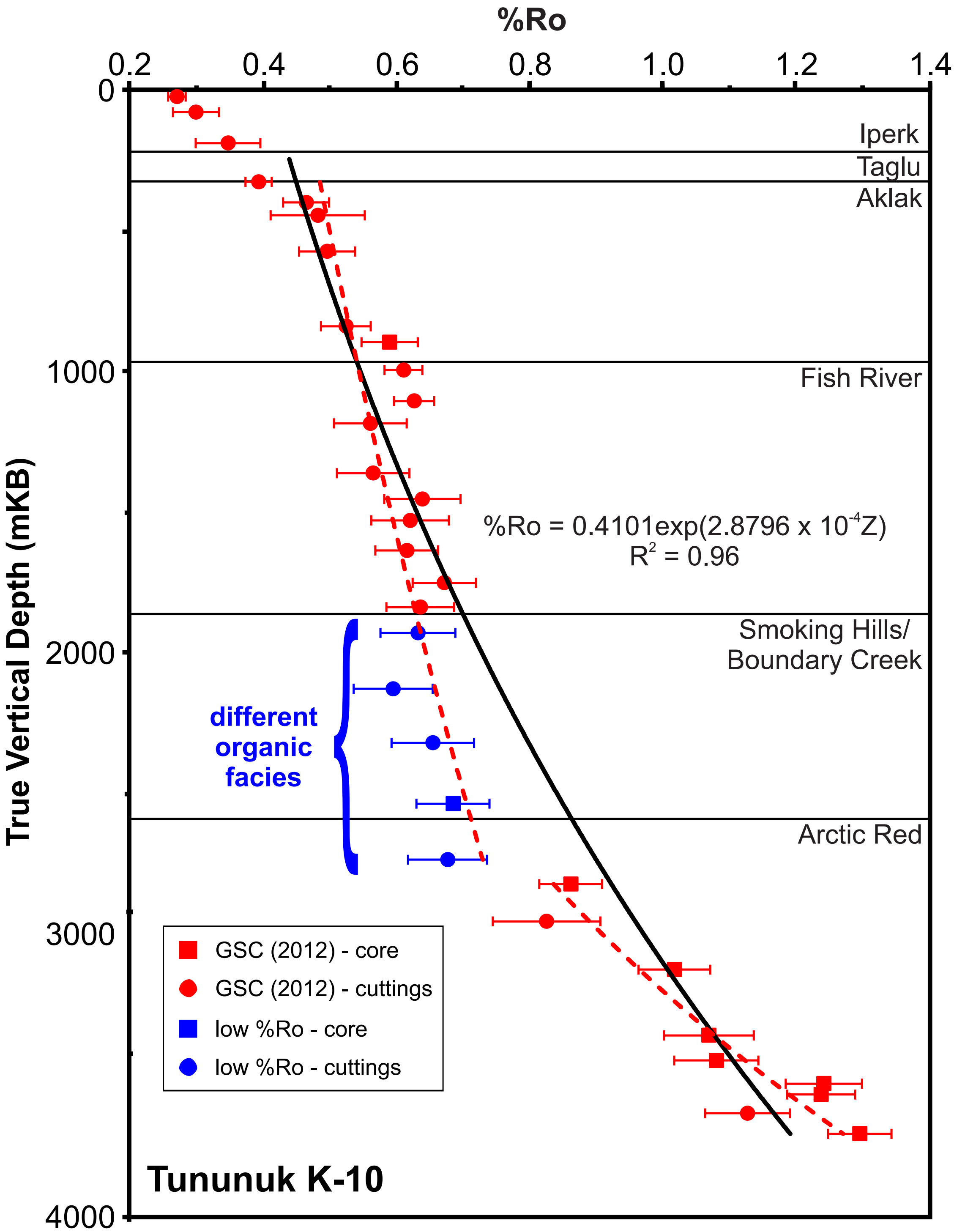

Figure 7. Random percent vitrinite reflectance in oil (%Ro) for samples from the Tununuk K-10 well. Measured depths were corrected to true vertical depth with respect to Kelly Bushing using borehole deviation survey in well history report.

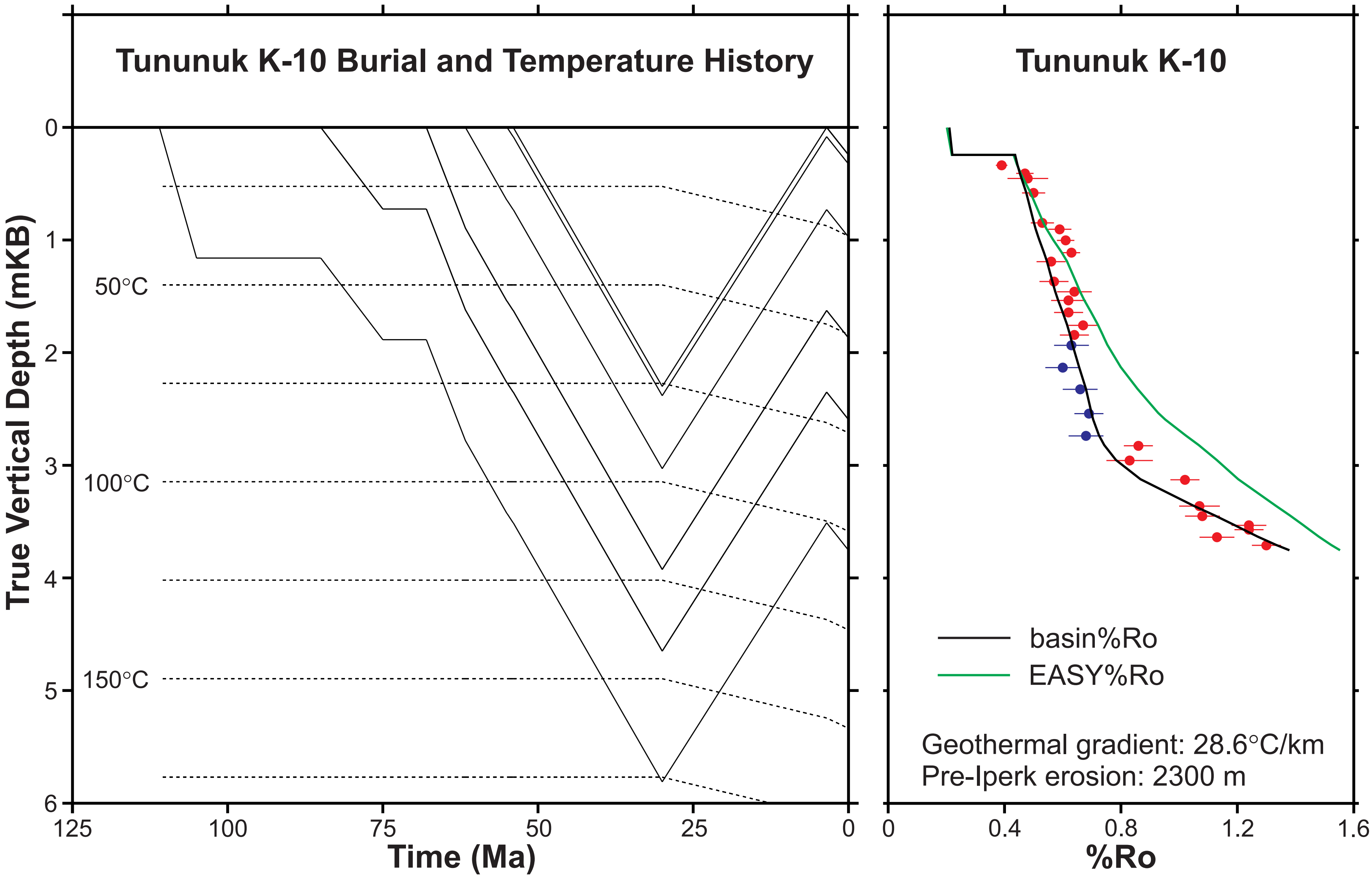

Figure 8. Left panel shows a simple thermal and burial history model for the Tununuk K-10 well assuming a constant geothermal gradient equal to the present value and 2300 m of pre-Iperk Sequence erosion. Right panel shows a comparison of observed and calculated %Ro values (using basin%Ro) derived from the thermal history reconstruction. EASY%Ro misfits the data if the present geothermal gradient is used.

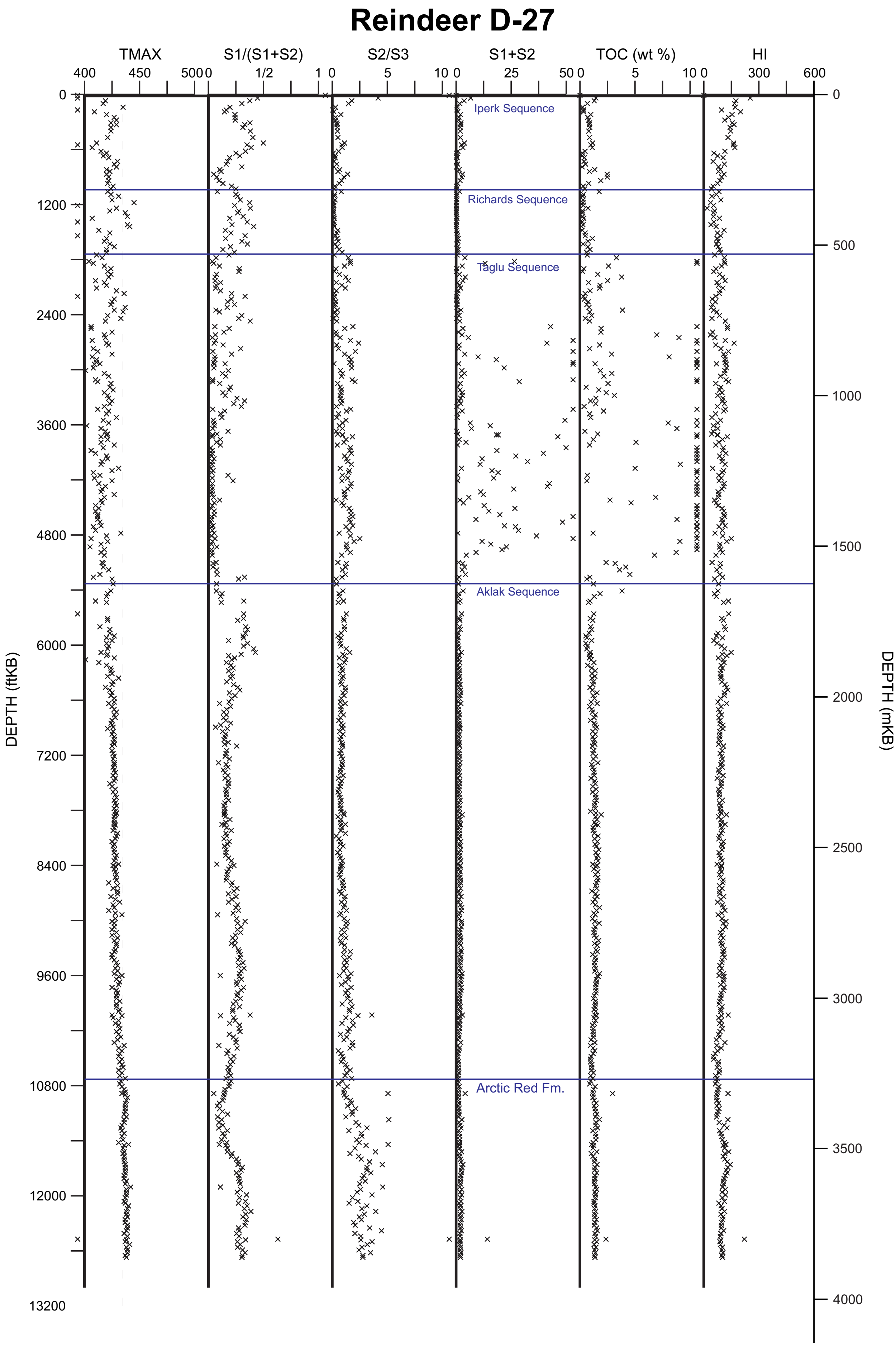

Figure 9. Selected Rock-Eval 6 parameters versus depth (displayed in Rock-Eval 2 format) for the Reindeer D-27 well.

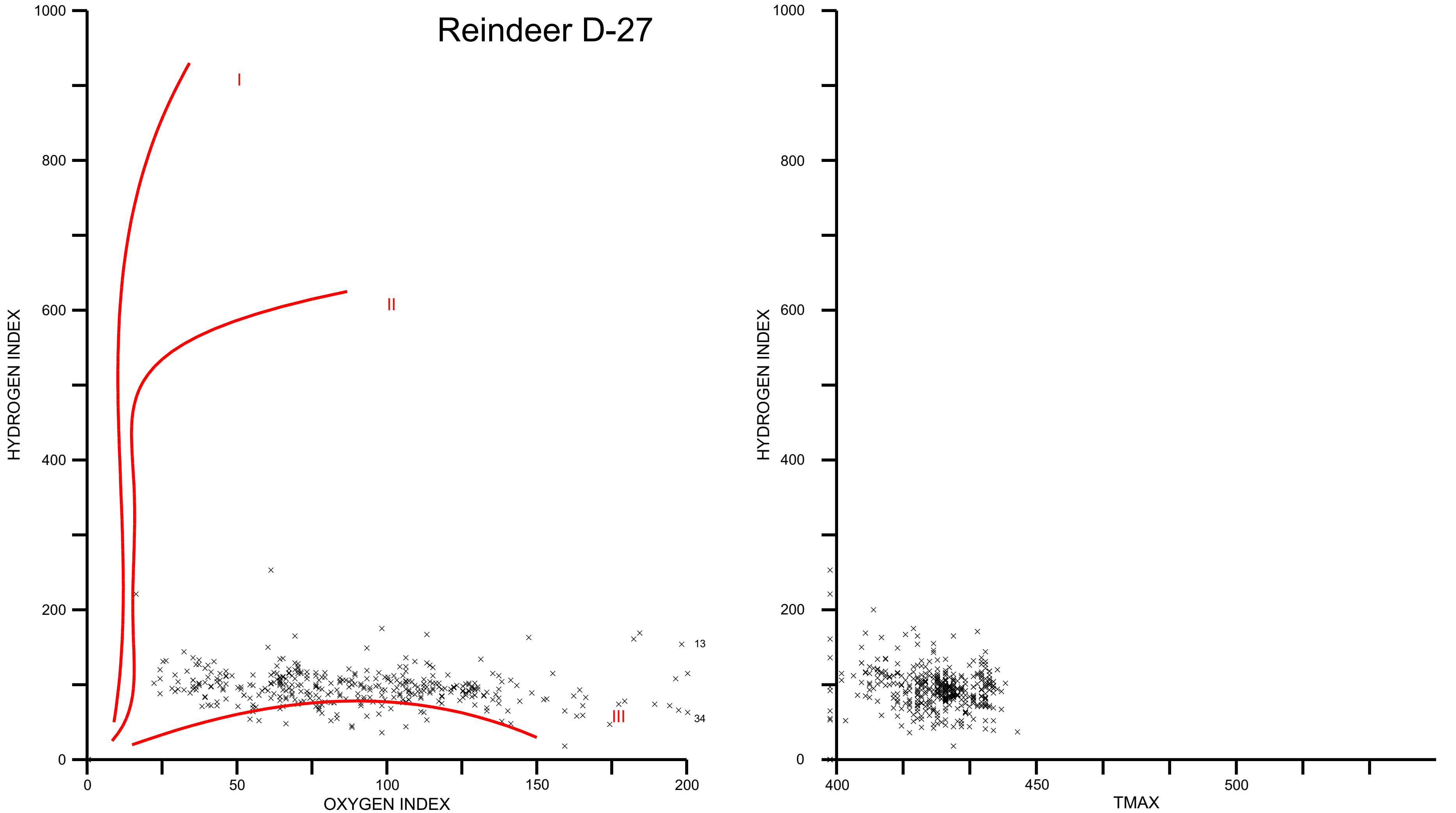

Figure 10. Whole rock HI versus OI (left) and HI versus Tmax (right) for the Reindeer D-27 well. Organic maturation pathways (red curves) are shown for different end member organic matter types - Type I (oil-prone, usually lacustrine), Type II (oil-prone, marine) and Type III (gas-prone, terrestrial).

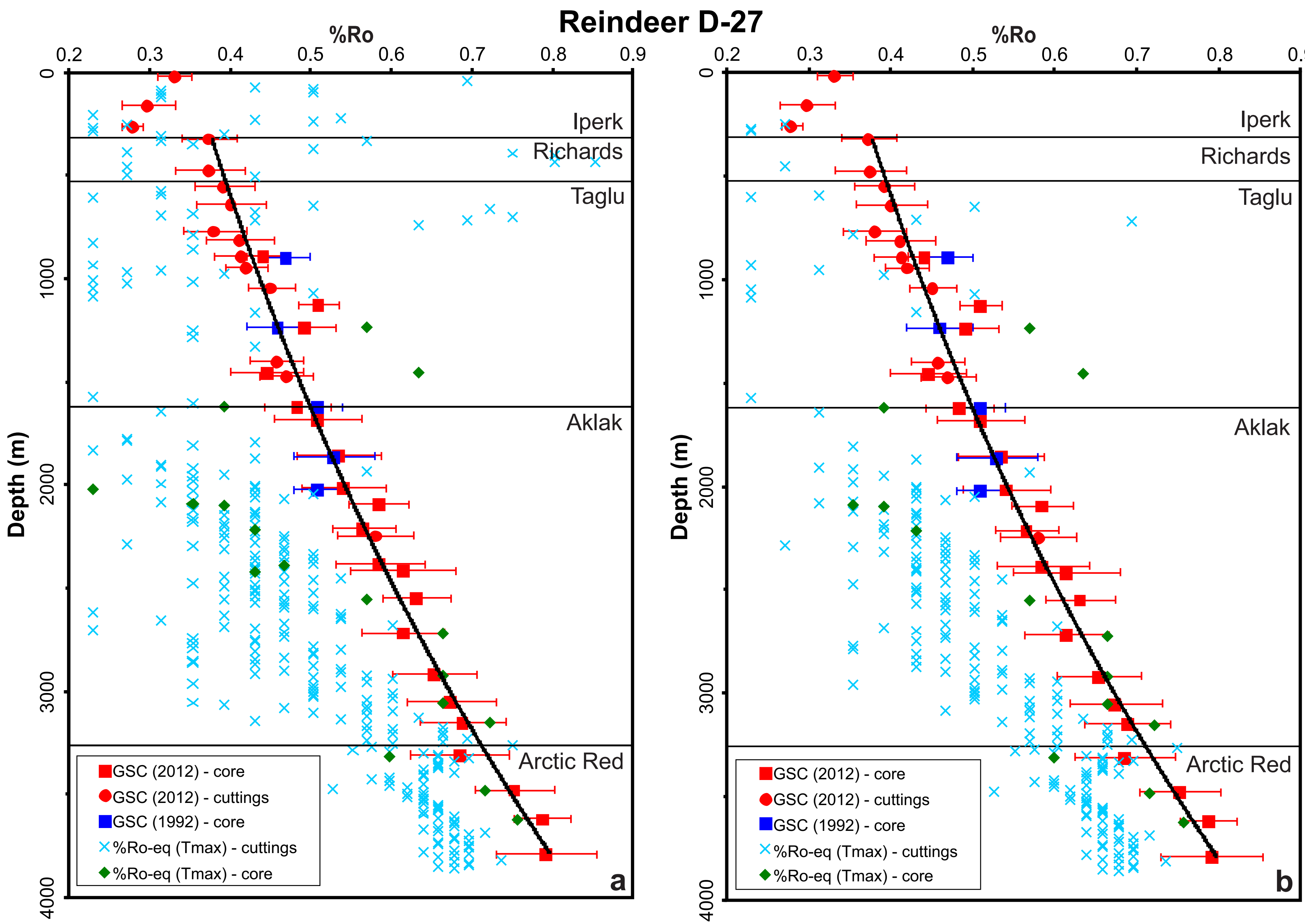

Figure 11. Comparison of measured %Ro with %Ro-equivalent values determined from Tmax for the Reindeer D-27 well. (a) All Tmax data and (b) Tmax values for least disturbed pyrograms.

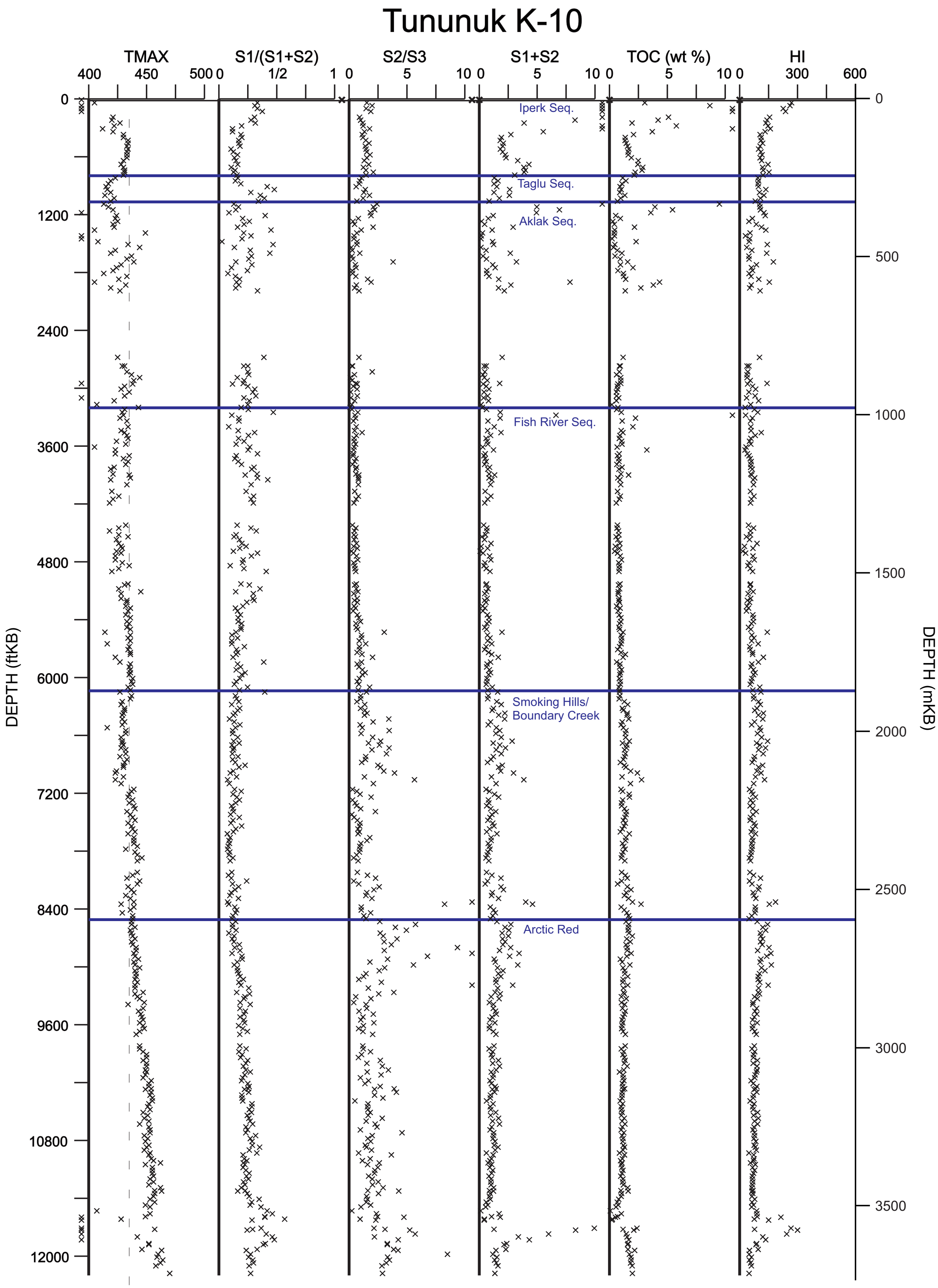

Figure 12. Selected Rock-Eval 6 parameters versus depth (displayed in Rock-Eval 2 format) for the Tununuk K-10 well.

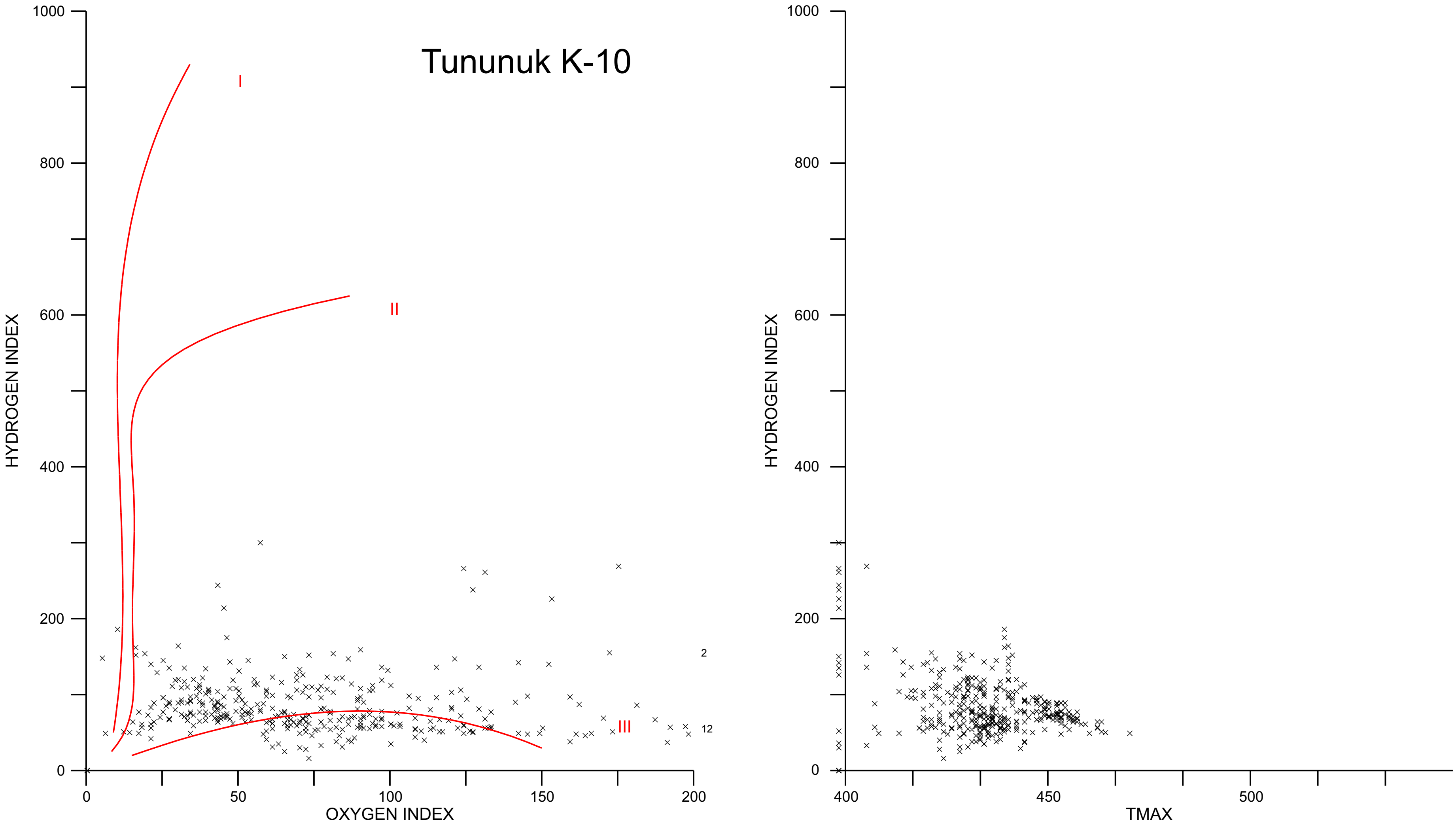

Figure 13. Whole rock HI versus OI (left) and HI versus Tmax (right) for the Tununuk K-10 well. Organic maturation pathways (red curves) are shown for different end member organic matter types - Type I (oil-prone, usually lacustrine), Type II (oil-prone, marine) and Type III (gas-prone, terrestrial).

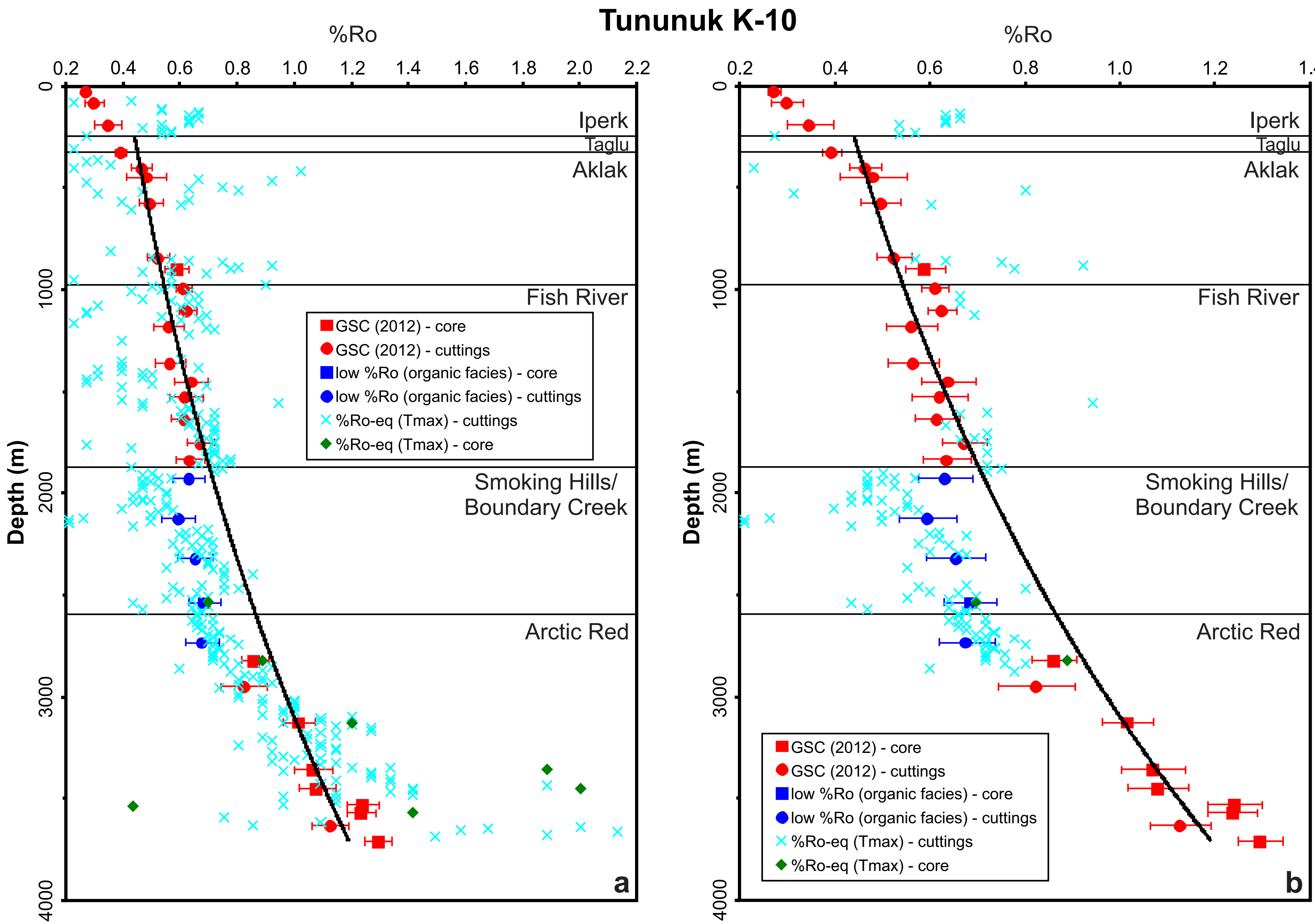

Figure 14. Comparison of measured %Ro with %Ro-equivalent values determined from Tmax for the Tununuk K-10 well. (a) All Tmax data and (b) Tmax values for least disturbed pyrograms.

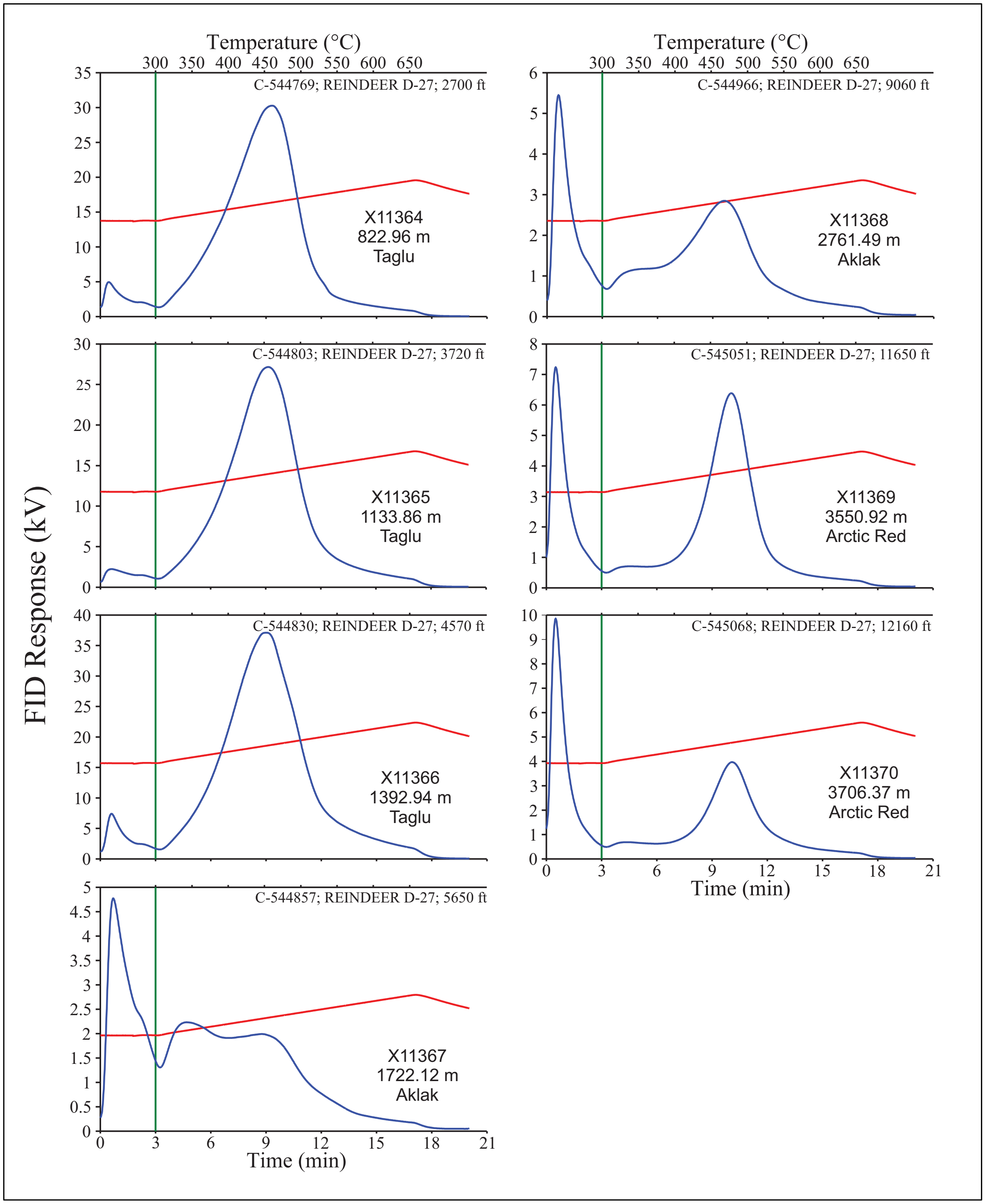

Figure 15. Rock-Eval pyrograms for cuttings samples from the Reindeer D-27 well that were selected for solvent extraction and GC and GC-MS analysis.

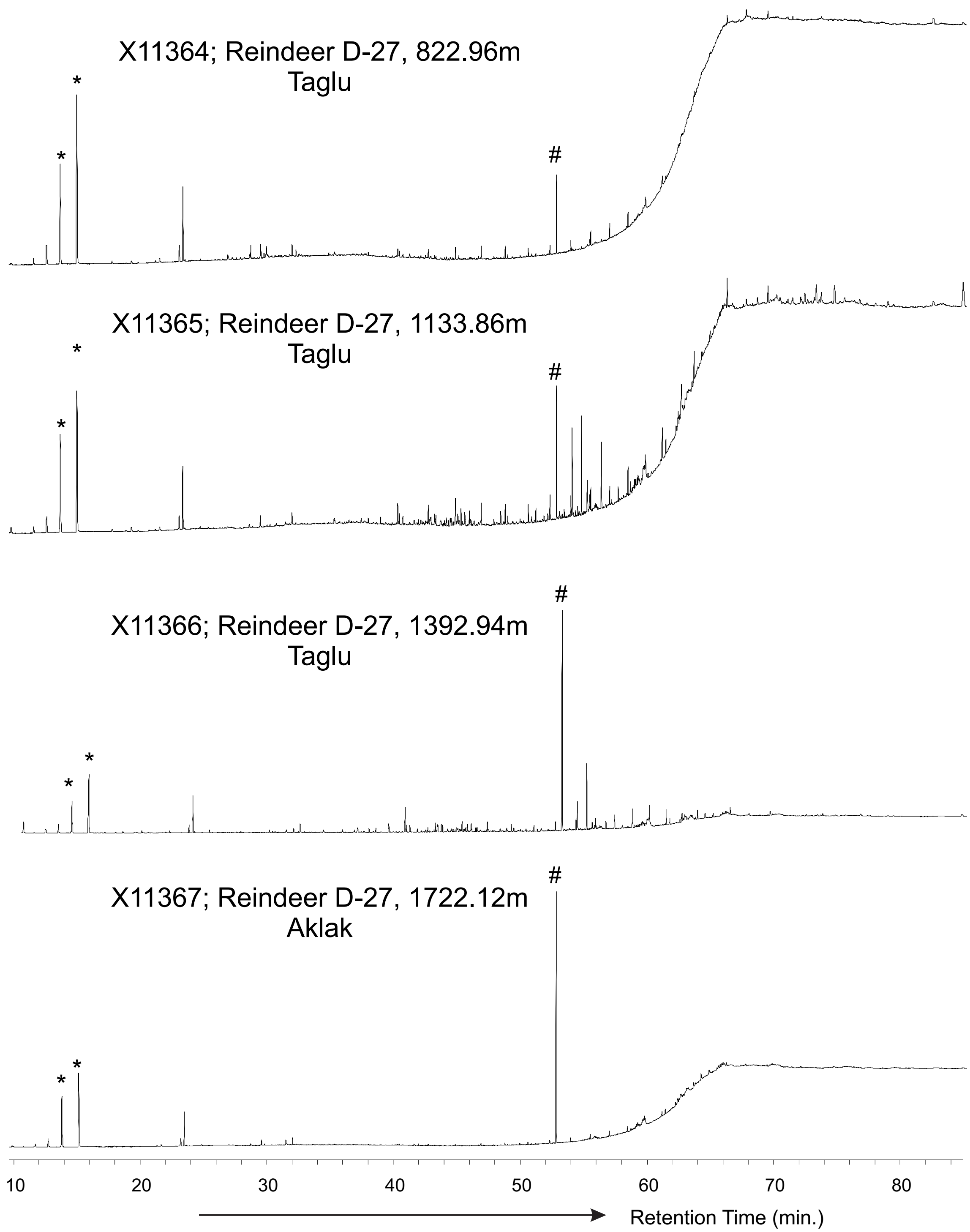

Figure 16. Traces from GC analysis of whole extracts for the cuttings samples from the Reindeer D-27 well. Peak # is plasticizer (see Figure 17); peaks * are impurity hydrocarbons (e.g. cyclohexane and methylhexanes) from solvent used for soxhlet extraction. Continued on next page.

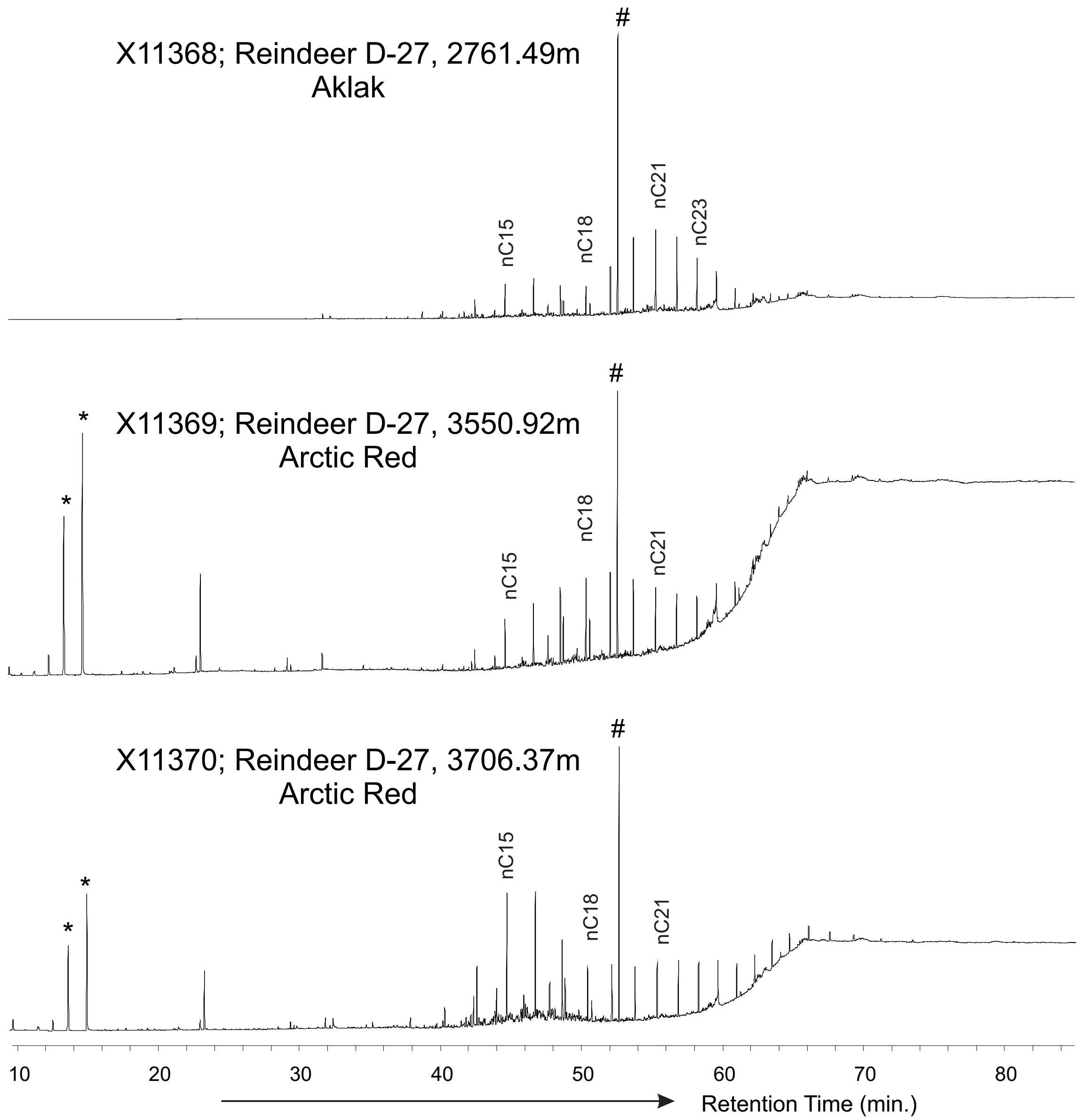

Figure 16. Continued.

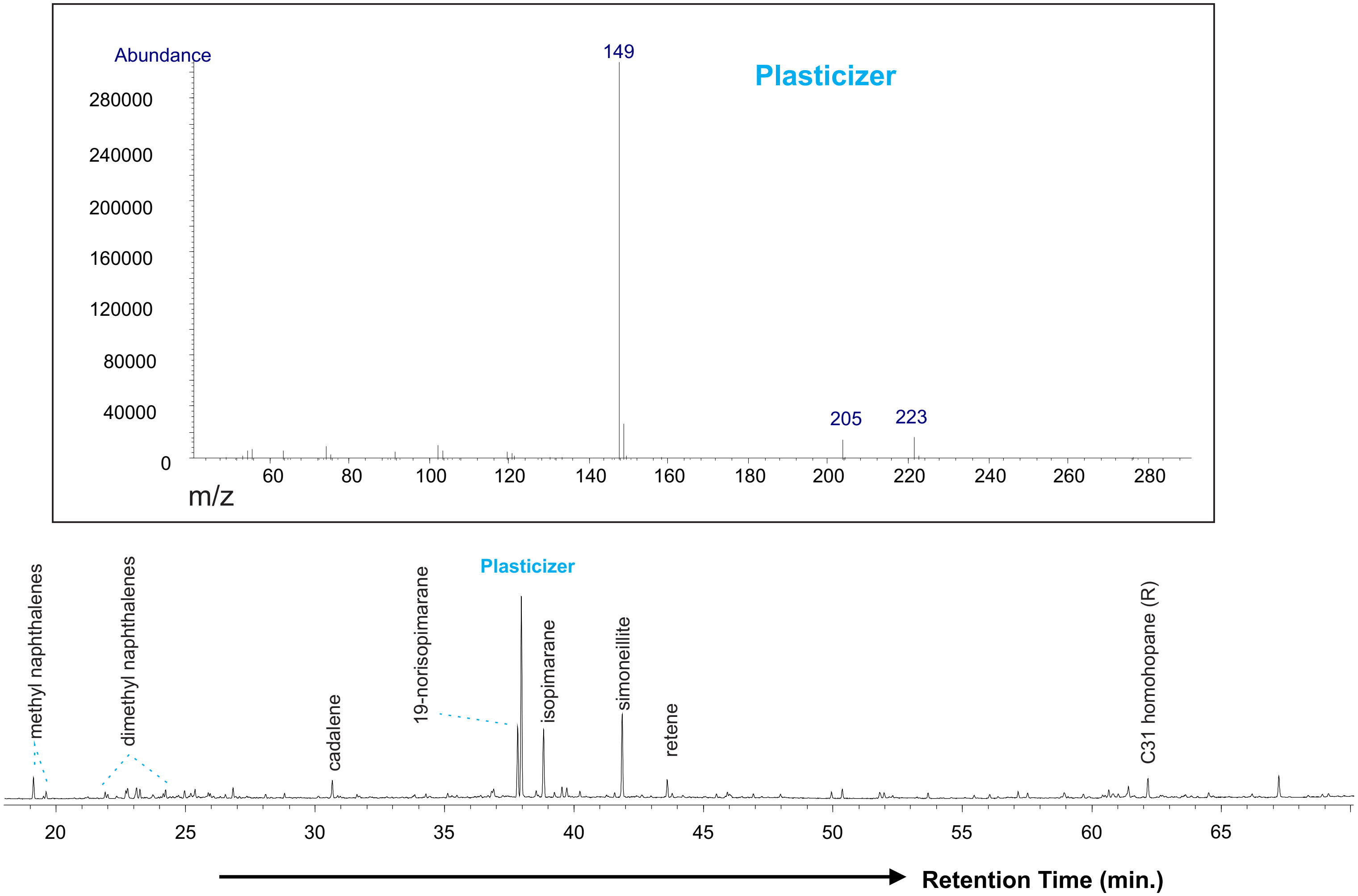

Figure 17. Plasticizer (peak # in Figure 16) is the major GC-amenable component as detected by GC-MS analysis of the total hydrocarbon fraction for sample X11365 from the Taglu Sequence.

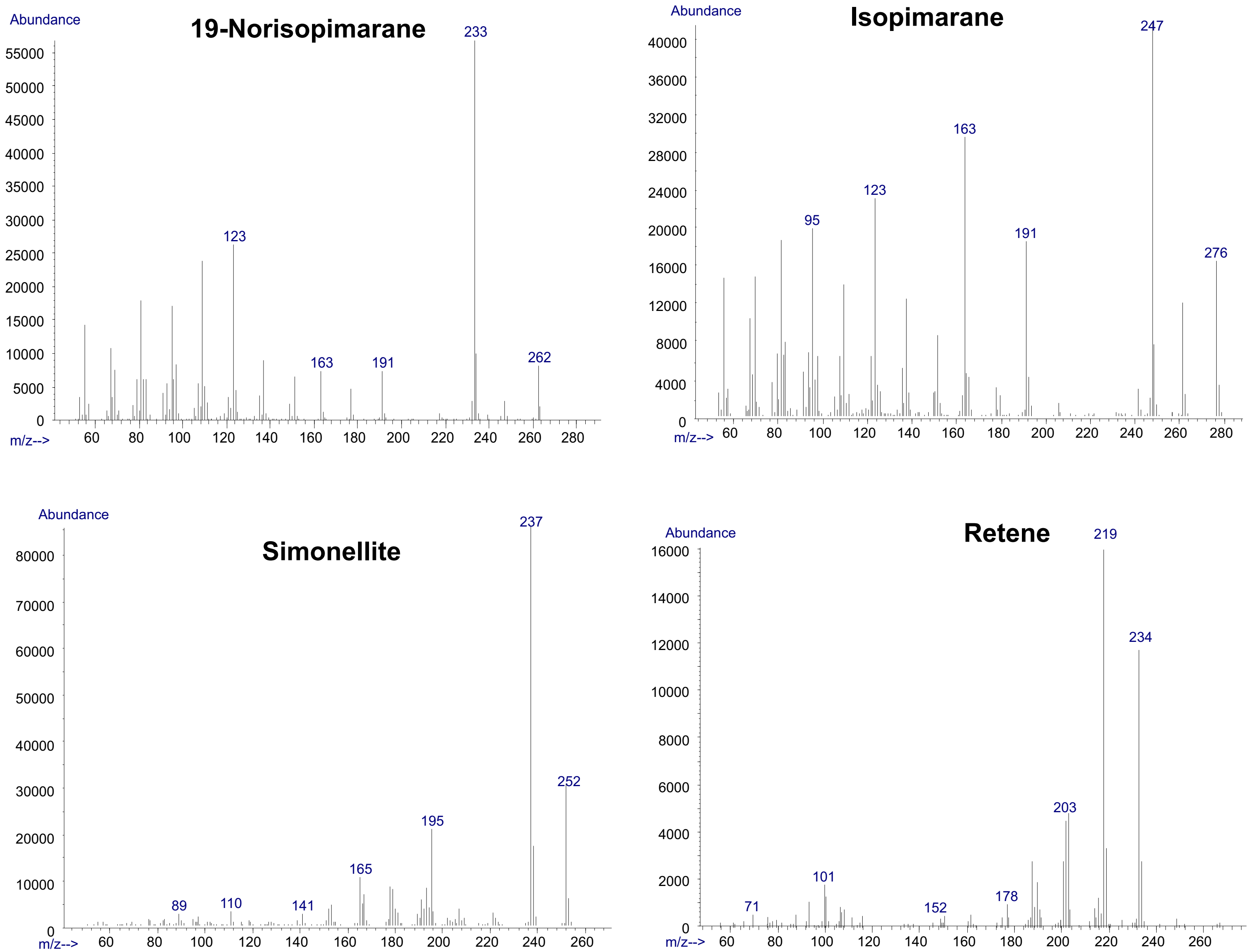

Figure 18. Mass spectra of the higher plant biomarkers present in the coaly cuttings sample X11365 from the Taglu Sequence in the Reindeer D-27 well. These are among the major hydrocarbon components as indicated in Figure 17.

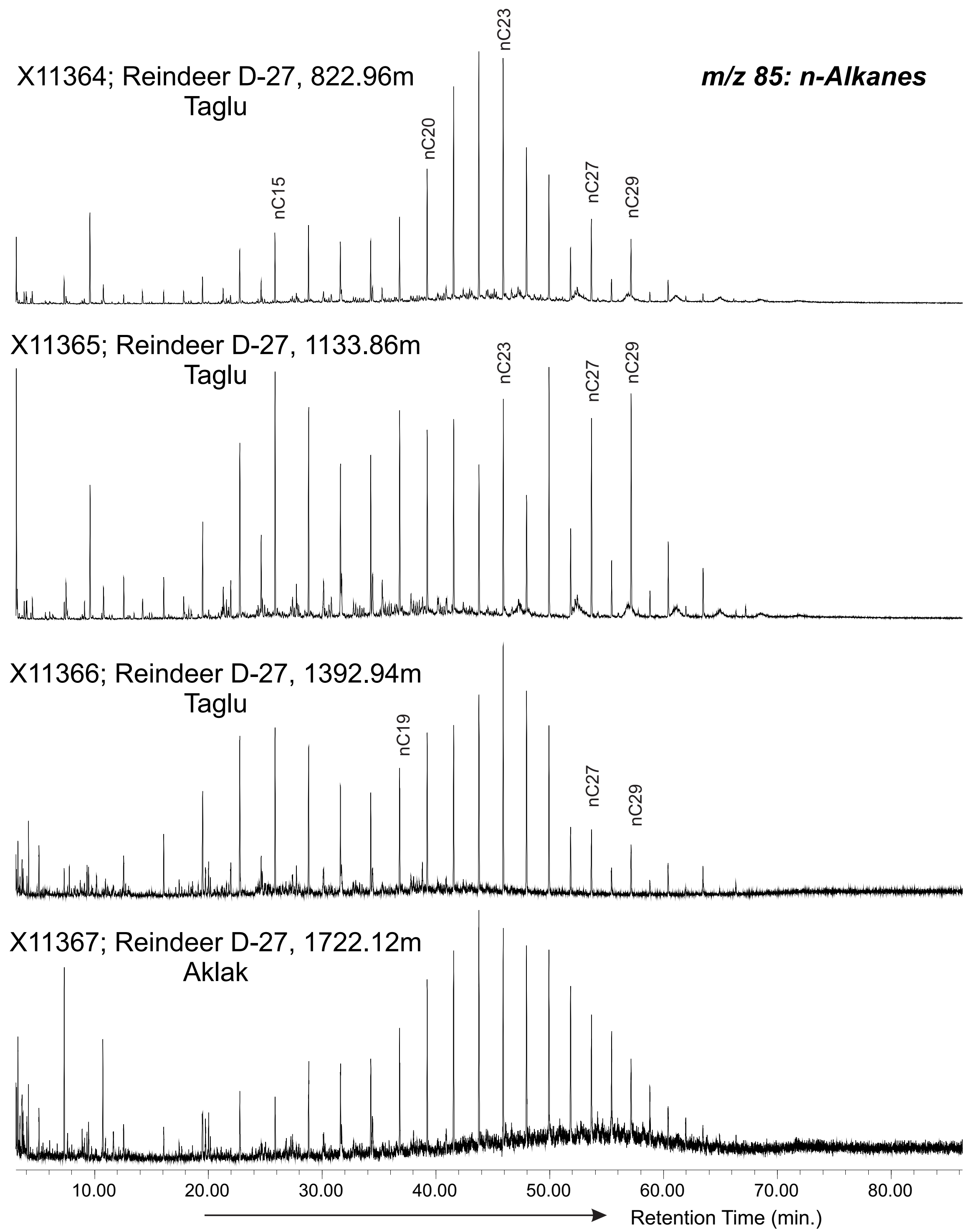

Figure 19. M/z 85 mass chromatograms showing the distribution of normal alkanes in cuttings samples from Reindeer D-27 well. Continued on next page.

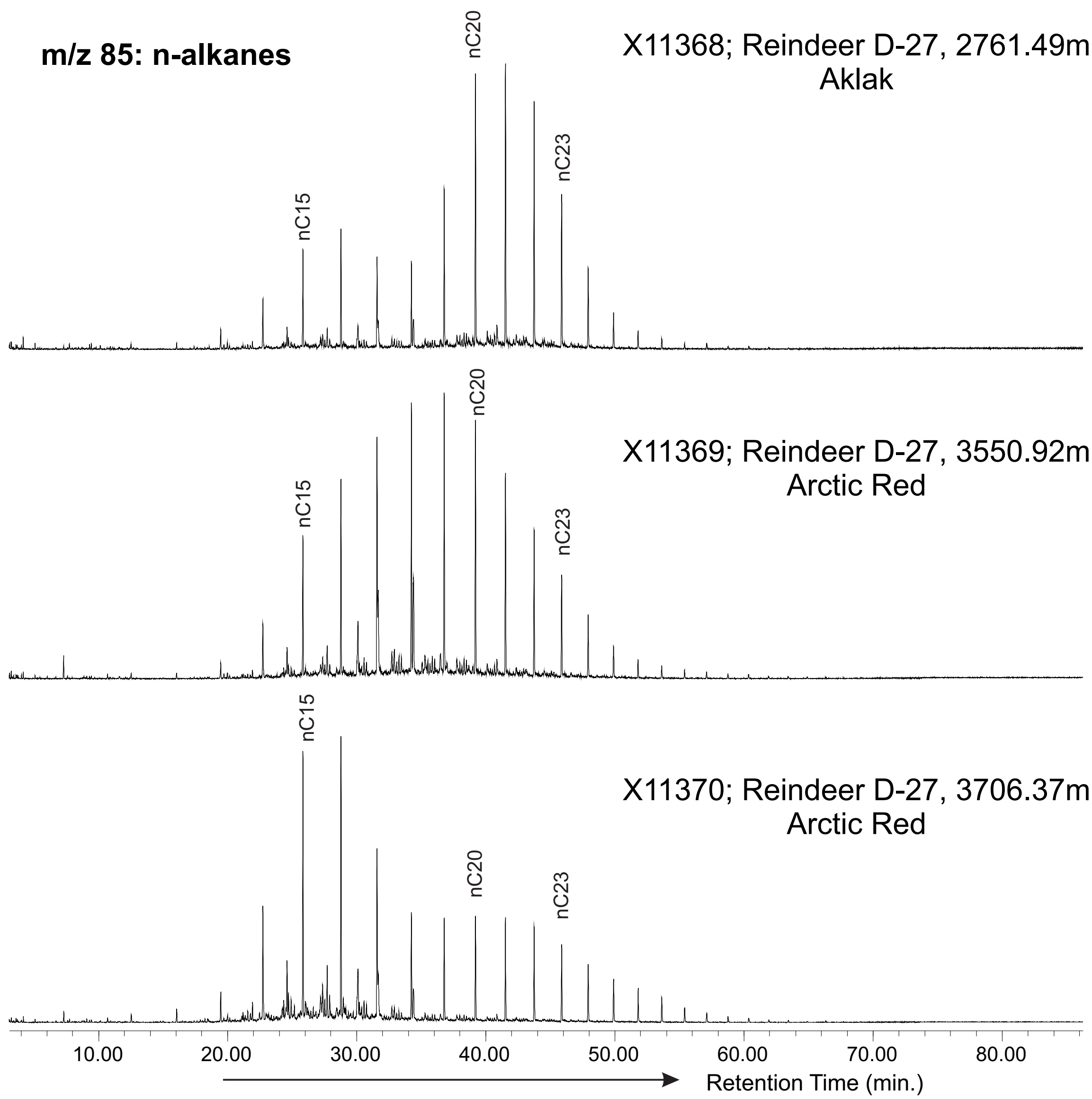

Figure 19. Continued.

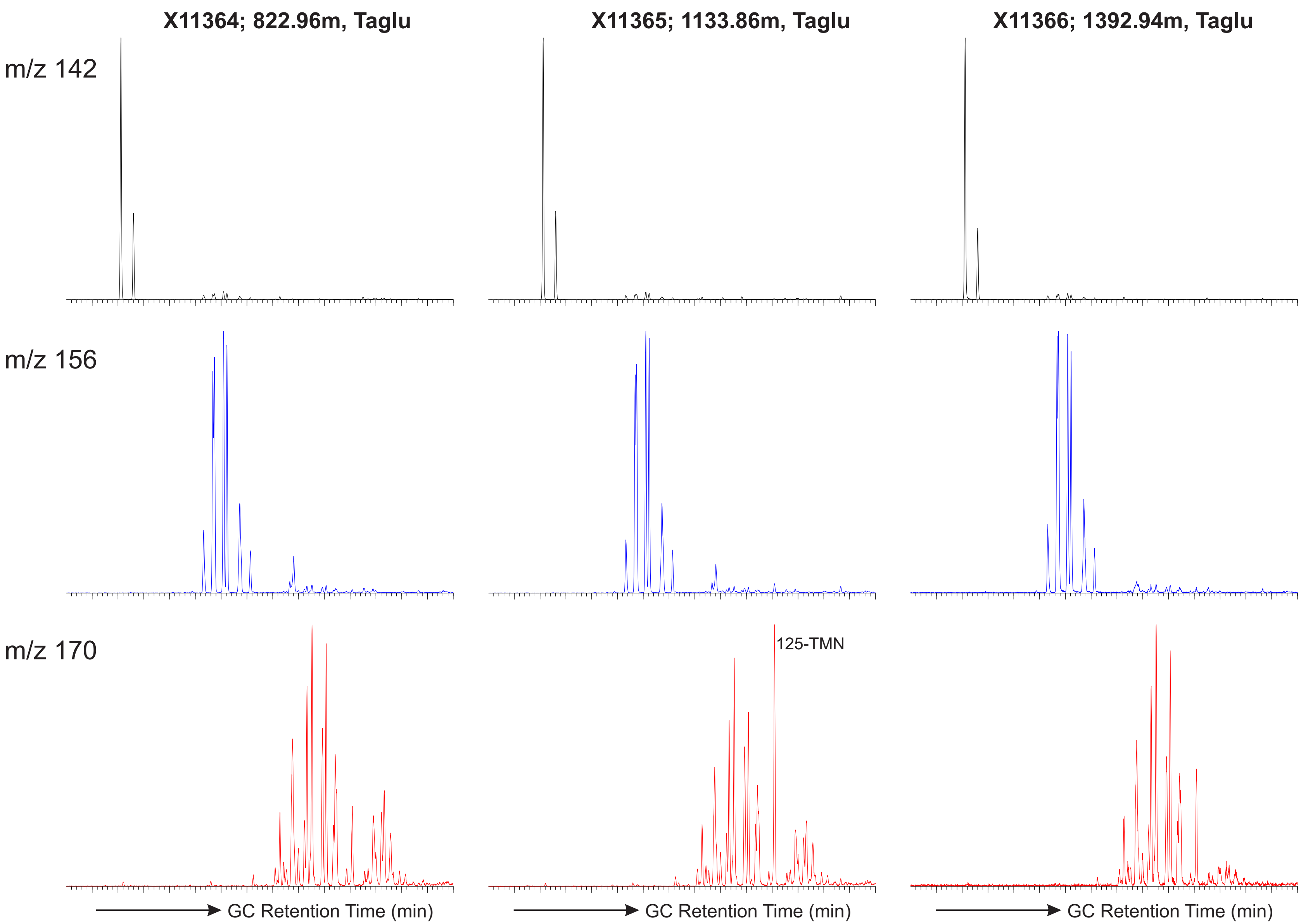

Figure 20. The distribution of methylnaphthalenes (m/z 142, black), dimethyl naphthalenes (m/z 156, blue) and trimethyl naphthalenes (m/z 170, red) for the cuttings samples from Reindeer D-27. 125-TMN: 1,2,5-trimethylnaphthalene. Continued on the next page.

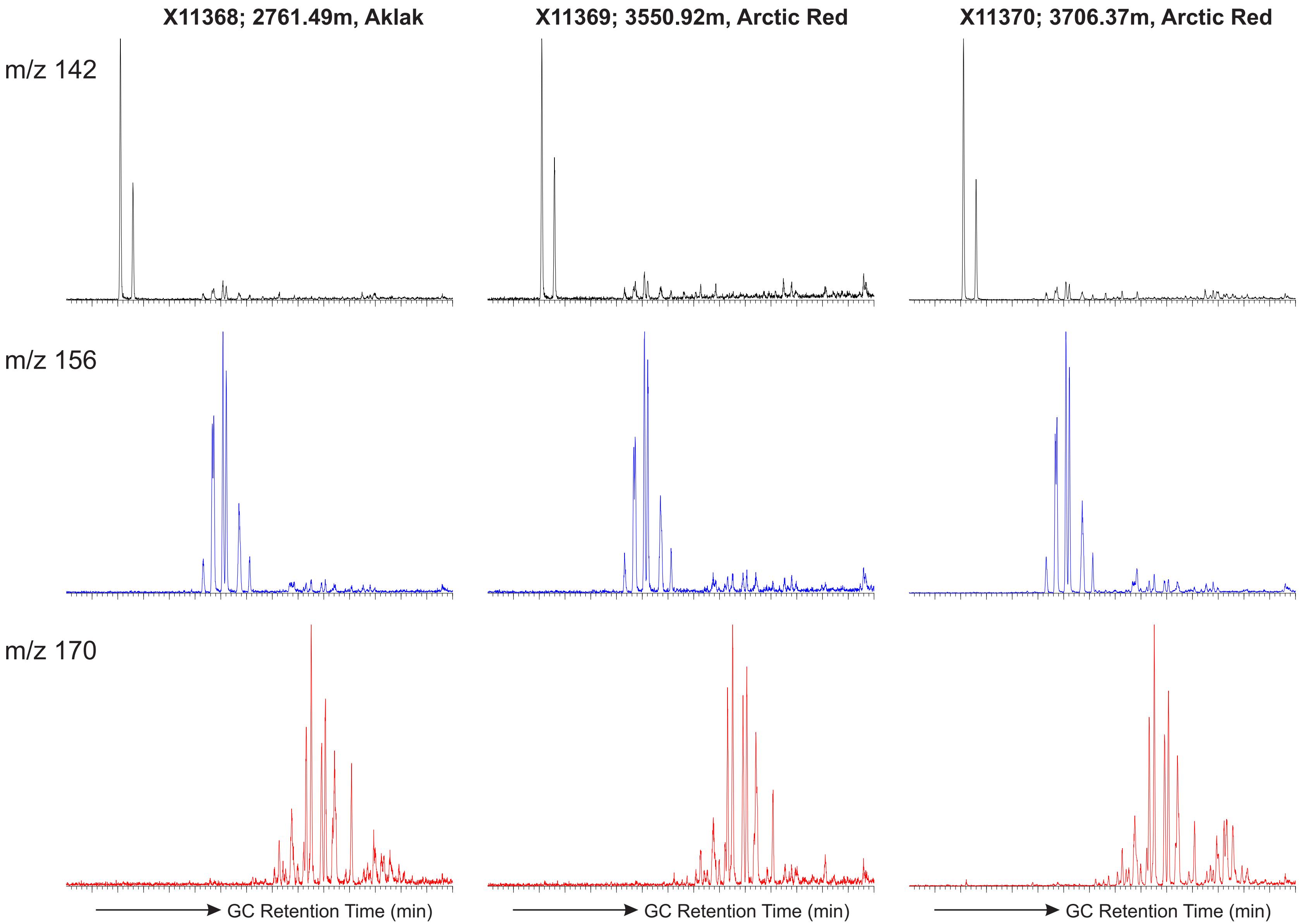

Figure 20. Continued.

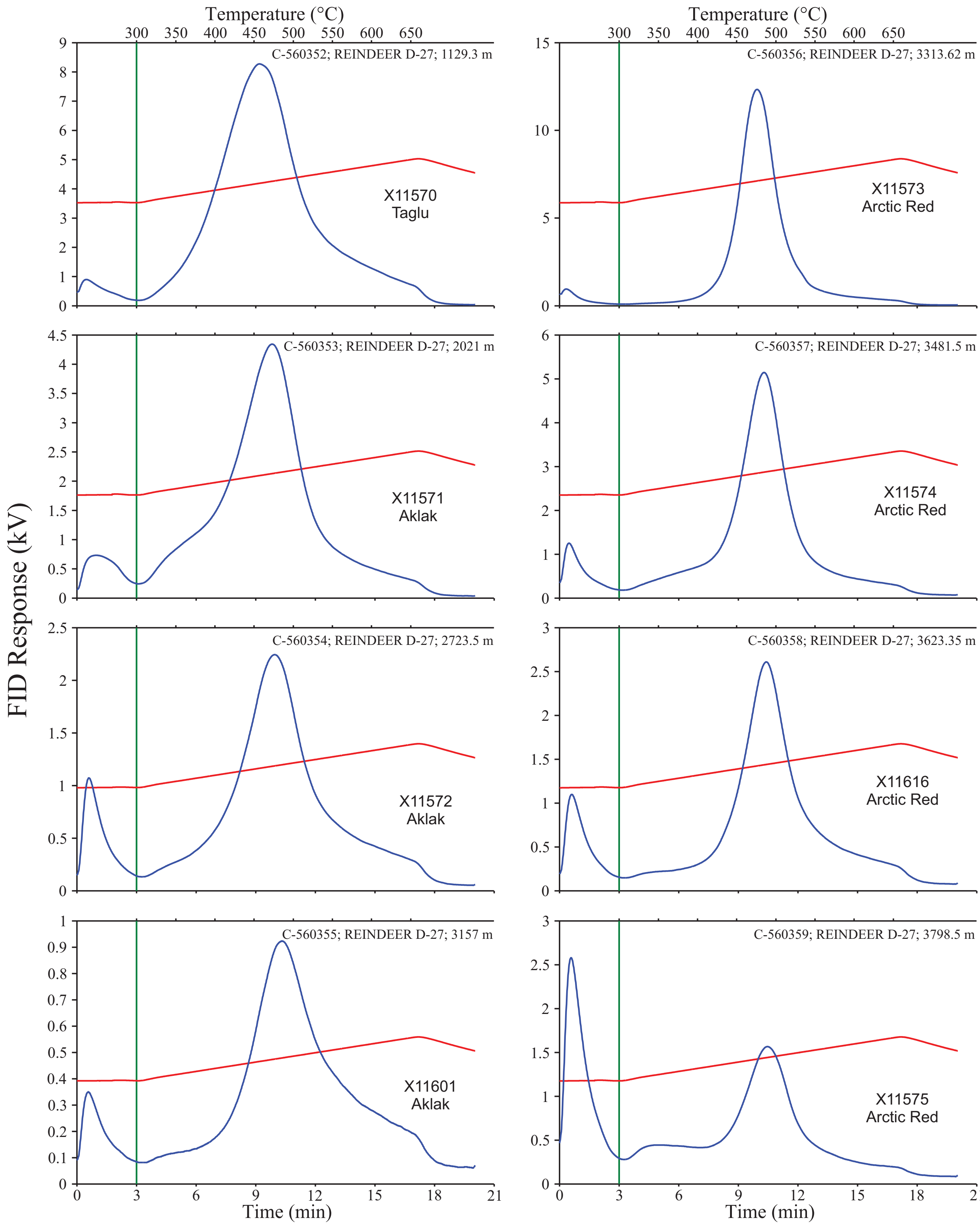

Figure 21. Rock-Eval pyrograms for core samples from the Reindeer D-27 and Tununuk K-10 wells that were selected for solvent extraction and GC and GC-MS analysis. Continued on next page.

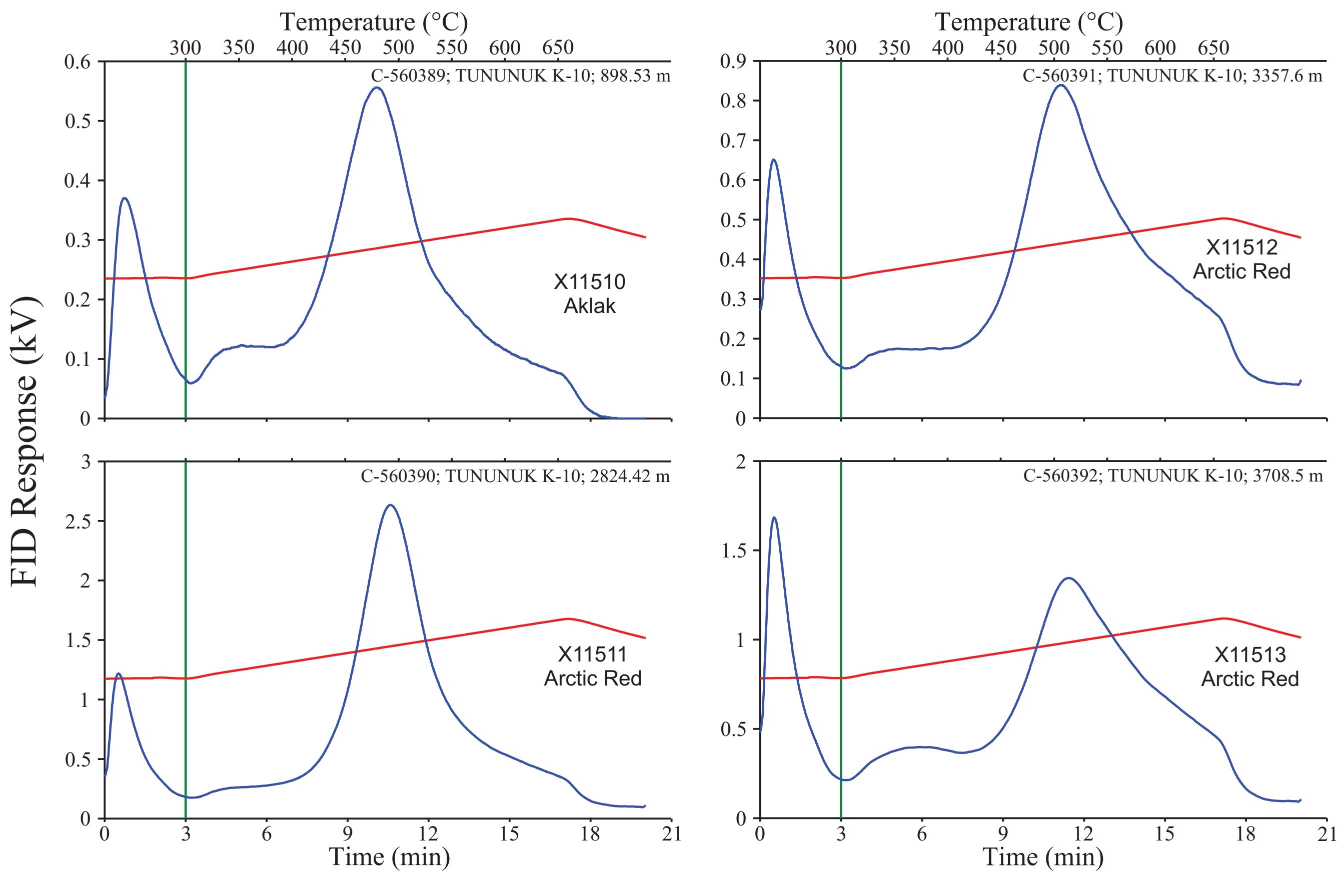

Figure 21. Continued.

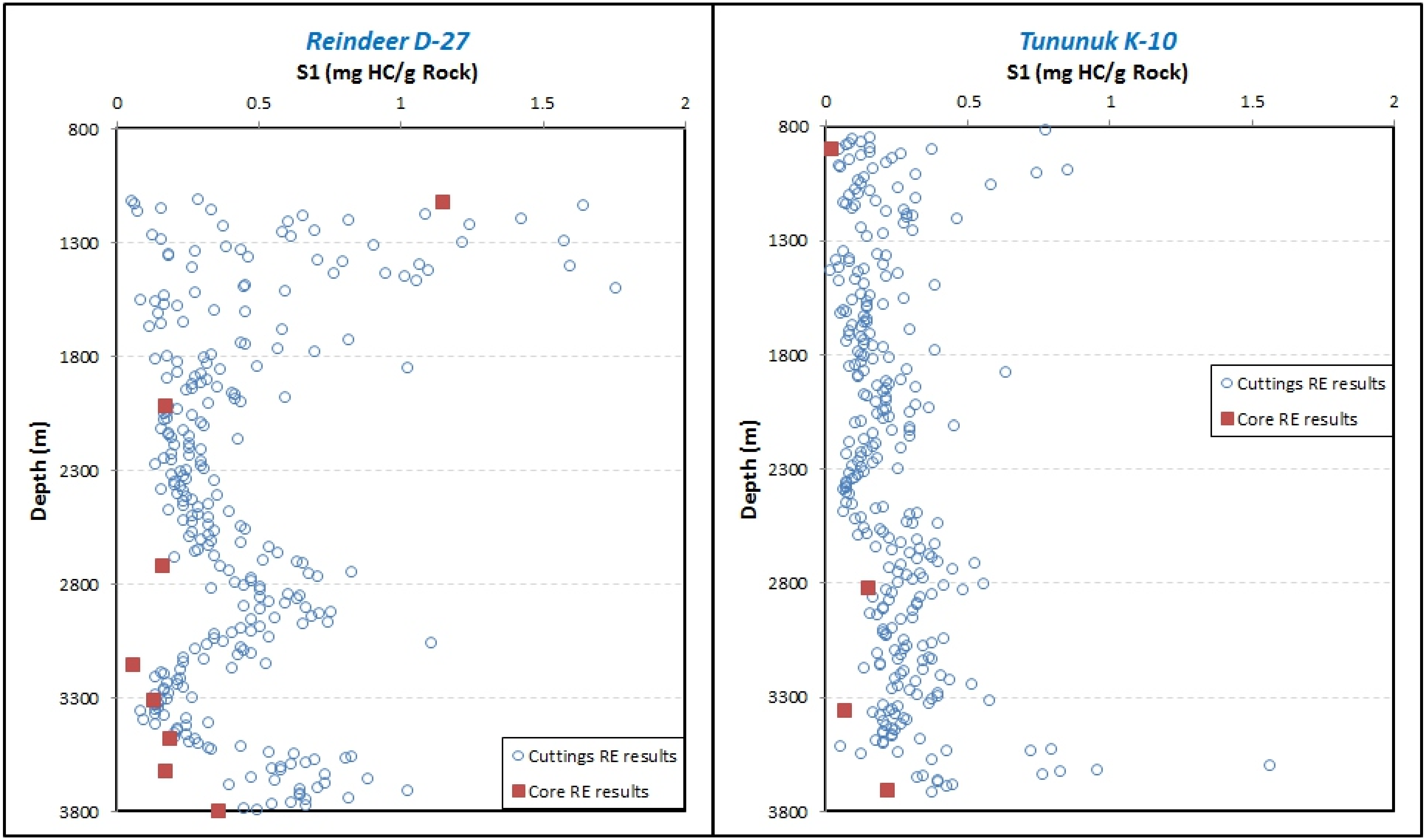

Figure 22. Depth profiles of Rock-Eval S1 values for core and cuttings samples from Reindeer D-27 and Tununuk K-10 wells. The cuttings samples seem to have generally higher S1 values than the core samples of corresponding depths, likely due to drilling mud contamination.

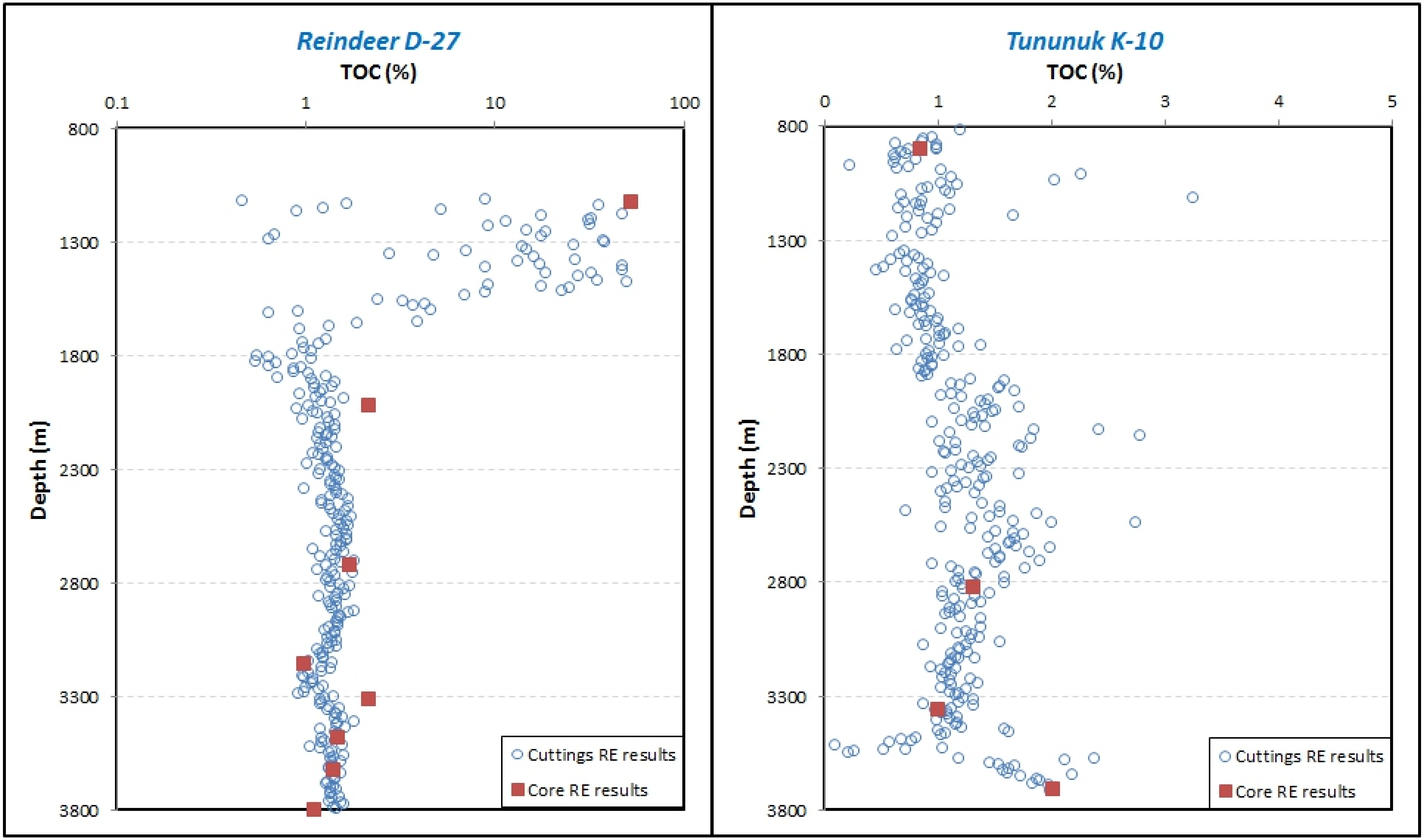

Figure 23. Depth profiles of Rock-Eval TOC content for core and cuttings samples from the Reindeer D-27 and Tununuk K-10 wells. TOC values are similar for both core and cuttings samples.

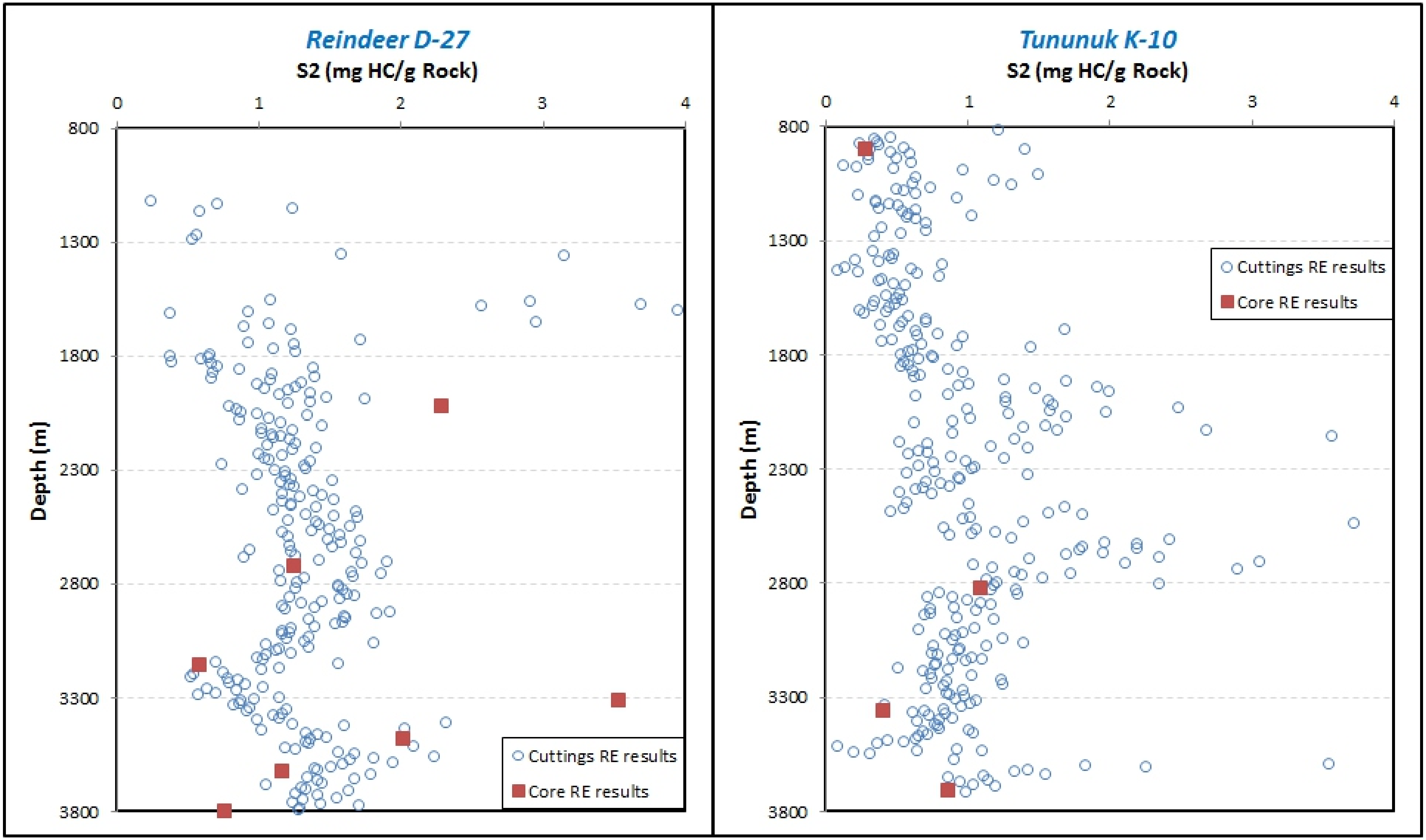

Figure 24. Depth profiles of Rock-Eval S2 values for core and cuttings samples from the Reindeer D-27 and Tununuk K-10 wells. S2 values are generally similar for both core and cuttings samples.

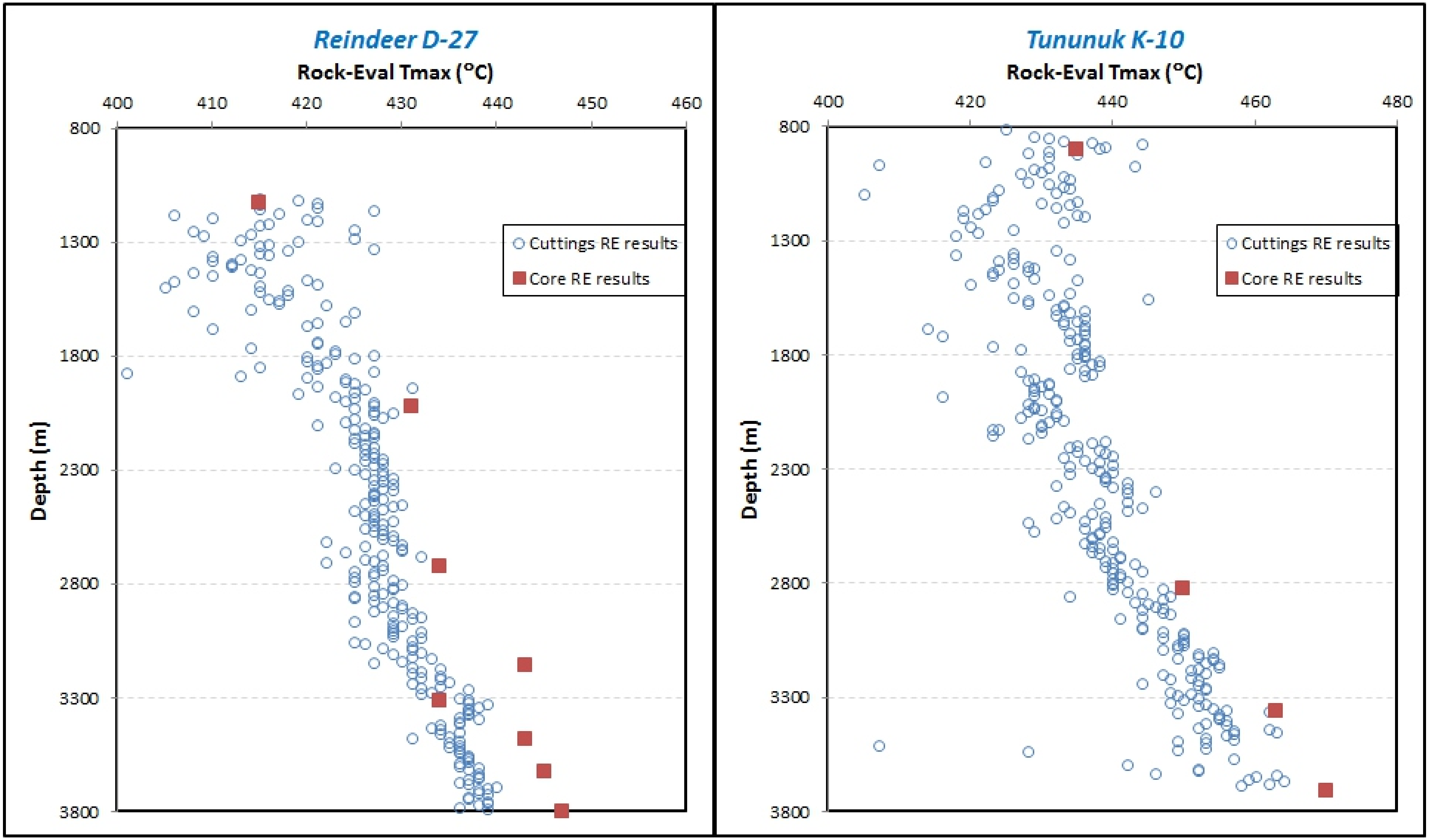

Figure 25. Depth profiles of Rock-Eval Tmax for Reindeer D-27 and Tununuk K-10 wells showing that Tmax values for cuttings samples are generally lower than those for core samples, probably due to drilling-related contamination of the cuttings samples.

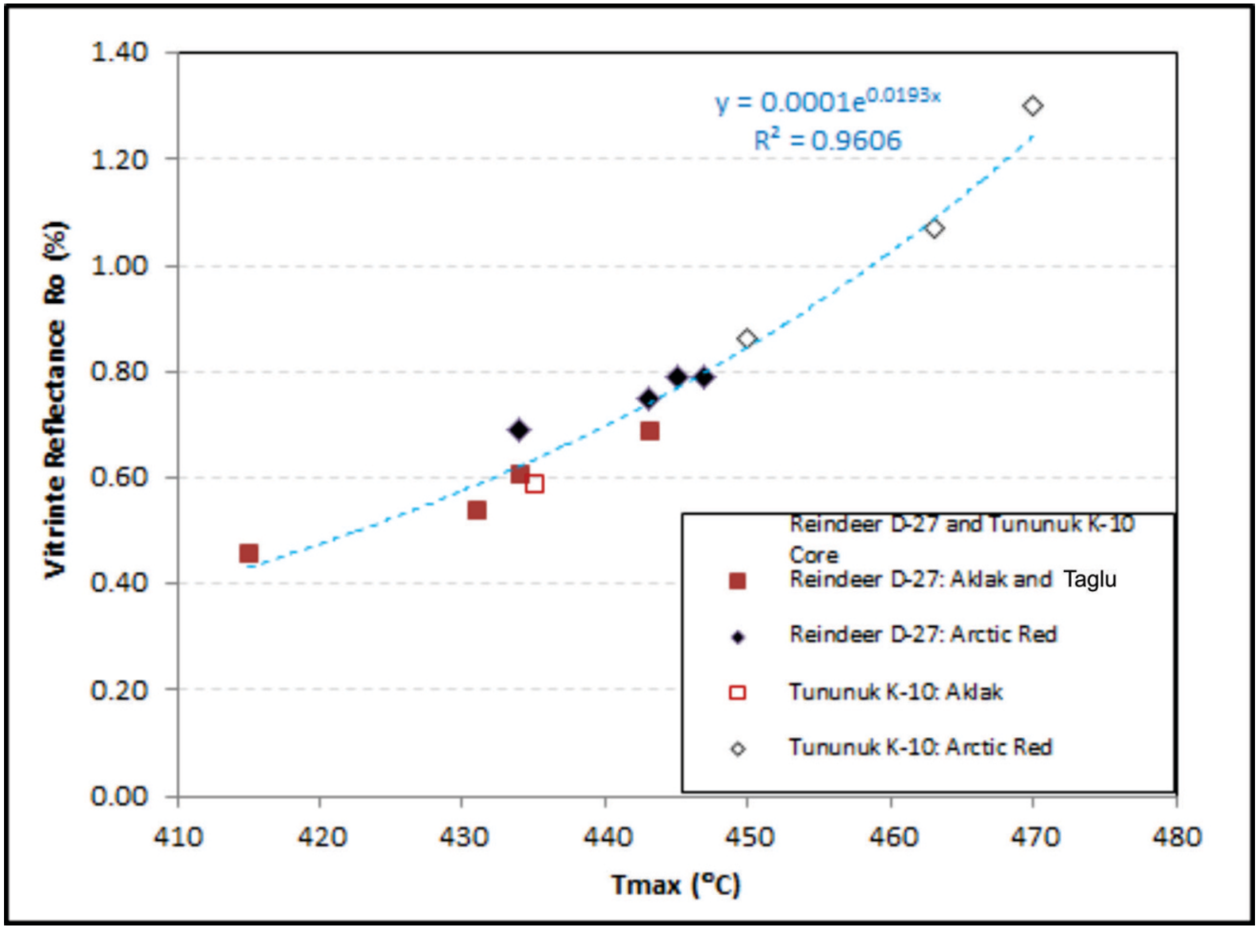

Figure 26. Relationship between Rock-Eval Tmax obtained on core samples and vitrinite reflectance measured on either core or cuttings samples of similar depth for the Reindeer D-27 and Tununuk K-10 wells.

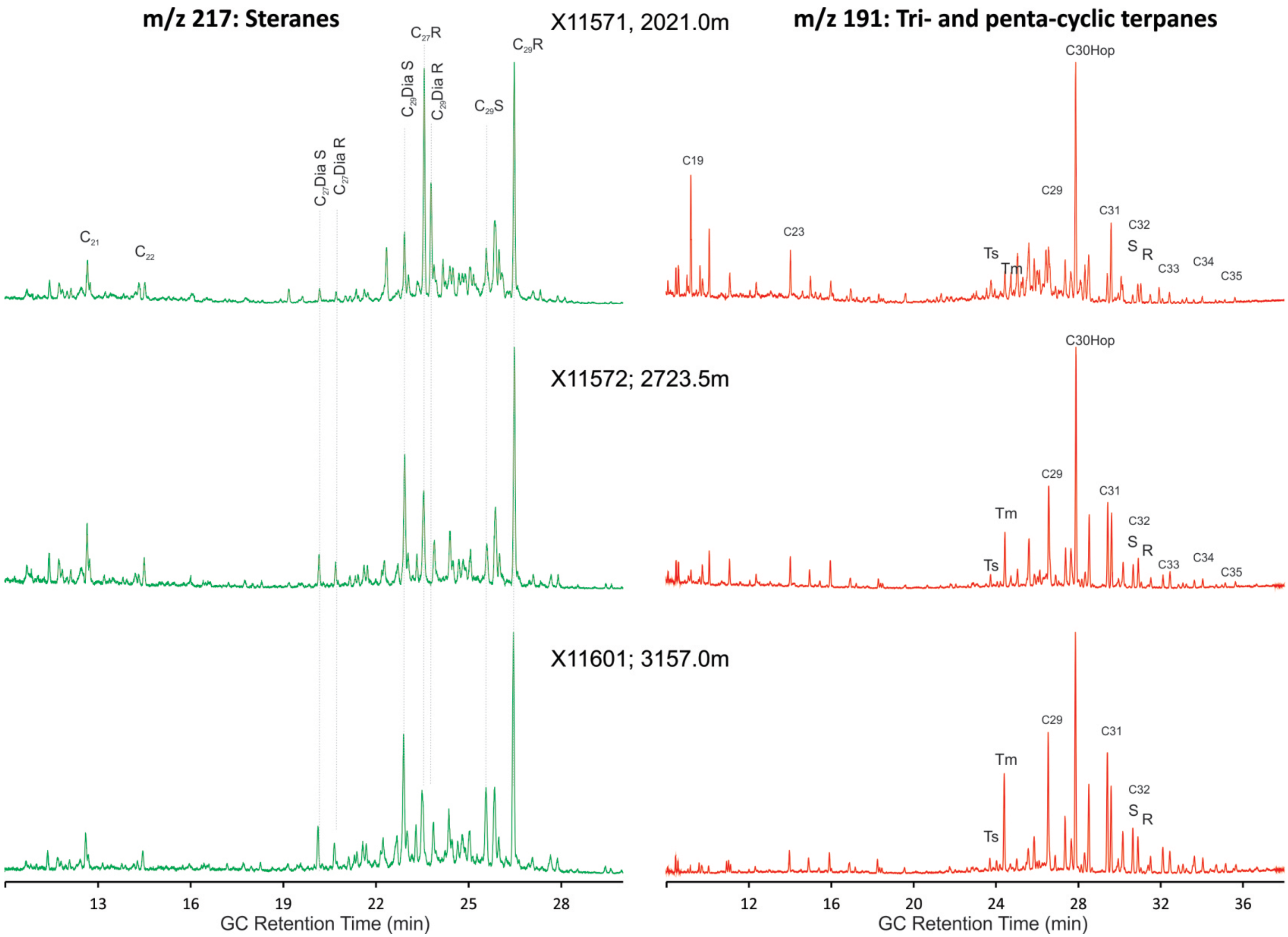

Figure 27. Mass chromatograms m/z 217 and 191 showing the distributions of steranes and terpanes for selected core samples from the Reindeer D-27 well. Continued on next page.

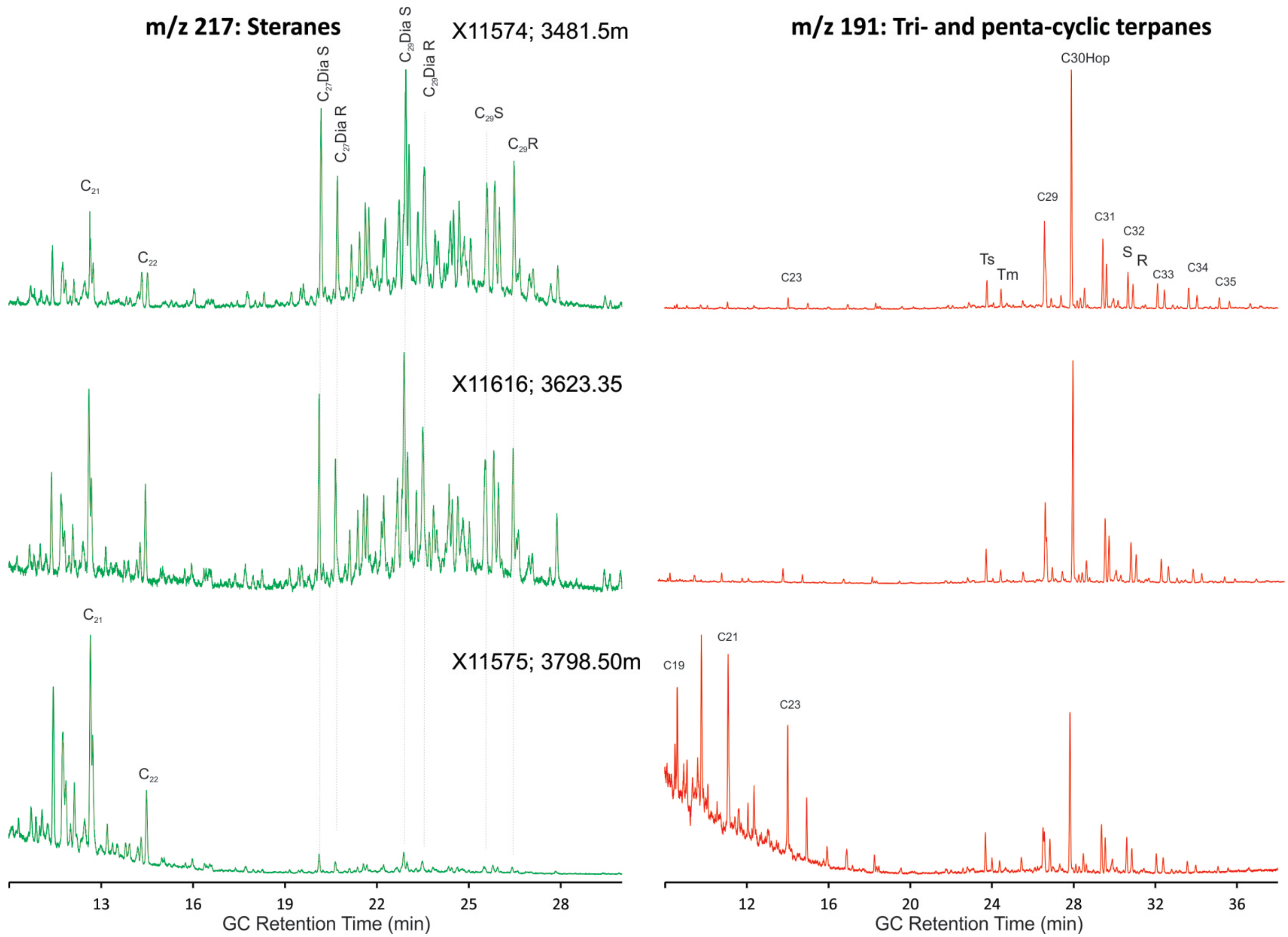

Figure 27. Continued.

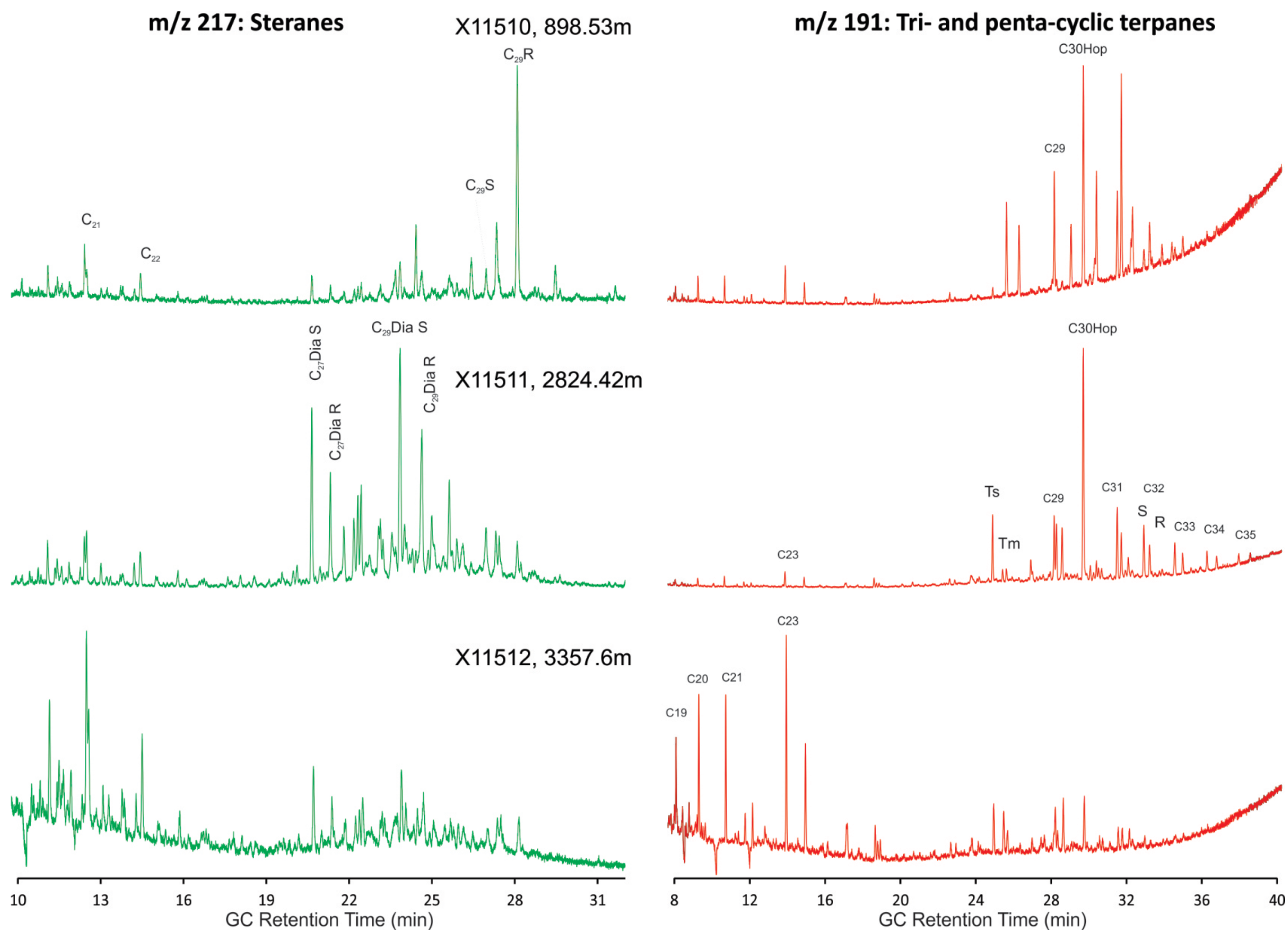

Figure 28. Mass chromatograms m/z 217 and 191 showing the distributions of steranes and terpanes for selected core samples from the Tununuk K-10 well.

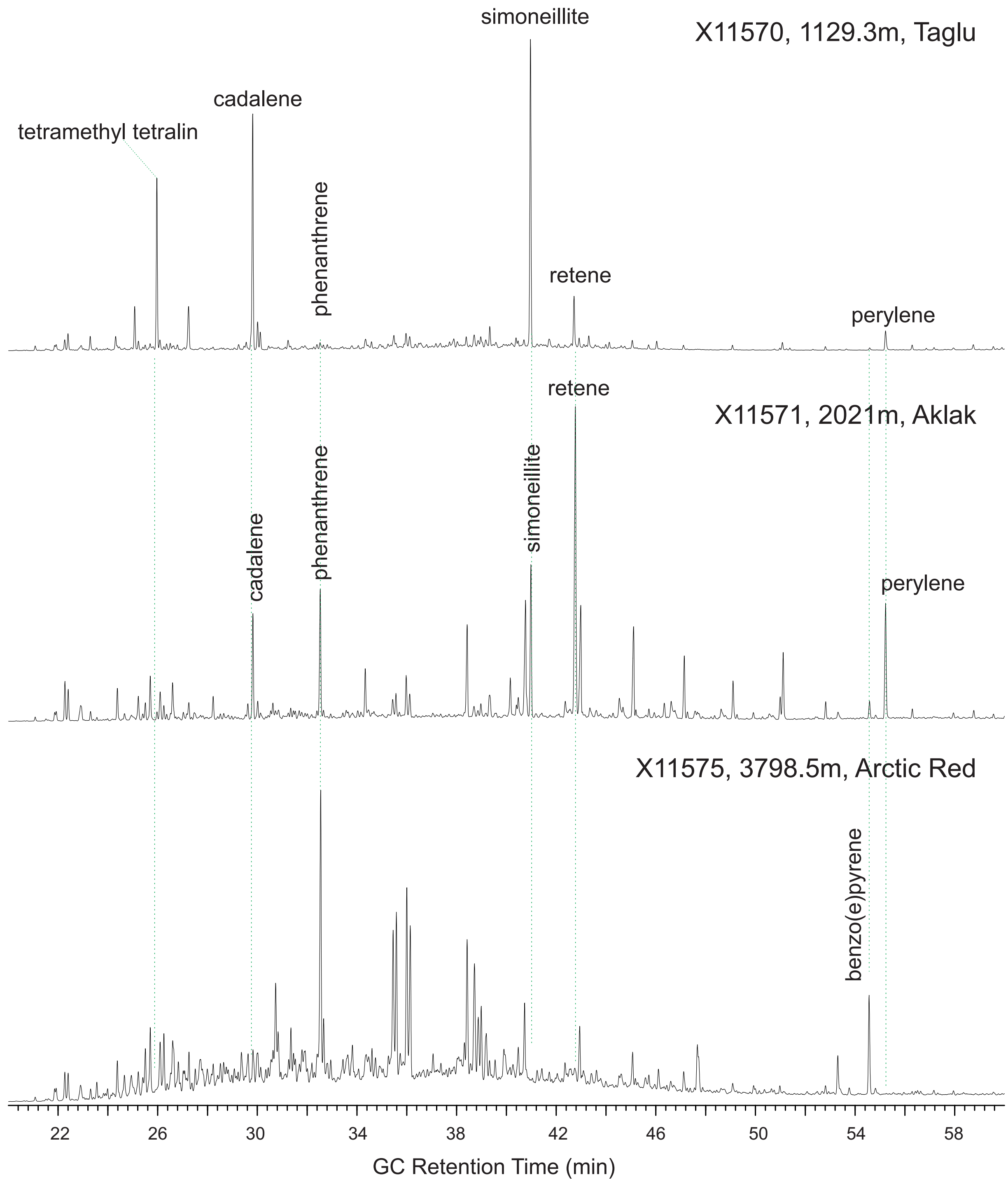

Figure 29. Partial total ion chromatograms (TIC) of aromatic fractions of selected core samples showing the distribution of higher plant derived biomarkers, tetramethyl tetralin, cadalene, simoneillite and retene.

Table 1. Mean random vitrinite reflectance (%Ro) data for various Reindeer D-27 samples. Lat: 69.1013 ºN, Long: 134.6177 ºW. Plotted %Ro values for primary vitrinite (Fig. 4) highlighted in yellow (cuttings) and green (core).

C #	Pellet #	Depth (ftKB)	Depth (mKB)	TVD (mKB)	TVD (mGL)	%Ro	S.D.	N	Stratigraphic Unit	Comments	Sample Type
									GSC 2012 (J. Reyes)		
C-544684	247/11	60	18.3	18.3	13.4	0.33	0.02	6	Iperk	rare indigenous organic matter, mainly recycled	CTG
C-544697	248/11	520	158.5	158.5	153.6	0.30	0.03	20	Iperk	rare indigenous organic matter, mainly recycled	CTG
C-544709	249/11	860	262.1	262.1	257.2	0.28	0.01	6	Iperk	rare indigenous organic matter, mainly recycled	CTG
C-544715	250/11	1050	320.0	320.0	315.1	0.37	0.03	26	Richards	rare indigenous organic matter, mainly recycled	CTG
C-544732	251/11	1560	475.5	475.5	470.6	0.38	0.04	48	Richards	rare indigenous organic matter, mainly recycled	CTG
C-544740	252/11	1810	551.7	551.7	546.8	0.39	0.04	36	Taglu	rare indigenous organic matter, mainly recycled	CTG
C-544750	253/11	2100	640.1	640.1	635.2	0.40	0.04	25	Taglu	rare indigenous organic matter, mainly recycled	CTG
C-544763	254/11	2520	768.1	768.1	763.2	0.38	0.04	52	Taglu	greenish-yellow fluorescing HCs, minor %Ro suppression?	CTG
C-544768	255/11	2670	813.8	813.8	808.9	0.41	0.04	51	Taglu	greenish-yellow fluorescing HCs, minor %Ro suppression?	CTG
C-544661	226/11	2925	891.5	891.5	886.6	0.44	0.02	25	Taglu	minor orange fluorescing solid bitumen	CORE
C-544777	256/11	2930	893.1	893.1	888.2	0.41	0.03	51	Taglu	greenish-yellow fluorescing HCs, minor %Ro suppression?	CTG
C-544782	257/11	3100	944.9	944.9	940.0	0.42	0.03	50	Taglu	liptinite-rich coaly matrix, trace HC inclusions	CTG
C-544793	258/11	3420	1042.4	1042.4	1037.5	0.45	0.03	45	Taglu	greenish-yellow fluorescing HCs, minor %Ro suppression?	CTG
C-544662	227/11	3700	1127.8	1127.5	1122.6	0.51	0.02	60	Taglu	minor orange fluorescing solid bitumen	CORE
C-544663	228/11	4064	1238.7	1238.3	1233.4	0.49	0.04	59	Taglu	intergranular greenish yellow fluorescing oil	CORE
C-544831	259/11	4590	1399.0	1398.4	1393.5	0.46	0.03	51	Taglu	greenish-yellow fluorescing HCs, minor %Ro suppression?	CTG
C-544664	229/11	4770	1453.9	1453.2	1448.3	0.45	0.05	39	Taglu		CORE
C-544838	260/11	4830	1472.2	1471.5	1466.6	0.47	0.03	51	Taglu	greenish-yellow fluorescing HCs, minor %Ro suppression?	CTG
C-544665	230/11	5322.5	1622.3	1621.3	1616.4	0.48	0.04	31	Taglu		CORE
C-544666	231/11	5525	1684.0	1683.0	1678.1	0.51	0.05	40	Aklak		CORE
C-544667	232/11	6105	1860.8	1859.5	1854.6	0.53	0.05	42	Aklak		CORE
C-544668	233/11	6626	2019.6	2018.1	2013.2	0.54	0.05	46	Aklak		CORE
C-544670	234/11	6883.5	2098.1	2096.5	2091.6	0.58	0.04	48	Aklak		CORE
C-544671	235/11	7271.5	2216.4	2214.5	2209.6	0.57	0.04	42	Aklak		CORE
C-544911	261/11	7380	2249.4	2247.5	2242.6	0.58	0.05	43	Aklak	greenish-yellow fluorescing HCs, minor %Ro suppression?	CTG
C-544672	236/11	7837.5	2388.9	2386.5	2381.6	0.59	0.06	44	Aklak		CORE
C-544673	237/11	7942.5	2420.9	2418.3	2413.4	0.62	0.07	46	Aklak		CORE
C-544674	238/11	8376.5	2553.2	2550.0	2545.1	0.63	0.04	50	Aklak		CORE
C-544675	239/11	8928	2721.3	2717.6	2712.7	0.61	0.05	51	Aklak		CORE
C-544676	240/11	9590	2923.0	2918.9	2914.0	0.65	0.05	43	Aklak		CORE
C-544677	241/11	10028	3056.5	3052.2	3047.3	0.68	0.06	49	Aklak		CORE
C-544678	242/11	10351.5	3155.1	3150.5	3145.6	0.69	0.05	36	Aklak		CORE
C-544679	243/11	10875	3314.7	3309.2	3304.3	0.69	0.06	34	Arctic Red	orange to brown fluorescing bitumen, alginite	CORE

C #	Pellet #	Depth (ftKB)	Depth (mKB)	TVD (mKB)	TVD (mGL)	%Ro	S.D.	N	Stratigraphic Unit	Comments	Sample Type
C-544680	244/11	11431	3484.2	3477.7	3472.8	0.75	0.05	27	Arctic Red	orange to brown fluorescing bitumen, alginite	CORE
C-544681	245/11	11894	3625.3	3618.6	3613.7	0.79	0.03	6	Arctic Red	orange to brown fluorescing bitumen, alginite	CORE
C-544682	246/11	12462	3798.4	3791.2	3786.3	0.79	0.06	29	Arctic Red	orange to brown fluorescing bitumen, alginite, oil staining	CORE
									GSC 1992 (M. Tomica)		
C-186738	87/92	2936	894.9	894.8	889.9	0.47	0.03	50	Taglu		CORE
C-186739	88/92	4047	1233.5	1233.1	1228.2	0.46	0.04	25	Taglu		CORE
C-186740	89/92	5320	1621.5	1620.6	1615.7	0.51	0.03	50	Taglu		CORE
C-186741	90/92	6112.5	1863.1	1861.8	1856.9	0.53	0.05	50	Aklak		CORE
C-186742	91/92	6637	2023.0	2021.5	2016.6	0.51	0.03	30	Aklak		CORE

Table 2. Mean random vitrinite reflectance (%Ro) data for various Tununuk K-10 samples. Lat: 68.9955 ºN, Long: 134.7788 ºW. Plotted %Ro values for primary vitrinite (Fig. 7) highlighted in yellow (cuttings) and green (core).

C #	Pellet #	Depth (ftKB)	Depth (mKB)	TVD (mKB)	TVD (mGL)	%Ro	S.D.	N	Stratigraphic Unit	Comments	Sample Type
						GSC 2012 (J. Reyes)					
C-544008	194/11	90	27.4	27.4	22.0	0.27	0.01	11	Qy/Iperk		CTG
C-544014	195/11	270	82.3	82.3	76.9	0.30	0.03	25	Qy/Iperk		CTG
C-544026	196/11	630	192.0	192.0	186.6	0.35	0.05	16	Qy/Iperk		CTG
C-544041	197/11	1080	329.2	329.2	323.8	0.39	0.02	18	Aklak	coaly matrix; some recycled OM	CTG
C-544049	198/11	1320	402.3	402.3	396.9	0.47	0.03	16	Aklak	rare indigenous OM; mainly recycled	CTG
C-544054	199/11	1470	448.1	448.1	442.7	0.48	0.07	25	Aklak	rare indigenous OM; mainly recycled	CTG
C-544068	200/11	1890	576.1	576.1	570.7	0.50	0.04	26	Aklak	minor coaly lenses; mainly recycled	CTG
C-544073	201/11	2760	841.2	841.2	835.8	0.53	0.04	17	Aklak	organically lean siltstone; rare coal lenses	CTG
C-543995	202/11	2946	897.9	897.9	892.5	0.59	0.04	8	Aklak	organically lean siltstone; rare coal lenses	CORE
C-544090	203/11	3270	996.7	996.6	991.2	0.61	0.03	52	Fish River		CTG
C-544101	204/11	3630	1106.4	1106.3	1100.9	0.63	0.03	23	Fish River		CTG
C-544110	205/11	3890	1185.7	1185.6	1180.2	0.56	0.05	29	Fish River		CTG
C-544120	206/11	4470	1362.5	1362.3	1356.9	0.57	0.05	14	Fish River		CTG
C-544130	207/11	4770	1453.9	1453.7	1448.3	0.64	0.06	14	Fish River		CTG
C-544135	208/11	5020	1530.1	1529.8	1524.4	0.62	0.06	25	Fish River		CTG
C-544147	209/11	5370	1636.8	1636.3	1630.9	0.62	0.05	27	Fish River		CTG
C-544160	210/11	5750	1752.6	1751.0	1745.6	0.67	0.05	19	Fish River		CTG
C-544169	211/11	6030	1837.9	1837.3	1831.9	0.64	0.05	29	Fish River		CTG
C-544180	212/11	6360	1938.5	1928.7	1923.3	0.63	0.06	24	Smoking Hills	reduced %Ro; different OM type	CTG
C-544201	213/11	6980	2127.5	2126.8	2121.4	0.60	0.06	19	Smoking Hills	reduced %Ro; different OM type	CTG
C-544221	214/11	7610	2319.5	2318.6	2313.2	0.66	0.06	37	Smoking Hills	reduced %Ro; different OM type	CTG
C-543996	218/11	8318	2535.3	2534.2	2528.8	0.69	0.05	36	Smoking Hills	reduced %Ro; different OM type	CORE
C-544262	215/11	8970	2734.1	2732.5	2727.1	0.68	0.06	30	Arctic Red	reduced %Ro; different OM type	CTG
C-543997	219/11	9255	2820.9	2819.1	2813.7	0.86	0.05	32	Arctic Red		CORE
C-544285	216/11	9690	2953.5	2951.3	2945.9	0.83	0.08	18	Arctic Red		CTG
C-543998	220/11	10254	3125.4	3122.3	3116.9	1.02	0.05	29	Arctic Red		CORE
C-543999	221/11	11023	3359.8	3355.8	3350.4	1.07	0.07	13	Arctic Red		CORE
C-544000	222/11	11315	3448.8	3444.5	3439.1	1.08	0.06	44	Arctic Red	carbonate in microfractures	CORE
C-544001	223/11	11586	3531.4	3526.8	3521.4	1.24	0.06	10	Arctic Red	carbonate in microfractures	CORE
C-544004	224/11	11712	3569.8	3565.4	3560.0	1.24	0.05	24	Arctic Red	carbonate in microfractures	CORE
C-544357	217/11	11930	3636.3	3631.8	3626.4	1.13	0.06	15	Arctic Red		CTG
C-544005	225/11	12169	3709.1	3704.6	3699.2	1.30	0.05	17	Arctic Red	carbonate in microfractures	CORE

Table 3. Reindeer D-27 Rock-Eval 6 data (Rock-Eval 2 format).

pale yellow	%Ro analysis
green	acceptable pyrogram
purple	anomalous pyrogram
orange	PI ≥ 0.2
yellow	TOC ≥ 5 wt%

Depth (ftKB)	Depth (mKB)	Qty (mg)	Tmax	S1	S2	S3	PI	S2/S3	PC (%)	TOC (%)	HI	OI	MINC (%)	Organic Type	%Roeq	Comments
													Iperk			
30	9.14	70.6	389	2.96	3.67	0.88	0.45	4.17	0.59	1.45	253	61	0.5	III		broad S2 curve
60	18.29	70.5	419	1.37	2.27	1.28	0.38	1.77	0.36	1.30	175	98	0.7	III		small S2, large left shoulder
90	27.43	70.3	417	0.49	1.12	0.76	0.31	1.47	0.16	0.67	167	113	0.5	III		left shoulder on S2
130	39.62	70.0	435	0.10	0.41	1.39	0.20	0.29	0.09	0.24	171	579	0.8	III	0.69	bimodal S2
160	48.77	70.5	363	0.06	0.31	5.67	0.16	0.05	0.20	0.32	97	1772	1.2	III		bimodal S2
180	54.86	70.4	409	0.11	0.64	4.28	0.15	0.15	0.19	0.32	200	1338	1.0	III		highly irregular S2, left and right shoulders
210	64.01	70.8	420	0.48	1.51	1.94	0.24	0.78	0.24	0.98	154	198	1.0	III	0.14	triangular shaped S2; left and right shoulders
240	73.15	70.5	427	0.30	0.94	3.14	0.24	0.30	0.21	0.70	134	449	1.3	III	0.43	large left shoulder on S2
270	82.30	70.8	429	0.29	0.90	2.94	0.24	0.31	0.21	0.79	114	372	1.1	III	0.50	left shoulder on S2; dominantly recycled
300	91.44	70.5	424	0.82	1.35	3.23	0.38	0.42	0.30	0.87	155	371	1.0	III	0.31	large left shoulder on S2
320	97.54	69.7	429	0.70	1.42	3.24	0.33	0.44	0.31	0.86	165	377	1.0	III	0.50	large left shoulder on S2
350	106.68	70.5	424	0.58	1.27	2.76	0.31	0.46	0.26	0.89	143	310	0.8	III	0.31	small left shoulder on S2
390	118.87	70.7	424	0.72	1.17	2.45	0.38	0.48	0.26	0.80	146	306	0.7	III	0.31	large left shoulder on S2
460	140.21	70.5	421	0.78	1.15	2.22	0.40	0.52	0.26	0.87	132	255	0.6	III	0.18	left shoulder on S2
520	158.50	69.9	411	1.87	1.88	1.69	0.50	1.11	0.39	1.15	163	147	0.7	III		small, broad S2 curve
540	164.59	69.9	392	0.86	1.59	1.80	0.35	0.88	0.27	0.99	161	182	0.7	III		small, broad S2 curve
570	173.74	70.1	407	1.20	1.89	2.06	0.39	0.92	0.34	1.12	169	184	0.7	III		small, broad S2 curve
610	185.93	70.8	415	0.27	0.53	0.92	0.34	0.58	0.11	0.46	115	200	0.2	III		small S2 curve skewed to left
630	192.02	71.0	420	0.04	0.12	1.17	0.22	0.10	0.05	0.22	55	532	0.1	III	0.14	small ragged S2
660	201.17	71.0	417	0.06	0.15	0.60	0.29	0.25	0.04	0.20	75	300	0.1	III		small, broad S2 curve
680	207.26	70.2	422	0.10	0.42	1.57	0.19	0.27	0.10	0.40	105	393	0.2	III	0.23	bimodal S2
720	219.46	70.1	430	0.04	0.19	1.18	0.19	0.16	0.06	0.37	51	319	0.1	III	0.54	ragged S2, left shoulder
750	228.60	70.1	427	0.11	0.57	1.40	0.15	0.41	0.10	0.51	112	275	0.2	III	0.43	S2 curve skewed slightly to the left; recycled component
780	237.74	70.0	429	0.07	0.16	1.00	0.29	0.16	0.05	0.20	80	500	0.1	III	0.50	ragged S2, left shoulder
810	246.89	69.8	420	0.14	1.21	1.78	0.10	0.68	0.18	1.34	90	133	0.1	III	0.14	
830	252.98	70.7	423	0.09	0.69	1.31	0.12	0.53	0.12	0.86	80	152	0.1	III	0.27	
860	262.13	69.9	420	0.14	2.72	1.94	0.05	1.40	0.34	2.47	110	79	0.2	III	0.14	
890	271.27	71.0	422	0.20	2.41	2.28	0.08	1.06	0.34	2.48	97	92	0.2	III	0.23	
930	283.46	70.6	422	0.18	1.67	1.97	0.10	0.85	0.26	1.89	88	104	0.1	III	0.23	
960	292.61	70.7	421	0.09	0.59	0.93	0.13	0.63	0.10	0.79	75	118	0.1	III	0.18	
990	301.75	70.6	426	0.04	0.15	0.63	0.22	0.24	0.04	0.30	50	210	0.1	III	0.39	broad ragged S2
1020	310.90	70.7	424	0.06	0.18	0.97	0.27	0.19	0.06	0.43	42	226	0.2	III	0.31	broad ragged S2
AVE			**418.1**													all values (32)
SD			**14.0**													

Depth (ftKB)	Depth (mKB)	Qty (mg)	Tmax	S1	S2	S3	PI	S2/S3	PC (%)	TOC (%)	HI	OI	MINC (%)	Organic Type	%Roeq	Comments
AVE			**421.3**													selected values (7)
SD			**1.1**													
										Richards						
1050	320.04	70.1	421	0.13	1.46	1.78	0.08	0.82	0.23	1.75	83	102	0.1	III	0.18	
1080	329.18	71.0	424	0.07	0.21	1.00	0.24	0.21	0.06	0.31	68	323	0.1	III	0.31	small, broad ragged S2
1100	335.28	70.9	431	0.04	0.11	0.59	0.27	0.19	0.03	0.25	44	236	0.1	III	0.57	small, broad ragged S2
1140	347.47	70.4	425	0.11	0.27	1.04	0.29	0.26	0.07	0.29	93	359	0.1	III	0.35	small, broad ragged S2
1170	356.62	70.0	445	0.06	0.10	0.70	0.36	0.14	0.05	0.27	37	259	0.1	III	0.94	small, broad ragged bimodal S2
1200	365.76	70.6	398	0.05	0.16	1.18	0.22	0.14	0.06	0.30	53	393	0.1	III		irregular ragged S2 with left shoulder
1230	374.90	70.9	429	0.08	0.13	1.16	0.38	0.11	0.07	0.73	18	159	0.1	III	0.50	small, broad ragged bimodal S2
1260	384.05	70.0	423	0.05	0.13	1.15	0.29	0.11	0.06	0.22	59	523	0.1	III	0.27	small, broad ragged S2
1280	390.14	69.9	437	0.04	0.11	0.92	0.26	0.12	0.04	0.21	52	438	0.1	III	0.75	small, broad ragged S2
1320	402.34	70.5	439	0.06	0.13	0.98	0.32	0.13	0.05	0.25	52	392	0.1	III	0.80	small, broad ragged bimodal S2
1340	408.43	69.9	407	0.07	0.29	1.64	0.19	0.18	0.08	0.34	85	482	0.2	III		irregular ragged S2 with left shoulder
1380	420.62	70.1	339	0.06	0.11	0.83	0.35	0.13	0.05	0.20	55	415	0.1	III		small, broad ragged bimodal S2
1410	429.77	70.3	439	0.03	0.11	0.86	0.19	0.13	0.04	0.28	39	307	0.1	III	0.80	small, broad ragged bimodal S2
1430	435.86	70.0	441	0.07	0.10	0.52	0.40	0.19	0.03	0.15	67	347	0.0	III	0.85	small, broad ragged bimodal S2
1470	448.06	70.8	413	0.04	0.22	0.44	0.14	0.50	0.04	0.20	110	220	0.1	III		irregular S2 with left shoulder
1500	457.20	70.2	423	0.09	0.35	0.83	0.21	0.42	0.07	0.47	74	177	0.2	III	0.27	somewhat irregular with left shoulder
1530	466.34	70.3	313	0.22	0.44	1.44	0.33	0.31	0.12	0.48	92	300	0.1	III		small, broad ragged bimodal S2
1560	475.49	70.1	420	0.15	0.81	1.87	0.16	0.43	0.16	1.13	72	165	0.2	III	0.14	large left shoulder on S2
1590	484.63	70.7	418	0.25	0.57	1.05	0.31	0.54	0.11	0.73	78	144	0.1	III		small, broad irregular S2 curve
1620	493.78	70.3	423	0.11	0.20	0.75	0.36	0.27	0.05	0.29	69	259	0.1	III	0.27	small, broad ragged bimodal S2
1650	502.92	70.7	427	0.14	0.56	1.29	0.20	0.43	0.11	0.72	78	179	0.1	III	0.43	large left shoulder on S2
1680	512.06	71.0	420	0.12	0.79	1.24	0.13	0.64	0.13	0.91	87	136	0.1	III	0.14	large left shoulder on S2
1710	521.21	70.5	420	0.17	0.55	0.61	0.23	0.90	0.09	0.60	92	102	0.1	III	0.14	large left shoulder on S2
AVE			**416.3**													all values (23)
SD			**30.7**													
AVE			**422.0**													selected values (2)
SD			**1.4**													
										Taglu						
1740	530.35	70.6	411	0.09	0.39	2.14	0.20	0.18	0.11	0.66	59	324	0.2	III		irregular triangle shaped S2
1770	539.50	69.9	416	0.28	3.70	2.53	0.07	1.46	0.48	3.31	112	76	0.2	III		coal
1810	551.69	25.3	404	0.95	25.54	15.60	0.04	1.64	3.20	22.88	112	68	0.8	III		broad S2; coal
1830	557.78	70.4	408	0.64	12.55	7.63	0.05	1.64	1.57	10.91	115	70	0.4	III		broad S2; coal
1860	566.93	70.7	418	0.28	2.50	2.25	0.10	1.11	0.34	2.59	97	87	0.2	III		
1890	576.07	70.9	424	0.09	0.23	0.69	0.29	0.33	0.06	0.35	66	197	0.1	III	0.31	small, broad S2 curve
1920	585.22	70.0	421	0.05	0.13	0.64	0.27	0.20	0.05	0.24	54	267	0.1	III	0.18	bimodal ragged S2
1950	594.36	70.4	424	0.11	1.39	2.13	0.08	0.65	0.23	1.61	86	132	0.3	III	0.31	left shoulder on S2
1980	603.50	70.5	422	0.25	3.91	3.17	0.06	1.23	0.52	3.79	103	84	0.2	III	0.23	coal
2020	615.70	70.4	410	0.19	2.90	1.99	0.06	1.46	0.36	2.51	116	79	0.2	III		asymmetric S2 peak
2040	621.79	70.6	418	0.07	0.56	1.51	0.11	0.37	0.11	0.78	72	194	0.1	III		broad, left-shoulder on S2
2070	630.94	70.4	420	0.11	1.45	1.67	0.07	0.87	0.22	1.82	80	92	0.2	III	0.14	

Depth (ftKB)	Depth (mKB)	Qty (mg)	Tmax	S1	S2	S3	PI	S2/S3	PC (%)	TOC (%)	HI	OI	MINC (%)	Organic Type	%Roeq	Comments
2100	640.08	70.4	411	0.13	1.86	1.56	0.06	1.19	0.26	1.79	104	87	0.1	III		flat-top S2
2130	649.22	70.6	429	0.10	0.81	2.16	0.10	0.38	0.17	0.92	88	235	0.7	III	0.50	broad base, left shoulder
2160	658.37	70.0	436	0.11	0.41	2.13	0.21	0.19	0.13	0.48	85	444	0.6	III	0.72	large left shoulder on S2
2190	667.51	70.3	375	0.10	0.20	0.92	0.34	0.22	0.08	0.31	65	297	0.4	III		small, broad S2 curve
2220	676.66	70.8	427	0.05	0.19	1.38	0.20	0.14	0.08	0.41	46	337	0.4	III	0.43	left shoulder on S2
2250	685.80	71.0	425	0.10	0.47	1.50	0.18	0.31	0.14	0.75	63	200	0.7	III	0.35	left shoulder on S2
2280	694.94	70.4	424	0.09	0.29	1.08	0.24	0.27	0.09	0.62	47	174	0.7	III	0.31	small, broad S2 curve
2310	704.09	70.9	437	0.07	0.34	1.74	0.16	0.20	0.12	0.83	41	210	0.5	III	0.75	triangular shaped S2
2340	713.23	70.1	427	0.15	2.05	4.37	0.07	0.47	0.42	3.86	53	113	0.7	III	0.43	
2360	719.33	70.5	435	0.07	0.63	2.82	0.10	0.22	0.19	0.89	71	317	1.8	III	0.69	
2400	731.52	70.7	421	0.39	0.90	2.28	0.30	0.39	0.20	1.06	85	215	0.7	III	0.18	large left shoulder on S2
2430	740.66	70.4	433	0.08	0.21	2.82	0.26	0.07	0.30	0.48	44	588	2.2	III	0.63	bimodal S2
2460	749.81	70.3	419	0.63	1.03	2.53	0.38	0.41	0.23	0.88	117	288	0.6	III		small, broad S2 curve
2520	768.10	20.5	406	2.51	40.39	21.57	0.06	1.87	4.90	31.21	129	69	1.6	III		liptinite-rich coal with HCs in pores; **oil stain**
2540	774.19	70.7	406	0.58	2.49	2.19	0.19	1.14	0.42	1.93	129	113	1.5	III		broad S2 peak
2580	786.38	70.9	425	0.15	0.91	2.68	0.14	0.34	0.27	1.90	48	141	1.9	III	0.35	
2610	795.53	70.2	418	0.17	2.51	6.83	0.06	0.37	0.63	6.98	36	98	1.0	III		asymmetric S2; coal component
2640	804.67	70.4	419	0.20	5.38	7.49	0.04	0.72	0.90	8.99	60	83	2.4	III		asymmetric S2; coal component
2670	813.82	10.8	407	3.79	54.51	33.09	0.07	1.65	6.77	46.40	117	71	1.3	III		broad S2; slightly irregular peak, coal; **oil stain**
2700	822.96	25.6	420	2.17	39.07	16.29	0.05	2.40	4.41	23.67	165	69	0.9	III	0.14	bituminous shale with coal
2720	829.06	69.9	422	0.18	1.17	2.84	0.13	0.41	0.34	1.79	65	159	2.3	III	0.23	small shoulder on left side of S2
2760	841.25	70.5	408	0.34	0.82	1.44	0.29	0.57	0.18	0.88	93	164	1.2	III		multiple left shoulders and broad S2
2790	850.39	25.2	412	2.22	52.26	24.93	0.04	2.10	6.06	39.14	134	64	1.3	III		coal
2820	859.54	70.0	425	0.83	3.11	2.76	0.21	1.13	0.48	2.88	108	96	0.6	III	0.35	left shoulder on S2, coaly
2850	868.68	70.7	407	0.59	9.39	6.18	0.06	1.52	1.22	8.10	116	76	2.7	III		odd-shaped S2 peak, a bit broad
2880	877.82	70.7	411	1.09	17.18	10.07	0.06	1.71	2.12	15.00	115	67	1.8	III		a little asymmetric S2; coal
2910	886.97	10.4	411	2.53	51.27	32.08	0.05	1.60	6.39	43.89	117	73	1.4	III		coal
2925	891.54	70.2	414	0.17	0.95	6.54	0.15	0.15	0.36	1.38	69	474	1.3	III		irregular shaped S2; **core;** solid bitumen
2930	893.06	10.6	409	3.22	58.87	33.79	0.05	1.74	7.25	48.11	122	70	1.5	III		coal; oil stain
2970	905.26	70.2	408	1.10	20.71	11.73	0.05	1.77	2.57	16.74	124	70	2.9	III		coal
3000	914.40	70.1	401	0.47	2.13	2.86	0.18	0.74	0.47	1.85	115	155	1.9	III		irregular S2; left and right asymmetry
3030	923.54	70.1	418	0.48	3.27	3.48	0.13	0.94	0.50	2.89	113	120	1.1	III		S2 a bit broad, coaly
3060	932.69	70.6	422	0.37	1.97	2.32	0.16	0.85	0.32	2.17	91	107	0.9	III	0.23	small left shoulder, coaly
3100	944.88	20.3	410	2.26	56.20	31.05	0.04	1.81	6.74	46.41	121	67	1.6	III		coal; trace HC fluid inclusions
3120	950.98	70.4	412	1.14	27.54	13.31	0.04	2.07	3.17	20.33	135	65	0.7	III		coal
3140	957.07	70.1	424	0.19	1.67	3.40	0.10	0.49	0.33	2.55	65	133	1.6	III	0.31	broad base on S2, coaly
3180	969.26	70.4	423	0.13	0.52	0.72	0.20	0.72	0.09	0.56	93	129	0.4	III	0.27	left shoulder on S2
3210	978.41	70.6	426	0.34	1.47	1.78	0.19	0.83	0.24	1.71	86	104	0.6	III	0.39	small left shoulder
3240	987.55	70.9	418	0.36	2.37	2.93	0.13	0.81	0.37	2.39	99	123	1.4	III		small left shoulder
3270	996.70	70.9	421	0.43	2.38	3.28	0.15	0.73	0.44	3.12	76	105	3.8	III	0.18	small left shoulder, broad base on S2
3300	1005.84	70.0	422	0.53	1.51	2.00	0.26	0.76	0.25	1.45	104	138	0.5	III	0.23	large left shoulder on S2
3330	1014.98	71.0	425	0.48	0.98	1.10	0.33	0.89	0.17	0.96	102	115	0.5	III	0.35	large left shoulder on S2
3360	1024.13	69.8	423	0.48	1.60	1.96	0.23	0.82	0.26	1.43	112	137	0.8	III	0.27	multiple left shoulders on S2

Depth (ftKB)	Depth (mKB)	Qty (mg)	Tmax	S1	S2	S3	PI	S2/S3	PC (%)	TOC (%)	HI	OI	MINC (%)	Organic Type	%Roeq	Comments
3390	1033.27	70.2	418	0.12	0.28	0.72	0.30	0.39	0.07	0.38	74	189	1.3	III		large left shoulder on S2
3420	1042.42	10.5	412	2.57	62.06	36.90	0.04	1.68	7.67	52.52	118	70	1.6	III		coal; oil stain
3440	1048.51	70.0	422	0.41	2.34	1.81	0.15	1.29	0.33	2.15	109	84	0.3	III	0.23	small left shoulder on S2
3470	1057.66	69.9	420	0.07	0.56	0.98	0.11	0.57	0.11	0.88	64	111	0.3	III	0.14	
3510	1069.85	70.1	429	0.06	0.43	1.03	0.11	0.42	0.10	0.97	44	106	2.2	III	0.50	broad base on S2; recycled component?
3540	1078.99	20.5	417	2.22	47.22	37.77	0.04	1.25	6.28	51.86	91	73	1.5	III		coal
3570	1088.14	70.0	422	0.33	6.08	6.48	0.05	0.94	0.87	8.01	76	81	0.8	III	0.23	coal
3600	1097.28	69.7	402	0.84	14.66	22.53	0.05	0.65	2.62	27.94	52	81	1.3	III		asymmetric, irregular S2, coal
3630	1106.42	70.0	415	0.28	6.71	7.23	0.04	0.93	0.99	8.80	76	82	0.8	III		coal
3660	1115.57	70.3	419	0.05	0.23	0.62	0.18	0.37	0.06	0.45	51	138	0.3	III		asymmetric, irregular S2 peak
3690	1124.71	70.7	421	0.06	0.70	1.42	0.08	0.49	0.14	1.61	43	88	0.2	III	0.18	asymmetric S2, right-skewed
3700	**1127.76**	70.5	420	0.74	18.42	19.98	0.04	0.92	2.72	24.37	76	82	0.8	III	0.14	**core**; coaly
3700	**1127.76**	20.3	420	0.71	17.65	18.83	0.04	0.94	2.66	24.11	73	78	0.8	III	0.14	**core**; coaly
3720	1133.86	20.3	415	1.64	44.54	24.25	0.04	1.84	5.24	34.70	128	70	1.1	III		coal
3750	1143.00	69.7	421	0.15	1.23	0.98	0.11	1.26	0.17	1.21	102	81	0.2	III	0.18	
3780	1152.14	70.6	415	0.33	4.15	3.91	0.07	1.06	0.61	5.09	82	77	0.5	III		
3810	1161.29	70.3	427	0.07	0.57	1.23	0.10	0.46	0.11	0.88	65	140	2.9	III	0.43	broad base on S2; recycled component?
3840	1170.43	10.7	417	1.08	48.86	29.63	0.02	1.65	6.03	46.05	106	64	1.4	III		coal
3870	1179.58	70.7	406	0.65	17.84	11.19	0.04	1.59	2.26	17.35	103	64	2.3	III		irregular S2, right shoulder
3900	1188.72	50.6	410	1.42	38.23	22.00	0.04	1.74	4.56	31.97	120	69	1.9	III		irregular S2, right shoulder
3930	1197.86	20.6	420	0.81	26.32	23.45	0.03	1.12	3.64	30.77	86	76	1.9	III	0.14	two peaks on S2, coal
3960	1207.01	70.9	421	0.60	11.22	8.58	0.05	1.31	1.44	11.24	100	76	0.8	III	0.18	coal
3990	1216.15	20.2	416	1.24	31.21	22.16	0.04	1.41	4.01	31.15	100	71	1.5	III		coal
4020	1225.30	70.7	415	0.37	10.54	6.08	0.03	1.73	1.27	9.11	116	67	0.9	III		coal
4064	**1238.71**	70.6	431	0.06	2.41	3.33	0.03	0.72	0.40	5.01	48	66	0.4	III	0.57	**core; coaly, oil stain**
4090	1246.63	70.5	425	0.69	15.61	10.04	0.04	1.55	1.93	14.46	108	69	1.1	III	0.35	irregular S2 peak skewed to right, coal
4110	1252.73	70.7	408	0.58	18.50	12.45	0.03	1.49	2.30	18.41	100	68	1.1	III		irregular S2 peak skewed to left, coal
4140	1261.87	71.1	414	0.12	0.55	0.60	0.18	0.92	0.10	0.67	82	90	0.2	III		somewhat irregular, broad base
4170	1271.02	70.3	409	0.61	16.48	11.74	0.04	1.40	2.12	17.41	95	67	1.1	III		irregular S2, right shoulder, coal, bituminous shale
4200	1280.16	70.3	425	0.15	0.52	0.59	0.23	0.88	0.09	0.63	83	94	0.9	III	0.35	broad S2, left & right shoulders
4230	1289.30	20.8	413	1.57	40.82	23.76	0.04	1.72	4.99	36.79	111	65	1.2	III		coal
4260	1298.45	20.2	419	1.21	40.26	24.53	0.03	1.64	4.89	37.19	108	66	1.2	III		coal
4290	1307.59	70.1	416	0.90	25.31	17.87	0.03	1.42	3.18	25.61	99	70	1.3	III		coal
4320	1316.74	70.6	415	0.38	10.80	9.93	0.03	1.09	1.51	13.82	78	72	0.8	III		asymmetric S2, right-skewed, coaly
4350	1325.88	70.3	427	0.43	11.93	10.75	0.03	1.11	1.67	14.57	82	74	1.5	III	0.43	two peaks on S2, coal
4380	1335.02	70.1	418	0.27	5.51	4.75	0.05	1.16	0.76	6.88	80	69	0.6	III		broad S2
4410	1344.17	70.7	415	0.18	1.57	4.44	0.10	0.35	0.39	2.73	58	163	1.2	III		irregular S2, right shoulder
4440	1353.31	70.9	416	0.18	3.14	3.55	0.05	0.88	0.50	4.64	68	77	0.8	III		
4470	1362.46	70.1	410	0.46	12.26	11.77	0.04	1.04	1.72	15.68	78	75	0.9	III		coal
4500	1371.60	20.7	413	0.70	25.99	16.89	0.03	1.54	3.27	26.06	100	65	1.6	III		somewhat irregular S2, coal
4530	1380.74	70.8	410	0.79	14.10	8.27	0.05	1.70	1.74	12.96	109	64	1.0	III		irrgular asymmetric peak, coal
4570	1392.94	69.7	412	1.06	18.83	11.05	0.05	1.70	2.33	17.09	110	65	1.1	III		somewhat irregular, broad S2, coal, oil stain
4590	1399.03	10.7	412	1.59	51.99	27.89	0.03	1.86	6.22	46.09	113	61	1.4	III		somewhat irregular, broad S2, coal, oil stain

Depth (ftKB)	Depth (mKB)	Qty (mg)	Tmax	S1	S2	S3	PI	S2/S3	PC (%)	TOC (%)	HI	OI	MINC (%)	Organic Type	%Roeq	Comments
4620	1408.18	70.7	412	0.26	8.75	5.66	0.03	1.55	1.10	8.81	99	64	0.4	III		somewhat irregular S2, right-skewed, coal
4650	1417.32	20.8	414	1.09	47.24	28.34	0.02	1.67	5.68	46.40	102	61	1.3	III		coal
4690	1429.51	70.7	415	0.94	21.00	11.24	0.04	1.87	2.50	18.14	116	62	1.0	III		irrgular asymmetric peak, coal
4700	1432.56	50.2	408	0.76	26.20	20.90	0.03	1.25	3.50	31.65	83	66	2.0	III		irregular S2, right shoulder, coal
4740	1444.75	50.5	410	1.01	27.30	17.94	0.04	1.52	3.41	26.98	101	66	1.3	III		coal
4770	**1453.90**	70.6	433	0.04	0.73	1.16	0.05	0.63	0.11	1.19	61	97	0.4	III	0.63	**core**
4800	1463.04	50.4	420	1.05	35.45	21.44	0.03	1.65	4.29	34.41	103	62	0.8	III	0.14	coal
4830	1472.18	20.5	406	4.74	74.11	29.58	0.06	2.51	8.38	49.42	150	60	1.2	III		asymmetric broad S2; coal; oil stain
4860	1481.33	70.5	421	0.45	11.34	5.71	0.04	1.99	1.33	9.08	125	63	1.1	III	0.18	coal
4890	1490.47	70.0	415	0.44	15.34	11.87	0.03	1.29	1.99	17.42	88	68	1.5	III		coal
4920	1499.62	70.2	405	1.75	21.09	16.61	0.08	1.27	2.88	24.42	86	68	2.2	III		somewhat asymmetric broad S2, coal
4950	1508.76	70.8	418	0.59	20.25	14.69	0.03	1.38	2.58	22.13	92	66	1.0	III		coal cavings?
4980	1517.90	70.2	415	0.27	8.80	5.36	0.03	1.64	1.08	8.74	101	61	0.5	III		coal cavings?
5010	1527.05	70.3	418	0.16	4.46	5.19	0.03	0.86	0.69	6.77	66	77	1.6	III		broad, flat-topped S2, coal caving?
5090	1551.43	70.6	416	0.08	1.07	2.10	0.07	0.51	0.21	2.38	45	88	0.9	III		broad base in S2, right-skewed
5100	1554.48	70.4	417	0.13	2.90	2.26	0.04	1.28	0.39	3.20	91	71	0.4	III		
5140	1566.67	70.5	417	0.16	3.68	3.06	0.04	1.20	0.48	4.16	88	74	0.8	III		
5170	1575.82	70.1	422	0.21	2.56	2.77	0.07	0.92	0.38	3.60	71	77	1.2	III	0.23	
5220	1591.06	70.6	414	0.34	3.94	3.30	0.08	1.19	0.55	4.53	87	73	1.2	III		broad S2
5250	1600.20	70.4	408	0.45	0.92	1.04	0.33	0.88	0.18	0.90	102	116	0.8	III		bimodal S2
5270	1606.30	70.8	425	0.14	0.37	1.04	0.27	0.36	0.11	0.63	59	165	1.1	III	0.35	broad S2 has large left shoulder, right shoulder
5322.5	**1622.30**	70.5	426	0.08	0.99	2.53	0.08	0.39	0.18	1.22	81	207	0.5	III	0.39	**core**; asymmetric S2
AVE			**417.1**													all values (120)
SD			**8.3**													
AVE			**417.4**													selected values (75)
SD			**6.6**													
AVE			**422.1**													selected values excluding TOC>5 wt% (30)
SD			**5.3**													
													Aklak			
5400	1645.92	70.0	424	0.23	2.94	3.02	0.07	0.97	0.43	3.82	77	79	0.9	III	0.31	
5430	1655.06	70.2	421	0.15	1.06	1.71	0.12	0.62	0.19	1.83	58	93	0.7	III	0.18	small left shoulder on S2
5460	1664.21	70.3	420	0.11	0.88	1.31	0.11	0.67	0.14	1.30	68	101	0.7	III	0.14	left shoulder on S2, switched to gel chem system, oil stain
5510	1679.45	70.5	410	0.58	1.22	1.19	0.32	1.03	0.22	0.91	134	131	1.0	III		large shoulder on S2
5525	**1684.02**	70.0	420	0.11	0.83	1.51	0.12	0.55	0.14	0.77	108	196	0.5	III	0.14	irregular S2 curve skewed to left; **core**
5650	1722.12	70.5	304	0.81	1.71	1.34	0.32	1.28	0.27	1.26	136	106	0.9	III		bimodal S2
5700	1737.36	71.1	421	0.43	0.92	0.90	0.32	1.02	0.17	0.94	98	96	1.6	III	0.18	large left shoulder on S2
5720	1743.46	70.1	421	0.45	1.24	1.16	0.27	1.07	0.20	1.16	107	100	0.8	III	0.18	large left shoulder on S2; trace oil stain & fluorescence; gas kick
5790	1764.79	70.7	414	0.56	1.09	0.99	0.34	1.10	0.19	0.97	112	102	0.9	III		large left shoulder on S2
5820	1773.94	70.0	423	0.69	1.25	1.12	0.35	1.12	0.22	1.06	118	106	0.9	III	0.27	large left shoulder on S2
5860	1786.13	70.7	423	0.33	0.65	0.80	0.34	0.81	0.13	0.84	77	95	1.1	III	0.27	large left shoulder on S2
5890	1795.27	70.8	427	0.17	0.37	0.72	0.31	0.51	0.10	0.54	69	133	1.0	III	0.43	left shoulder on S2
5910	1801.37	70.1	420	0.30	0.64	0.80	0.32	0.80	0.13	0.63	102	127	0.8	III	0.14	left shoulder on S2
5940	1810.51	70.6	425	0.13	0.58	0.88	0.18	0.66	0.11	1.06	55	83	1.0	III	0.35	small left shoulder on S2, broad base

Depth (ftKB)	Depth (mKB)	Qty (mg)	Tmax	S1	S2	S3	PI	S2/S3	PC (%)	TOC (%)	HI	OI	MINC (%)	Organic Type	%Roeq	Comments
5970	1819.66	70.0	420	0.21	0.38	0.52	0.36	0.73	0.08	0.53	72	98	1.7	III	0.14	large left shoulder on S2
6000	1828.80	70.7	422	0.31	0.66	0.83	0.32	0.80	0.13	0.68	97	122	1.6	III	0.23	large left shoulder on S2
6030	1837.94	70.0	421	0.49	0.70	0.55	0.41	1.27	0.14	0.62	113	89	0.8	III	0.18	large left shoulder on S2
6070	1850.14	70.1	415	1.02	1.37	0.86	0.43	1.59	0.28	0.92	149	93	1.2	III		large left shoulder on S2
6090	1856.23	70.6	421	0.36	0.85	0.89	0.29	0.96	0.16	0.85	100	105	1.5	III	0.18	left shoulder on S2
6105	**1860.80**	70.9	420	0.27	1.20	1.08	0.19	1.11	0.20	0.95	126	114	0.9	III	0.14	bimodal S2; **core**
6130	1868.42	70.6	427	0.21	0.67	1.05	0.24	0.64	0.13	0.85	79	124	0.9	III	0.43	small left shoulder on S2
6150	1874.52	70.9	401	0.29	1.08	0.88	0.21	1.23	0.17	1.02	106	86	0.5	III		irregular S2, large left shoulder
6180	1883.66	70.0	413	0.27	1.38	1.26	0.16	1.10	0.21	1.26	110	100	1.0	III		broad S2, left shoulder
6210	1892.81	70.8	420	0.17	0.66	0.96	0.21	0.69	0.13	0.70	94	137	0.9	III	0.14	left shoulder on S2
6240	1901.95	70.7	424	0.31	1.07	1.19	0.23	0.90	0.18	1.06	101	112	1.5	III	0.31	large left shoulder on S2
6270	1911.10	71.0	424	0.29	1.29	1.38	0.18	0.93	0.20	1.39	93	99	0.9	III	0.31	small left shoulder on S2
6300	1920.24	70.6	425	0.26	0.98	1.32	0.21	0.74	0.19	1.09	90	121	1.1	III	0.35	small left shoulder on S2
6330	1929.38	70.5	421	0.35	1.25	1.27	0.22	0.98	0.20	1.35	93	94	1.0	III	0.18	small left shoulder on S2
6350	1935.48	70.6	431	0.26	1.03	1.15	0.20	0.90	0.17	1.09	94	106	0.9	III	0.57	small left shoulder on S2
6390	1947.67	70.6	426	0.24	1.20	1.56	0.16	0.77	0.19	1.22	98	128	0.6	III	0.39	small left shoulder on S2
6420	1956.82	71.1	425	0.40	1.35	1.58	0.23	0.85	0.22	1.17	115	135	0.7	III	0.35	left shoulder on S2
6450	1965.96	70.5	419	0.41	1.13	0.95	0.27	1.19	0.17	0.91	124	104	0.6	III		irregular S2, large left shoulder
6480	1975.10	70.4	423	0.59	1.47	1.22	0.29	1.20	0.23	1.12	131	109	0.7	III	0.27	irregular S2, large left shoulder
6510	1984.25	70.9	425	0.41	1.74	1.78	0.19	0.98	0.26	1.55	112	115	0.7	III	0.35	small left shoulder on S2
6540	1993.39	70.3	424	0.43	1.35	1.26	0.24	1.07	0.21	1.20	112	105	0.7	III	0.31	large left shoulder on S2, trace fluorescence
6570	2002.54	70.6	427	0.32	1.20	1.47	0.21	0.82	0.21	1.32	91	111	0.8	III	0.43	small left shoulder on S2, fair fluorescence
6610	2014.73	70.5	427	0.18	0.78	1.07	0.19	0.73	0.13	1.01	77	106	0.7	III	0.43	small left shoulder on S2
6626	**2019.60**	70.1	422	0.22	1.94	1.65	0.10	1.18	0.26	1.56	124	106	0.7	III	0.23	large left shoulder on S2; **core**
6660	2029.97	70.6	425	0.21	0.83	1.04	0.20	0.80	0.14	0.88	94	118	0.8	III	0.35	large left shoulder on S2
6690	2039.11	70.7	427	0.17	0.86	1.12	0.16	0.77	0.14	1.07	80	105	0.8	III	0.43	small left shoulder on S2
6720	2048.26	70.2	429	0.16	0.98	1.21	0.14	0.81	0.15	1.13	87	107	0.7	III	0.50	
6750	2057.40	70.7	427	0.26	1.33	1.31	0.16	1.02	0.20	1.39	96	94	0.7	III	0.43	small left shoulder on S2
6780	2066.54	70.8	428	0.17	1.06	1.43	0.14	0.74	0.19	1.29	82	111	0.8	III	0.47	small left shoulder on S2
6810	2075.69	70.4	425	0.16	0.85	1.41	0.16	0.60	0.15	0.95	89	148	1.0	III	0.35	small left shoulder on S2, trace fluorescence
6840	2084.83	70.7	424	0.29	1.14	1.40	0.20	0.81	0.20	1.30	88	108	0.8	III	0.31	small left shoulder on S2
6862	**2091.54**	70.5	425	0.18	1.43	1.46	0.11	0.98	0.21	1.38	104	106	0.6	III	0.35	left shoulder on S2 curve; **core; trace to fair fluorescence**
6883.5	**2098.09**	70.0	426	0.10	1.43	1.64	0.06	0.87	0.20	1.53	93	107	0.7	III	0.39	asymmetric S2, left shoulder; **core**
6900	2103.12	70.8	421	0.30	1.44	1.50	0.17	0.96	0.23	1.39	104	108	0.7	III	0.18	left shoulder on S2
6930	2112.26	70.6	426	0.15	1.01	1.48	0.13	0.68	0.17	1.17	86	126	0.7	III	0.39	small left shoulder on S2
6960	2121.41	70.9	425	0.23	1.23	1.25	0.16	0.98	0.19	1.39	88	90	0.6	III	0.35	small left shoulder on S2
6990	2130.55	70.3	427	0.18	1.01	1.27	0.15	0.80	0.16	1.16	87	109	0.6	III	0.43	small left shoulder on S2
7020	2139.70	70.4	427	0.18	1.08	1.52	0.14	0.71	0.18	1.29	84	118	0.9	III	0.43	small left shoulder on S2
7050	2148.84	70.9	426	0.25	1.14	1.37	0.18	0.83	0.19	1.25	91	110	0.6	III	0.39	left shoulder on S2
7070	2154.94	70.1	427	0.19	1.09	1.16	0.15	0.94	0.16	1.35	81	86	0.7	III	0.43	small left shoulder on S2
7090	2161.03	70.8	425	0.42	1.21	1.27	0.26	0.95	0.21	1.13	107	112	0.8	III	0.35	large left shoulder on S2
7140	2176.27	70.4	425	0.25	1.25	1.59	0.17	0.79	0.20	1.25	100	127	0.7	III	0.35	left shoulder on S2
7170	2185.42	70.8	426	0.20	1.05	1.49	0.16	0.70	0.18	1.18	89	126	0.9	III	0.39	small left shoulder on S2

Depth (ftKB)	Depth (mKB)	Qty (mg)	Tmax	S1	S2	S3	PI	S2/S3	PC (%)	TOC (%)	HI	OI	MINC (%)	Organic Type	%Roeq	Comments
7200	2194.56	70.6	427	0.25	1.39	1.67	0.15	0.83	0.20	1.43	97	117	0.7	III	0.43	small left shoulder on S2
7230	2203.70	70.5	426	0.29	1.23	1.29	0.19	0.95	0.18	1.22	101	106	0.6	III	0.39	small left shoulder on S2
7271.5	**2216.35**	70.8	427	0.16	1.58	1.80	0.09	0.88	0.23	1.63	97	110	0.6	III	0.43	small left shoulder; **core; exudatinite**
7290	2221.99	70.8	427	0.19	0.99	1.05	0.16	0.94	0.15	1.07	93	98	0.5	III	0.43	small left shoulder on S2
7320	2231.14	70.3	426	0.25	1.16	1.29	0.18	0.90	0.18	1.15	101	112	0.9	III	0.39	small left shoulder on S2
7350	2240.28	70.7	427	0.16	1.03	1.37	0.13	0.75	0.17	1.28	80	107	0.7	III	0.43	small left shoulder on S2
7380	2249.42	70.5	428	0.19	1.06	1.40	0.15	0.76	0.18	1.26	84	111	0.7	III	0.47	small left shoulder on S2; oil stain
7410	2258.57	70.0	426	0.29	1.35	1.37	0.17	0.99	0.20	1.29	105	106	0.9	III	0.39	large left shoulder on S2
7440	2267.71	71.1	428	0.13	0.73	1.29	0.15	0.57	0.14	1.00	73	129	0.7	III	0.47	small left shoulder on S2
7470	2276.86	70.9	427	0.29	1.31	1.52	0.18	0.86	0.20	1.35	97	113	0.6	III	0.43	small left shoulder on S2
7500	2286.00	70.0	423	0.30	1.32	1.80	0.19	0.73	0.25	1.39	95	129	1.1	III	0.27	small left shoulder on S2
7530	2295.14	71.1	425	0.24	1.10	1.52	0.18	0.72	0.20	1.17	94	130	0.9	III	0.35	small left shoulder on S2
7560	2304.29	70.8	428	0.22	1.18	1.99	0.16	0.59	0.20	1.47	80	135	0.6	III	0.47	small left shoulder on S2
7590	2313.43	70.2	426	0.19	0.98	1.86	0.16	0.53	0.19	1.15	85	162	1.2	III	0.39	small left shoulder on S2
7620	2322.58	70.0	428	0.23	1.18	1.81	0.16	0.65	0.19	1.41	84	128	0.6	III	0.47	small left shoulder on S2
7650	2331.72	69.8	429	0.24	1.22	1.70	0.16	0.72	0.20	1.44	85	118	0.6	III	0.50	small left shoulder on S2
7680	2340.86	70.5	427	0.34	1.51	1.87	0.18	0.81	0.23	1.49	101	126	0.6	III	0.43	small left shoulder on S2
7710	2350.01	70.8	428	0.20	1.14	1.58	0.15	0.72	0.19	1.34	85	118	0.7	III	0.47	small left shoulder on S2
7740	2359.15	70.2	429	0.20	1.21	1.67	0.14	0.72	0.19	1.32	92	127	0.6	III	0.50	small left shoulder on S2
7770	2368.30	70.9	427	0.22	1.24	1.58	0.15	0.78	0.19	1.39	89	114	0.6	III	0.43	small left shoulder on S2
7800	2377.44	69.9	428	0.15	0.87	1.09	0.14	0.80	0.13	0.96	91	114	0.4	III	0.47	small left shoulder on S2
7820	2383.54	71.0	429	0.23	1.37	1.33	0.15	1.03	0.20	1.44	95	92	0.5	III	0.50	small left shoulder on S2
7837.5	**2388.87**	70.5	428	0.40	2.38	2.22	0.14	1.07	0.32	1.93	123	115	0.5	III	0.47	bimodal S2; **core; pore filling exudatinite**
7860	2395.73	70.1	427	0.21	1.16	2.19	0.15	0.53	0.25	1.43	81	153	1.0	III	0.43	small left shoulder on S2
7890	2404.87	70.3	427	0.35	1.44	1.86	0.20	0.77	0.24	1.54	94	121	0.6	III	0.43	small left shoulder on S2
7920	2414.02	70.5	427	0.24	1.28	1.71	0.16	0.75	0.21	1.32	97	130	0.6	III	0.43	small left shoulder on S2
7942.5	**2420.87**	71.0	427	0.23	1.64	1.37	0.12	1.20	0.23	1.41	116	97	0.6	III	0.43	bimodal S2; **core; pore filling exudatinite**
7950	2423.16	70.7	428	0.26	1.52	1.89	0.15	0.80	0.23	1.64	93	115	0.6	III	0.47	small left shoulder on S2
7980	2432.30	70.9	427	0.23	1.16	1.34	0.16	0.87	0.18	1.20	97	112	0.6	III	0.43	small left shoulder on S2
8010	2441.45	70.2	426	0.32	1.22	1.55	0.21	0.79	0.19	1.20	102	129	0.6	III	0.39	left shoulder on S2
8040	2450.59	70.4	430	0.23	1.22	1.02	0.16	1.20	0.17	1.30	94	78	0.4	III	0.54	small left shoulder on S2
8070	2459.74	70.9	429	0.28	1.39	3.74	0.17	0.37	0.31	1.65	84	227	1.0	III	0.50	small left shoulder on S2
8100	2468.88	70.7	428	0.18	1.09	1.82	0.14	0.60	0.20	1.33	82	137	0.6	III	0.47	small left shoulder on S2
8130	2478.02	70.3	425	0.39	1.67	2.22	0.19	0.75	0.27	1.58	106	141	0.8	III	0.35	small left shoulder on S2
8160	2487.17	70.2	427	0.28	1.32	1.77	0.18	0.75	0.22	1.38	96	128	0.6	III	0.43	small left shoulder on S2
8180	2493.26	70.1	426	0.26	1.52	1.55	0.14	0.98	0.22	1.49	102	104	0.6	III	0.39	Two left shoulders on S2
8220	2505.46	70.9	427	0.32	1.69	2.45	0.16	0.69	0.28	1.71	99	143	0.8	III	0.43	small left shoulder on S2
8250	2514.60	71.1	427	0.23	1.20	2.40	0.16	0.50	0.25	1.45	83	166	1.1	III	0.43	small left shoulder on S2
8280	2523.74	70.4	429	0.26	1.39	2.07	0.16	0.67	0.22	1.61	86	129	0.6	III	0.50	small left shoulder on S2
8310	2532.89	70.7	428	0.32	1.42	1.94	0.18	0.73	0.24	1.52	93	128	0.9	III	0.47	small left shoulder on S2
8340	2542.03	70.2	427	0.43	1.63	1.78	0.21	0.92	0.26	1.64	99	109	0.7	III	0.43	left shoulder on S2
8376.5	**2553.16**	70.5	431	0.07	0.84	1.05	0.08	0.80	0.14	1.16	72	91	0.6	III	0.57	**core; trace HC fluid inclusions**
8390	2557.27	70.4	426	0.45	1.49	1.60	0.23	0.93	0.23	1.55	96	103	0.7	III	0.39	left shoulder on S2

Depth (ftKB)	Depth (mKB)	Qty (mg)	Tmax	S1	S2	S3	PI	S2/S3	PC (%)	TOC (%)	HI	OI	MINC (%)	Organic Type	%Roeq	Comments
8400	2560.32	70.3	428	0.34	1.36	1.73	0.20	0.79	0.22	1.42	96	122	0.8	III	0.47	small left shoulder on S2
8430	2569.46	70.3	427	0.26	1.15	1.57	0.18	0.73	0.19	1.26	91	125	0.7	III	0.43	small left shoulder on S2
8460	2578.61	70.6	428	0.32	1.56	1.98	0.17	0.79	0.25	1.62	96	122	0.6	III	0.47	small left shoulder on S2
8490	2587.75	70.9	429	0.25	1.20	1.87	0.17	0.64	0.21	1.42	85	132	0.7	III	0.50	small left shoulder on S2
8520	2596.90	70.6	428	0.29	1.48	2.06	0.16	0.72	0.24	1.62	91	127	0.6	III	0.47	small left shoulder on S2
8550	2606.04	70.8	429	0.33	1.71	1.75	0.16	0.98	0.25	1.63	105	107	0.6	III	0.50	small left shoulder on S2
8580	2615.18	70.5	422	0.43	1.57	1.72	0.21	0.91	0.25	1.51	104	114	0.8	III	0.23	left shoulder on S2; asymmetric peak
8640	2633.47	70.2	426	0.53	1.51	1.47	0.26	1.03	0.25	1.52	99	97	0.7	III	0.39	large left shoulder on S2
8610	2624.33	70.0	430	0.32	1.21	1.20	0.21	1.01	0.19	1.43	85	84	0.6	III	0.54	small left shoulder on S2
8670	2642.62	70.6	430	0.28	0.93	1.39	0.23	0.67	0.16	1.08	86	129	0.5	III	0.54	small left shoulder on S2
8700	2651.76	70.4	430	0.27	1.22	1.48	0.18	0.82	0.19	1.42	86	104	0.6	III	0.54	small left shoulder on S2
8730	2660.90	70.6	424	0.56	1.67	1.44	0.25	1.16	0.26	1.55	108	93	0.8	III	0.31	large left shoulder on S2
8760	2670.05	70.3	428	0.34	1.25	1.12	0.21	1.12	0.18	1.35	93	83	0.6	III	0.47	small left shoulder on S2
8790	2679.19	70.5	432	0.20	0.89	1.07	0.19	0.83	0.15	1.18	75	91	0.8	III	0.60	small left shoulder on S2
8820	2688.34	71.0	426	0.51	1.41	1.27	0.26	1.11	0.23	1.39	101	91	0.8	III	0.39	small left shoulder on S2
8850	2697.48	70.8	427	0.63	1.89	1.83	0.25	1.03	0.30	1.78	106	103	0.7	III	0.43	small left shoulder on S2
8880	2706.62	70.9	422	0.65	1.72	1.33	0.27	1.29	0.26	1.50	115	89	0.8	III	0.23	left shoulder on S2
8910	2715.77	70.1	428	0.36	1.24	1.58	0.22	0.78	0.21	1.26	98	125	1.5	III	0.47	small left shoulder on S2
8928	**2721.25**	70.4	434	0.10	1.09	1.62	0.09	0.67	0.17	1.39	78	117	0.4	III	0.66	**core; trace HC fluid inclusions**
8970	2734.06	70.2	428	0.39	1.13	1.04	0.26	1.09	0.18	1.14	99	91	0.6	III	0.47	small left shoulder on S2
9000	2743.20	70.5	425	0.82	1.64	1.18	0.33	1.39	0.25	1.35	121	87	0.6	III	0.35	large left shoulder on S2
9020	2749.30	70.5	427	0.67	1.85	1.48	0.27	1.25	0.27	1.74	106	85	0.6	III	0.43	small left shoulder on S2
9060	2761.49	70.8	427	0.70	1.65	1.29	0.30	1.28	0.25	1.39	119	93	0.5	III	0.43	large left shoulder on S2
9090	2770.63	71.1	425	0.47	1.31	1.51	0.26	0.87	0.21	1.29	102	117	0.6	III	0.35	small left shoulder on S2
9120	2779.78	70.4	429	0.47	1.14	1.02	0.29	1.12	0.18	1.26	90	81	0.8	III	0.50	small left shoulder on S2
9150	2788.92	70.6	425	0.41	1.26	1.57	0.25	0.80	0.22	1.32	95	119	0.8	III	0.35	small left shoulder on S2
9180	2798.06	70.7	430	0.44	1.55	1.25	0.22	1.24	0.22	1.48	105	84	0.4	III	0.54	small left shoulder on S2
9210	2807.21	70.4	427	0.50	1.55	2.11	0.24	0.73	0.28	1.69	92	125	0.9	III	0.43	small left shoulder on S2
9240	2816.35	70.1	429	0.33	1.25	1.52	0.21	0.82	0.21	1.32	95	115	0.6	III	0.50	small left shoulder on S2
9260	2822.45	70.1	429	0.50	1.58	1.40	0.24	1.13	0.24	1.57	101	89	0.6	III	0.50	small left shoulder on S2
9310	2837.69	69.9	428	0.60	1.61	1.44	0.27	1.12	0.25	1.46	110	99	0.6	III	0.47	small left shoulder on S2
9330	2843.78	70.4	427	0.64	1.66	1.01	0.28	1.64	0.25	1.58	105	64	0.5	III	0.43	small left shoulder on S2
9360	2852.93	70.6	425	0.50	1.21	1.17	0.29	1.03	0.20	1.16	104	101	0.5	III	0.35	left shoulder on S2
9390	2862.07	70.0	425	0.63	1.56	1.01	0.29	1.54	0.23	1.39	112	73	0.7	III	0.35	left shoulder on S2
9420	2871.22	70.6	427	0.53	1.44	1.27	0.27	1.13	0.24	1.44	100	88	0.7	III	0.43	small left shoulder on S2; minute oil may be present
9450	2880.36	70.9	429	0.59	1.29	0.99	0.31	1.30	0.20	1.31	98	76	0.6	III	0.50	small left shoulder on S2; minute oil may be present
9480	2889.50	70.8	430	0.44	1.16	1.07	0.27	1.08	0.19	1.33	87	80	0.6	III	0.54	small left shoulder on S2; minute oil may be present
9510	2898.65	70.9	428	0.66	1.38	1.09	0.32	1.27	0.23	1.43	97	76	0.6	III	0.47	small left shoulder on S2; minute oil may be present
9540	2907.79	70.1	430	0.50	1.18	1.14	0.30	1.04	0.19	1.35	87	84	0.6	III	0.54	small left shoulder on S2
9570	2916.94	70.4	427	0.75	1.91	1.12	0.28	1.71	0.28	1.78	107	63	0.6	III	0.43	left shoulder on S2
9590	**2923.03**	70.3	434	0.16	1.32	1.99	0.11	0.66	0.20	1.59	83	125	0.5	III	0.66	small left shoulder; **core; trace HC fluid inclusions**
9600	2926.08	69.7	431	0.71	1.82	1.28	0.28	1.42	0.26	1.65	110	78	0.5	III	0.57	small left shoulder on S2
9630	2935.22	70.4	429	0.68	1.59	1.07	0.30	1.49	0.24	1.47	108	73	0.6	III	0.50	small left shoulder on S2

Depth (ftKB)	Depth (mKB)	Qty (mg)	Tmax	S1	S2	S3	PI	S2/S3	PC (%)	TOC (%)	HI	OI	MINC (%)	Organic Type	%Roeq	Comments
9660	2944.37	70.7	432	0.55	1.60	1.33	0.26	1.20	0.24	1.51	106	88	0.4	III	0.60	small left shoulder on S2
9690	2953.51	70.1	431	0.47	1.34	1.63	0.26	0.82	0.22	1.45	92	112	0.6	III	0.57	small left shoulder on S2
9720	2962.66	70.3	425	0.74	1.58	0.92	0.32	1.72	0.24	1.43	110	64	0.7	III	0.35	small left shoulder on S2
9750	2971.80	70.6	429	0.65	1.53	1.12	0.30	1.37	0.24	1.45	106	77	0.7	III	0.50	small left shoulder on S2
9780	2980.94	70.2	430	0.50	1.38	1.13	0.26	1.22	0.22	1.46	95	77	0.6	III	0.54	small left shoulder on S2
9810	2990.09	70.3	429	0.43	1.22	0.85	0.26	1.44	0.19	1.31	93	65	0.8	III	0.50	small left shoulder on S2
9840	2999.23	70.0	429	0.47	1.15	0.84	0.29	1.37	0.18	1.23	93	68	0.7	III	0.50	small left shoulder on S2
9870	3008.38	70.1	432	0.40	1.21	0.73	0.25	1.66	0.18	1.41	86	52	0.7	III	0.60	small left shoulder on S2
9900	3017.52	70.9	429	0.34	1.16	1.29	0.23	0.90	0.24	1.40	83	92	1.0	III	0.50	small left shoulder on S2
9930	3026.66	70.0	429	0.53	1.34	0.75	0.28	1.79	0.22	1.36	99	55	0.7	III	0.50	small left shoulder on S2
9960	3035.81	70.9	432	0.34	1.19	0.77	0.22	1.55	0.18	1.29	92	60	0.6	III	0.60	small left shoulder on S2
9980	3041.90	70.0	431	0.37	1.31	0.83	0.22	1.58	0.19	1.43	92	58	0.6	III	0.57	small left shoulder on S2
10020	3054.10	70.2	425	1.10	1.80	0.50	0.38	3.60	0.28	1.35	133	37	0.9	III	0.35	bimodal S2
10028	**3056.53**	70.6	434	0.18	1.45	0.62	0.11	2.34	0.18	1.50	97	41	1.0	III	0.66	left shoulder on S2 curve; **core; trace HC fluid inclusions**
10050	3063.24	69.9	426	0.31	1.04	0.84	0.23	1.24	0.17	1.28	81	66	0.8	III	0.39	left shoulder on S2; irregular peak
10080	3072.38	70.4	431	0.43	1.34	0.73	0.24	1.84	0.19	1.42	94	51	0.6	III	0.57	small left shoulder on S2
10110	3081.53	70.6	428	0.27	1.13	1.28	0.19	0.88	0.22	1.31	86	98	0.9	III	0.47	small left shoulder on S2; bituminous partings
10130	3087.62	70.0	431	0.44	1.11	0.58	0.28	1.91	0.17	1.14	97	51	0.6	III	0.57	left shoulder on S2
10170	3099.82	70.4	432	0.47	1.22	0.78	0.28	1.56	0.18	1.21	101	64	0.9	III	0.60	small left shoulder on S2; pyrobitumen - gilsonite-type
10200	3108.96	70.3	429	0.42	1.04	0.73	0.29	1.42	0.17	1.18	88	62	0.7	III	0.50	left shoulder on S2
10230	3118.10	70.6	431	0.23	0.98	1.30	0.19	0.75	0.15	1.22	80	107	0.6	III	0.57	small left shoulder on S2
10260	3127.25	70.4	433	0.30	1.02	0.78	0.23	1.31	0.14	1.22	84	64	0.5	III	0.63	small left shoulder on S2
10290	3136.39	70.1	430	0.23	0.69	0.65	0.25	1.06	0.11	1.01	68	64	0.6	III	0.54	small left shoulder on S2; black bituminous partings
10320	3145.54	70.6	427	0.52	1.55	0.85	0.25	1.82	0.22	1.35	115	63	0.5	III	0.43	large left shoulder on S2
10351.5	**3155.14**	70.3	436	0.07	0.67	0.36	0.10	1.86	0.08	0.95	71	38	0.3	III	0.72	left shoulder on S2 curve; **core; trace HC fluid inclusions**
10380	3163.82	69.9	431	0.40	1.13	0.70	0.26	1.61	0.17	1.19	95	59	0.4	III	0.57	left shoulder on S2
10410	3172.97	70.8	434	0.22	1.01	1.83	0.18	0.55	0.20	1.34	75	137	0.5	III	0.66	small left shoulder on S2
10440	3182.11	70.5	432	0.15	0.74	0.94	0.17	0.79	0.11	1.20	62	78	0.6	III	0.60	small left shoulder on S2
10470	3191.26	69.8	431	0.16	0.53	0.58	0.23	0.91	0.09	1.01	52	57	0.4	III	0.57	small left shoulder on S2
10500	3200.40	70.8	434	0.13	0.51	0.51	0.21	1.00	0.07	0.94	54	54	0.6	III	0.66	small left shoulder on S2
10530	3209.54	70.0	432	0.22	0.77	0.95	0.22	0.81	0.13	0.96	80	99	1.1	III	0.60	small left shoulder on S2
10560	3218.69	70.9	434	0.21	0.84	0.69	0.20	1.22	0.12	1.07	79	64	0.5	III	0.66	small left shoulder on S2
10590	3227.83	70.1	435	0.17	0.78	0.59	0.18	1.32	0.11	1.07	73	55	0.6	III	0.69	small left shoulder on S2
10620	3236.98	70.4	431	0.21	0.90	0.55	0.19	1.64	0.12	1.05	86	52	0.6	III	0.57	left shoulder on S2; brown bituminous shale partings
10650	3246.12	70.6	434	0.23	1.02	0.78	0.18	1.31	0.14	1.22	84	64	0.5	III	0.66	left shoulder on S2
10680	3255.26	70.6	432	0.16	0.63	0.54	0.20	1.17	0.09	0.98	64	55	0.9	III	0.60	left shoulder on S2
10710	3264.41	69.9	437	0.16	0.83	0.47	0.16	1.77	0.10	1.16	72	41	0.3	III	0.75	small left shoulder on S2
AVE			**426.2**													all values (180)
SD			**10.2**													
AVE			**428.5**													selected values(128)
SD			**2.9**													
												Arctic Red				
10740	3273.55	70.5	433	0.18	0.69	0.74	0.20	0.93	0.15	0.97	71	76	1.6	II	0.58	small left shoulder on S2

Depth (ftKB)	Depth (mKB)	Qty (mg)	Tmax	S1	S2	S3	PI	S2/S3	PC (%)	TOC (%)	HI	OI	MINC (%)	Organic Type	%Roeq	Comments
10770	3282.70	70.5	432	0.13	0.56	1.00	0.19	0.56	0.20	0.89	63	112	2.7	II	0.55	small left shoulder on S2
10800	3291.84	70.4	434	0.26	1.13	0.84	0.19	1.35	0.18	1.37	82	61	0.9	II	0.60	small left shoulder on S2
10830	3300.98	69.9	436	0.17	0.96	0.88	0.15	1.09	0.18	1.24	77	71	1.4	II	0.64	high gas kicks
10860	3310.13	70.2	437	0.15	0.86	0.82	0.15	1.05	0.16	1.17	74	70	1.5	II	0.66	
10875	**3314.70**	70.4	434	0.20	3.90	0.77	0.05	5.06	0.39	2.96	132	26	0.3	II	0.60	**core;** bitumen; gas in fractures
10890	3319.27	70.8	437	0.14	0.85	0.77	0.14	1.10	0.16	1.19	71	65	1.3	II	0.66	
10920	3328.42	70.0	439	0.13	0.81	0.64	0.14	1.27	0.14	1.17	69	55	1.0	II	0.70	
10950	3337.56	70.8	438	0.14	0.93	0.56	0.13	1.66	0.13	1.30	72	43	0.9	II	0.68	
10980	3346.70	70.7	437	0.13	1.19	0.68	0.10	1.75	0.16	1.47	81	46	1.4	II	0.66	
11010	3355.85	70.7	437	0.08	0.91	0.65	0.08	1.40	0.14	1.29	71	50	1.8	II	0.66	
11040	3364.99	71.0	437	0.13	1.15	0.54	0.10	2.13	0.15	1.39	83	39	1.4	II	0.66	
11070	3374.14	71.1	437	0.16	1.09	0.61	0.13	1.79	0.15	1.42	77	43	1.2	II	0.66	
11100	3383.28	70.0	436	0.24	1.13	0.62	0.17	1.82	0.16	1.54	73	40	1.3	II	0.64	
11130	3392.42	70.1	438	0.09	0.98	0.79	0.08	1.24	0.16	1.40	70	56	1.7	II	0.68	
11160	3401.57	70.7	436	0.32	2.31	0.45	0.12	5.13	0.24	1.77	131	25	0.6	II	0.64	
11190	3410.71	70.2	436	0.13	1.23	0.57	0.09	2.16	0.17	1.46	84	39	1.7	II	0.64	
11220	3419.86	70.0	434	0.24	1.59	0.66	0.13	2.41	0.20	1.43	111	46	1.1	II	0.60	trace oil stain
11250	3429.00	70.3	433	0.21	2.02	0.64	0.09	3.16	0.23	1.60	126	40	0.8	II	0.58	
11280	3438.14	69.8	434	0.21	1.01	0.67	0.18	1.51	0.14	1.17	86	57	0.7	II	0.60	very small left shoulder on S2
11310	3447.29	70.1	436	0.20	1.32	0.50	0.13	2.64	0.15	1.41	94	35	0.7	II	0.64	
11340	3456.43	70.6	434	0.24	1.40	0.52	0.15	2.69	0.17	1.45	97	36	0.8	II	0.60	
11380	3468.62	70.8	435	0.20	1.47	0.66	0.12	2.23	0.17	1.45	101	46	0.9	II	0.62	
11410	3477.77	70.1	431	0.27	1.35	0.55	0.17	2.45	0.18	1.20	112	46	0.7	II	0.53	very small left shoulder on S2
11431	**3484.17**	70.5	440	0.14	1.27	0.25	0.10	5.08	0.14	1.06	120	24	0.2	II	0.72	**core;** bitumen, alginite
11440	3486.91	70.4	436	0.25	1.32	0.43	0.16	3.07	0.16	1.24	106	35	0.9	II	0.64	very small left shoulder on S2
11470	3496.06	70.5	435	0.28	1.34	0.65	0.17	2.06	0.17	1.19	113	55	0.5	II	0.62	very small left shoulder on S2
11510	3508.25	70.1	436	0.43	2.08	0.53	0.17	3.92	0.24	1.53	136	35	0.5	II	0.64	very small left shoulder on S2
11530	3514.34	70.2	435	0.32	1.18	0.73	0.21	1.62	0.17	1.03	115	71	1.0	II	0.62	small left shoulder on S2
11560	3523.49	70.7	436	0.33	1.25	0.52	0.21	2.40	0.17	1.18	106	44	1.0	II	0.64	small left shoulder on S2
11590	3532.63	70.1	436	0.53	1.55	0.59	0.26	2.63	0.21	1.35	115	44	0.6	II	0.64	small left shoulder on S2
11620	3541.78	70.9	436	0.62	1.66	0.49	0.27	3.39	0.23	1.31	127	37	1.0	II	0.64	small left shoulder on S2
11650	3550.92	70.4	437	0.82	2.23	0.49	0.27	4.55	0.29	1.55	144	32	0.5	II	0.66	small left shoulder on S2
11680	3560.06	70.2	437	0.80	1.80	0.57	0.31	3.16	0.26	1.37	131	42	0.8	II	0.66	small left shoulder on S2
11710	3569.21	70.5	437	0.69	1.63	0.52	0.30	3.13	0.23	1.34	122	39	0.6	II	0.66	small left shoulder on S2
11740	3578.35	70.1	437	0.66	1.93	0.55	0.25	3.51	0.25	1.52	127	36	0.6	II	0.66	small left shoulder on S2
11770	3587.50	70.4	436	0.61	1.58	0.55	0.28	2.87	0.22	1.35	117	41	0.8	II	0.64	small left shoulder on S2
11800	3596.64	70.2	436	0.57	1.50	0.55	0.28	2.73	0.21	1.36	110	40	0.9	II	0.64	small left shoulder on S2
11830	3605.78	70.3	438	0.54	1.38	0.46	0.28	3.00	0.19	1.30	106	35	0.6	II	0.68	small left shoulder on S2
11860	3614.93	70.4	437	0.57	1.40	0.56	0.29	2.50	0.20	1.30	108	43	0.7	II	0.66	small left shoulder on S2
11894	**3625.29**	70.5	442	0.18	1.47	0.32	0.11	4.59	0.15	1.44	102	22	0.3	II	0.76	**core;** bitumen
11920	3633.22	70.5	438	0.73	1.78	0.69	0.29	2.58	0.25	1.51	118	46	0.7	II	0.68	small left shoulder on S2
11950	3642.36	70.0	438	0.47	1.33	0.59	0.26	2.25	0.20	1.35	99	44	1.2	II	0.68	small left shoulder on S2
11980	3651.50	70.3	438	0.88	1.66	0.46	0.35	3.61	0.24	1.41	118	33	0.8	II	0.68	left shoulder on S2

Depth (ftKB)	Depth (mKB)	Qty (mg)	Tmax	S1	S2	S3	PI	S2/S3	PC (%)	TOC (%)	HI	OI	MINC (%)	Organic Type	%Roeq	Comments
12010	3660.65	70.0	437	0.55	1.40	0.76	0.28	1.84	0.21	1.40	100	54	1.0	II	0.66	small left shoulder on S2
12050	3672.84	70.5	436	0.73	1.44	0.62	0.34	2.32	0.23	1.28	112	48	1.6	II	0.64	small left shoulder on S2; slightly bituminous
12070	3678.94	70.8	437	0.39	1.04	0.68	0.27	1.53	0.16	1.27	82	54	0.9	II	0.66	small left shoulder on S2
12100	3688.08	70.2	440	0.70	1.29	0.41	0.35	3.15	0.19	1.37	94	30	0.8	II	0.72	small left shoulder on S2
12130	3697.22	70.2	439	0.64	1.32	0.49	0.33	2.69	0.20	1.33	99	37	0.9	II	0.70	small left shoulder on S2
12160	3706.37	70.2	438	1.02	1.62	0.41	0.39	3.95	0.25	1.43	113	29	0.8	II	0.68	small left shoulder on S2
12190	3715.51	70.6	438	0.64	1.25	0.43	0.34	2.91	0.19	1.34	93	32	1.0	II	0.68	small left shoulder on S2
12220	3724.66	70.3	439	0.64	1.40	0.57	0.31	2.46	0.20	1.34	104	43	0.7	II	0.70	small left shoulder on S2
12250	3733.80	70.9	437	0.81	1.54	0.58	0.34	2.66	0.24	1.49	103	39	1.1	II	0.66	small left shoulder on S2
12280	3742.94	70.3	437	0.66	1.30	0.67	0.34	1.94	0.21	1.35	96	50	1.3	II	0.66	small left shoulder on S2
12310	3752.09	70.5	439	0.61	1.23	0.59	0.33	2.08	0.19	1.30	95	45	1.1	II	0.70	small left shoulder on S2
12340	3761.23	70.8	439	0.54	1.43	0.42	0.27	3.40	0.20	1.51	95	28	0.8	II	0.70	small left shoulder on S2
12370	3770.38	71.0	438	0.66	1.70	0.38	0.28	4.47	0.22	1.57	108	24	0.8	II	0.68	small left shoulder on S2
12400	3779.52	70.6	436	0.44	1.28	0.62	0.26	2.06	0.19	1.37	93	45	1.0	II	0.64	small left shoulder on S2
12430	3788.66	70.4	439	0.49	1.27	0.49	0.28	2.59	0.18	1.43	89	34	0.9	II	0.70	small left shoulder on S2
12462	**3798.42**	70.6	295	8.94	5.22	0.38	0.63	13.74	1.20	2.36	221	16	0.2	II		very large S1, bimodal S2; **core; oil stain**
12470	3800.86	70.4	438	0.64	1.25	0.48	0.34	2.60	0.19	1.34	93	36	1.1	II	0.68	bimodal S2
12490	3806.95	70.3	437	0.48	1.34	0.37	0.26	3.62	0.18	1.52	88	24	0.8	II	0.66	small left shoulder on S2
12520	3816.10	70.9	441	0.48	1.18	0.37	0.29	3.19	0.16	1.29	91	29	0.6	II	0.74	small left shoulder on S2
12550	3825.24	70.8	438	0.53	1.46	0.54	0.27	2.70	0.20	1.45	101	37	0.8	II	0.68	small left shoulder on S2
12580	3834.38	70.3	439	0.59	1.31	0.54	0.31	2.43	0.19	1.33	98	41	0.8	II	0.70	small left shoulder on S2
12610	3843.53	70.8	439	0.73	1.46	0.42	0.33	3.48	0.21	1.40	104	30	0.6	II	0.70	small left shoulder on S2
12640	3852.67	70.8	437	0.57	1.28	0.46	0.31	2.78	0.18	1.31	98	35	0.7	II	0.66	small left shoulder on S2
12660	3858.77	70.8	438	0.61	1.39	0.50	0.30	2.78	0.20	1.36	102	37	0.6	II	0.68	small left shoulder on S2
AVE			**434.8**													all values (68)
SD			**17.3**													
AVE			**436.8**													selected values (67)
SD			**2.0**													

Table 4. Tununuk K-10 Rock-Eval 6 data (Rock-Eval 2 format).

(pale yellow)	%Ro analysis
(green)	acceptable pyrogram
(purple)	anomalous pyrogram
(orange)	PI ≥ 0.2
(yellow)	TOC ≥ 5 wt%

Depth (ftKB)	Depth (mKB)	Qty (mg)	Tmax	S1	S2	S3	PI	S2/S3	PC (%)	TOC (%)	HI	OI	MINC (%)	Organic Type	%Roeq	Comments
										Iperk Sequence						
30	9.14	50.3	405	4.08	8.19	5.34	0.33	1.53	1.26	3.05	269	175	2.4	III		bimodal S2
60	18.29	50.5	326	10.21	22.65	11.38	0.31	1.99	3.38	8.67	261	131	1.6	III		S1 80% recovery, bimodal S2
90	27.43	25.2	318	19.95	40.10	27.26	0.33	1.47	6.43	17.78	226	153	1.5	III		S1 80% recovery, large right shoulder on S2
120	36.58	25.4	312	23.96	39.94	21.31	0.37	1.87	6.36	16.75	238	127	1.7	III		S1 80% recovery, bimodal S2
180	54.86	70.2	421	3.51	7.91	8.76	0.31	0.90	1.34	5.10	155	172	2.7	III	0.18	S1 90% recovery, bimodal S2
210	64.01	69.7	420	2.29	5.98	5.97	0.28	1.00	0.95	4.20	142	142	1.6	III	0.14	large left shoulder on S2
240	73.15	70.4	427	1.22	2.65	2.25	0.31	1.18	0.42	1.95	136	115	1.6	III	0.43	S1 90% recovery, large left shoulder on S2
270	82.30	70.2	422	2.07	8.47	6.98	0.20	1.21	1.21	5.78	147	121	1.7	III	0.23	S1 80% recovery, large left shoulder on S2
300	91.44	20.2	412	7.44	55.92	31.61	0.12	1.77	6.95	35.22	159	90	1.8	III		S1 60% recovery, left shoulder on S2
330	100.58	70.2	421	0.65	4.88	3.67	0.12	1.33	0.64	3.70	132	99	0.9	III	0.18	S1 80% recovery, asymmetrical S2
360	109.73	69.8	430	0.52	2.21	1.95	0.19	1.13	0.32	2.08	106	94	1.1	III	0.54	S1 80% recovery, left shoulder on S2
390	118.87	70.4	430	0.38	1.53	1.28	0.20	1.20	0.22	1.36	112	94	1.8	III	0.54	S1 80% recovery, left shoulder on S2
420	128.02	70.0	434	0.31	1.50	1.04	0.17	1.44	0.20	1.35	111	77	1.4	III	0.66	left shoulder on S2
450	137.16	70.5	434	0.36	1.72	1.00	0.17	1.72	0.22	1.45	119	69	1.0	III	0.66	
480	146.30	70.3	433	0.37	1.66	1.19	0.18	1.39	0.22	1.56	106	76	1.1	III	0.63	small left shoulder
510	155.45	70.0	434	0.19	1.63	1.11	0.11	1.47	0.21	1.67	98	66	0.8	III	0.66	
540	164.59	70.7	433	0.25	1.77	1.16	0.12	1.53	0.22	1.61	110	72	0.8	III	0.63	
570	173.74	70.0	433	0.36	1.88	1.04	0.16	1.81	0.24	1.62	116	64	0.8	III	0.63	small left shoulder
600	182.88	70.7	433	0.31	2.00	1.31	0.13	1.53	0.25	1.89	106	69	0.7	III	0.63	small left shoulder
630	192.02	70.9	430	0.49	2.83	2.16	0.15	1.31	0.39	2.49	114	87	0.9	III	0.54	
670	204.22	70.5	428	0.70	3.59	2.11	0.16	1.70	0.46	2.45	147	86	0.9	III	0.47	S1 80% recovery, small left shoulder on S2
700	213.36	70.2	430	0.41	3.44	2.79	0.11	1.23	0.47	2.88	119	97	1.0	III	0.54	S1 80% recovery, small left shoulder on S2
730	222.50	70.5	431	0.56	3.43	2.36	0.14	1.45	0.45	2.81	122	84	0.8	III	0.57	S1 80% recovery, left shoulder on S2
750	228.60	70.9	431	0.49	3.39	1.62	0.13	2.09	0.41	2.23	152	73	0.8	III	0.57	
780	237.74	70.9	430	0.48	2.58	1.76	0.16	1.47	0.34	2.14	121	82	0.8	III	0.54	small left shoulder
Ave			414.3													all values (25)
SD			36.8													
Ave			**432.3**													selected values (9)
SD			**1.6**													
										Taglu Sequence						
810	246.89	70.2	423	0.21	1.08	1.02	0.16	1.06	0.17	1.14	95	89	1.2	III	0.27	
840	256.03	70.6	419	0.23	1.39	1.51	0.14	0.92	0.21	1.42	98	106	1.3	III		S1 90% recovery, asymmetrical S2
870	265.18	70.4	417	0.24	1.03	1.18	0.19	0.87	0.17	1.08	95	109	1.1	III		asymmetrical S2
900	274.32	70.1	415	0.63	0.88	1.45	0.42	0.61	0.23	0.91	97	159	1.7	III		irregular S2

Depth (ftKB)	Depth (mKB)	Qty (mg)	Tmax	S1	S2	S3	PI	S2/S3	PC (%)	TOC (%)	HI	OI	MINC (%)	Organic Type	%Roeq	Comments
930	283.46	70.0	416	1.26	1.37	0.98	0.48	1.40	0.27	1.01	136	97	1.4	III		irregular S2
960	292.61	70.7	419	0.35	0.92	0.72	0.28	1.28	0.16	0.89	103	81	1.1	III		left shoulder on S2
990	301.75	70.4	414	0.93	1.67	0.95	0.36	1.76	0.29	1.33	126	71	1.4	III		low S2 with left shoulder
1020	310.90	70.6	422	0.68	1.05	0.87	0.39	1.21	0.21	0.97	108	90	1.4	III	0.23	irregular, low S2
1050	320.04	70.6	419	0.29	0.56	0.83	0.34	0.67	0.13	0.69	81	120	1.3	III		low S2 with left shoulder
Ave			418.2													all values (9)
SD			3.0													
Ave			**423.0**													selected values (1)
SD																
													Aklak Sequence			
1080	329.18	70.3	413	1.46	9.87	4.09	0.13	2.41	1.23	9.50	104	43	0.6	III		
1110	338.33	70.2	417	0.84	4.13	1.97	0.17	2.10	0.55	3.93	105	50	0.9	III		
1140	347.47	70.2	421	1.01	5.91	2.67	0.15	2.21	0.77	5.45	108	49	0.7	III	0.18	
1170	356.62	70.4	332	0.43	4.51	2.45	0.09	1.84	0.59	3.57	126	69	1.1	III		irregular S2 with large right shoulder
1200	365.76	70.7	424	0.48	0.72	0.38	0.40	1.89	0.14	0.54	133	70	1.8	III	0.31	irregular low S2
1230	374.90	70.9	423	0.16	0.62	0.78	0.20	0.79	0.11	0.94	66	83	1.2	III	0.27	broad S2
1260	384.05	70.1	425	0.05	0.14	0.42	0.25	0.33	0.04	0.29	48	145	2.3	III	0.35	left shoulder on S2
1290	393.19	70.0	421	0.10	0.36	0.76	0.22	0.47	0.10	0.42	86	181	1.9	III	0.18	left shoulder on S2
1320	402.34	70.9	422	0.47	2.45	1.18	0.16	2.08	0.33	2.16	113	55	2.1	III	0.23	small left shoulder on S2
1350	411.48	70.4	405	0.50	0.61	0.58	0.45	1.05	0.12	0.45	136	129	1.4	III		irregular S2
1380	420.62	70.6	449	0.06	0.22	0.33	0.22	0.67	0.05	0.41	54	80	1.2	III	1.03	large right and left shoulders on S2
1410	429.77	70.8	331	0.05	0.13	0.30	0.29	0.43	0.03	0.43	30	70	0.1	III		irregular S2
1440	438.91	70.2	334	0.03	0.12	0.29	0.21	0.41	0.02	0.23	52	126	0.5	III		bimodal S2
1470	448.06	70.8	408	0.03	1.12	1.62	0.03	0.69	0.20	2.30	49	70	1.3	III		large, broad S2; reworked solid bitumen
1500	457.20	71.0	434	0.58	0.66	0.98	0.47	0.67	0.15	0.46	143	213	0.7	III	0.66	irregular, low S2
1530	466.34	70.2	444	0.02	0.13	0.67	0.16	0.19	0.04	0.35	37	191	0.4	III	0.92	broad S2 with large right shoulder
1560	475.49	70.1	423	0.16	0.43	1.57	0.27	0.27	0.13	0.68	63	231	1.4	III	0.27	left shoulder on S2
1590	484.63	70.6	419	1.18	1.50	1.63	0.44	0.92	0.33	1.07	140	152	2.1	III		irregular, low S2
1620	493.78	70.7	437	0.09	0.23	0.95	0.27	0.24	0.07	0.48	48	198	1.6	III	0.75	left shoulder on S2
1650	502.92	70.9	433	0.16	0.46	1.39	0.26	0.33	0.13	0.93	49	149	1.9	III	0.63	left shoulder on S2
1680	512.06	70.5	439	0.47	2.74	0.72	0.15	3.81	0.30	1.57	175	46	2.0	III	0.80	
1710	521.21	70.2	428	0.33	0.83	1.54	0.29	0.54	0.19	0.95	87	162	1.9	III	0.47	left shoulder on S2
1740	530.35	71.0	424	0.15	1.23	2.03	0.11	0.61	0.21	2.03	61	100	1.6	III	0.31	small left shoulder on S2
1770	539.50	70.3	421	0.16	0.49	1.80	0.25	0.27	0.15	0.73	67	247	2.2	III	0.18	large left shoulder on S2
1800	548.64	70.2	413	0.05	0.59	1.99	0.08	0.30	0.16	1.20	49	166	2.6	III		right shoulder on S2
1830	557.78	70.4	433	0.12	0.72	1.24	0.14	0.58	0.16	1.23	59	101	1.7	III	0.63	broad S2
1860	566.93	70.2	426	0.30	1.38	0.86	0.18	1.60	0.20	1.40	99	61	0.7	III	0.39	large left shoulder on S2
1890	576.07	70.8	405	1.19	6.65	3.49	0.15	1.91	0.84	4.33	154	81	1.3	III		S1 80% recovery, asymmetrical S2
1920	585.22	70.5	432	0.47	2.26	3.59	0.17	0.63	0.43	3.79	60	95	1.7	III	0.60	
1950	594.36	70.8	419	0.24	1.42	2.98	0.15	0.48	0.30	2.71	52	110	1.2	III		S1 90% recovery
1980	603.50	70.4	427	0.72	1.44	1.67	0.33	0.86	0.26	1.36	106	123	1.4	III	0.43	left and right shoulders on S2
2670	813.82	70.6	425	0.77	1.21	1.42	0.39	0.85	0.23	1.18	103	120	0.5	III	0.35	small left and right shoulders on S2
2760	841.25	70.7	429	0.15	0.45	1.51	0.25	0.30	0.10	0.94	48	161	0.4	III	0.50	left shoulder on S2

Depth (ftKB)	Depth (mKB)	Qty (mg)	Tmax	S1	S2	S3	PI	S2/S3	PC (%)	TOC (%)	HI	OI	MINC (%)	Organic Type	%Roeq	Comments
2790	850.39	69.9	431	0.09	0.33	1.37	0.21	0.24	0.08	0.86	38	159	0.3	III	0.57	small left shoulder on S2
2820	859.54	70.7	433	0.12	0.36	0.18	0.25	2.00	0.04	0.85	42	21	0.1	III	0.63	small left shoulder on S2
2850	868.68	70.4	437	0.08	0.23	0.50	0.26	0.46	0.04	0.61	38	82	0.1	III	0.75	small left shoulder on S2
2880	877.82	70.0	444	0.07	0.37	3.46	0.16	0.11	0.30	0.97	38	357	1.9	III	0.92	S1 80% recovery, asymmetrical S2 small left shoulder; gas
2910	886.97	69.8	439	0.15	0.54	2.14	0.21	0.25	0.20	0.98	55	218	1.4	III	0.80	left shoulder on S2; occasional oil staining
2940	896.11	70.0	378	0.37	1.39	2.43	0.21	0.57	0.40	0.98	142	248	2.6	III		S1 60% recovery, bimodal S2
2946	897.94	70.4	438	0.04	0.30	0.43	0.13	0.70	0.04	0.73	41	59	0.1	III	0.78	**core**, S1 90% recovery, left and right shoulders on S2
2970	905.26	70.8	431	0.15	0.45	1.25	0.25	0.36	0.11	0.67	67	187	3.3	III	0.57	left shoulder and small right shoulder on S2
3000	914.40	70.1	428	0.26	0.58	0.84	0.30	0.69	0.18	0.70	83	120	5.4	III	0.47	large left shoulder on S2
3030	923.54	70.7	435	0.12	0.29	2.14	0.30	0.14	0.24	0.60	48	357	2.5	III	0.69	left shoulder and small right shoulder on S2
3070	935.74	70.5	431	0.23	0.49	0.69	0.32	0.71	0.10	0.61	80	113	0.5	III	0.57	large left peak on S2
3090	941.83	70.8	387	0.08	0.29	1.89	0.21	0.15	0.35	0.80	36	236	3.6	III		irregular S2
3120	950.98	70.0	422	0.21	0.59	1.23	0.26	0.48	0.12	0.60	98	205	0.5	III	0.23	S1 80% recovery, left and right shoulders on S2
3160	963.17	69.8	407	0.04	0.12	0.49	0.25	0.24	0.03	0.21	57	233	4.2	III		bimodal S2
3190	972.31	70.9	443	0.05	0.21	2.32	0.20	0.09	0.34	0.73	29	318	3.8	III	0.90	asymmetrical S2
Ave			419.2													all values (48)
SD			26.4													
Ave			**427.4**													selected values (14)
SD			**10.2**													
													Fish River Sequence			
3210	978.41	70.3	431	0.16	0.47	1.91	0.25	0.25	0.21	0.62	76	308	4.6	III	0.57	large left shoulder and right shoulder on S2
3240	987.55	71.1	429	0.85	0.96	1.27	0.47	0.76	0.31	1.02	94	125	1.7	III	0.50	low broad S2 with large left shoulder
3270	996.70	70.6	430	0.74	5.89	11.54	0.11	0.51	1.22	18.87	31	61	1.5	III	0.54	broad asymmetrical S2; coaly
3300	1005.84	70.7	427	0.31	1.49	2.67	0.17	0.56	0.29	2.25	66	119	1.0	III	0.43	S1 80% recovery, large left shoulder on S2
3330	1014.98	70.4	433	0.13	0.62	1.65	0.17	0.38	0.15	1.10	56	150	0.9	III	0.63	S1 90% recovery, small left shoulder on S2
3390	1033.27	70.2	434	0.11	1.18	1.91	0.09	0.62	0.19	2.02	58	95	0.4	III	0.66	S1 80% recovery, small left shoulder on S2
3430	1045.46	70.5	428	0.12	0.60	1.25	0.16	0.48	0.12	1.01	59	124	0.7	III	0.47	S1 90% recovery, broad S2
3450	1051.56	70.9	431	0.58	1.30	1.16	0.31	1.12	0.21	1.16	112	100	0.3	III	0.57	large left peak and a right shoulder on S2
3480	1060.70	70.8	433	0.25	0.73	1.16	0.25	0.63	0.13	0.90	81	129	0.5	III	0.63	S1 90% recovery, large left shoulder on S2
3510	1069.85	70.5	434	0.10	0.49	1.13	0.17	0.43	0.09	0.85	58	133	0.4	III	0.66	small left and right shoulder on S2
3540	1078.99	70.2	424	0.15	0.54	1.22	0.21	0.44	0.10	1.05	51	116	0.8	III	0.31	left shoulder on S2
3570	1088.14	70.4	432	0.11	0.63	1.12	0.15	0.56	0.12	1.09	58	103	0.4	III	0.60	left shoulder on S2
3600	1097.28	70.0	405	0.08	0.22	0.51	0.27	0.43	0.05	0.66	33	77	0.3	III		large left shoulder on S2
3630	1106.42	70.0	423	0.31	0.92	2.33	0.25	0.39	0.24	3.23	28	72	2.0	III	0.27	left shoulder and a large right shoulder on S2
3670	1118.62	70.3	423	0.17	0.34	0.93	0.33	0.37	0.09	0.84	40	111	1.0	III	0.27	large left shoulder on S2
3690	1124.71	70.6	435	0.06	0.34	0.98	0.15	0.35	0.08	0.69	49	142	0.7	III	0.69	S1 90% recovery, small left shoulder on S2
3720	1133.86	70.7	430	0.07	0.44	0.74	0.13	0.59	0.07	0.80	55	93	0.7	III	0.54	S1 80% recovery, left shoulder on S2
3750	1143.00	70.5	434	0.10	0.50	1.03	0.17	0.49	0.10	0.83	60	124	0.7	III	0.66	S1 90% recovery, left shoulder on S2
3780	1152.14	70.0	432	0.09	0.37	1.26	0.20	0.29	0.09	0.64	58	197	0.7	III	0.60	S1 90% recovery, left shoulder on S2, oil staining/fluor.
3810	1161.29	70.3	422	0.27	0.62	0.97	0.30	0.64	0.12	1.09	57	89	0.6	III	0.23	S1 90% recovery, large left shoulder on S2
3830	1167.38	70.8	419	0.21	0.53	0.93	0.29	0.57	0.11	0.82	65	113	0.6	III		S1 90% recovery, large left shoulder on S2
3880	1182.62	70.0	421	0.28	0.57	0.96	0.33	0.59	0.11	0.99	58	97	0.7	III	0.18	S1 90% recovery, large left shoulder on S2
3890	1185.67	70.5	435	0.30	1.02	1.21	0.23	0.84	0.17	1.65	62	73	0.4	III	0.69	S1 90% recovery, left shoulder on S2

Depth (ftKB)	Depth (mKB)	Qty (mg)	Tmax	S1	S2	S3	PI	S2/S3	PC (%)	TOC (%)	HI	OI	MINC (%)	Organic Type	%Roeq	Comments
3920	1194.82	70.3	436	0.28	0.56	0.70	0.34	0.80	0.17	0.72	78	97	1.6	III	0.72	broad S2 with large left shoulder
3940	1200.91	70.0	419	0.46	0.63	0.78	0.42	0.81	0.13	0.90	70	87	0.7	III		large left peak on S2
3990	1216.15	70.8	433	0.27	0.70	0.88	0.28	0.80	0.11	0.97	72	91	0.4	III	0.63	S1 90% recovery, large left peak on S2
4060	1237.49	70.4	420	0.12	0.39	0.80	0.23	0.49	0.07	0.70	56	114	0.5	III	0.14	S1 80% recovery, large left shoulder on S2
4110	1252.73	70.4	426	0.30	0.70	0.87	0.30	0.80	0.12	0.94	74	93	0.3	III	0.39	S1 90% recovery, large left peak on S2
4140	1261.87	70.4	421	0.20	0.52	0.85	0.28	0.61	0.10	0.85	61	100	0.3	III	0.18	S1 90% recovery, large left shoulder on S2
4180	1274.06	70.7	418	0.14	0.33	0.78	0.30	0.42	0.07	0.59	56	132	0.4	III		S1 80% recovery, bimodal S2
4410	1344.17	70.5	432	0.06	0.32	1.13	0.15	0.28	0.08	0.69	46	164	1.1	III	0.60	broad S2 with left and right shoulders
4440	1353.31	71.2	426	0.18	0.47	0.80	0.28	0.59	0.09	0.65	72	123	1.1	III	0.39	S1 90% recovery, large left peak on S2
4470	1362.46	70.5	418	0.21	0.44	0.95	0.33	0.46	0.10	0.78	56	122	0.7	III		S1 90% recovery, large left peak on S2
4510	1374.65	70.6	426	0.08	0.46	1.09	0.14	0.42	0.09	0.82	56	133	0.3	III	0.39	S1 80% recovery, large left shoulder on S2
4530	1380.74	70.0	434	0.03	0.20	0.36	0.12	0.56	0.04	0.57	35	63	0.4	III	0.66	large right shoulder on S2
4560	1389.89	69.8	424	0.08	0.37	0.84	0.18	0.44	0.08	0.72	51	117	0.9	III	0.31	left shoulder on S2
4600	1402.08	70.5	426	0.20	0.81	1.27	0.19	0.64	0.13	0.90	90	141	0.9	III	0.39	S1 80% recovery, bimodal S2
4630	1411.22	70.6	428	0.04	0.13	0.33	0.21	0.39	0.04	0.51	25	65	0.2	III	0.47	asymmetrical S2
4650	1417.32	70.6	429	0.13	0.59	0.83	0.18	0.71	0.10	0.86	69	97	0.6	III	0.50	S1 70% recovery, bimodal S2
4680	1426.46	69.9	424	0.01	0.07	0.33	0.15	0.21	0.03	0.45	16	73	0.2	III	0.31	large left shoulder on S2
4700	1432.56	69.8	428	0.11	0.22	0.59	0.33	0.37	0.06	0.70	31	84	0.6	III	0.47	large left shoulder on S2
4730	1441.70	69.6	423	0.25	0.64	1.00	0.28	0.64	0.12	0.93	69	108	0.6	III	0.27	large left shoulder on S2
4770	1453.90	70.7	423	0.21	0.79	1.06	0.21	0.75	0.14	1.04	76	102	0.4	III	0.27	S1 80% recovery, bimodal S2
4800	1463.04	70.3	429	0.10	0.39	0.99	0.21	0.39	0.08	0.80	49	124	0.5	III	0.50	S1 80% recovery, large left shoulder on S2
4830	1472.18	70.3	435	0.04	0.37	0.76	0.10	0.49	0.07	0.86	43	88	0.4	III	0.69	S1 80% recovery, right shoulder on S2
4860	1481.33	70.5	426	0.13	0.47	0.92	0.22	0.51	0.09	0.85	55	108	0.4	III	0.39	S1 90% recovery, large left shoulder on S2
4890	1490.47	71.1	420	0.38	0.55	0.95	0.41	0.58	0.12	0.82	67	116	0.4	III	0.14	large left peak on S2
5020	1530.10	70.0	434	0.12	0.51	0.82	0.20	0.62	0.10	0.91	56	90	0.6	III	0.66	left and right shoulder on S2
5030	1533.14	70.9	431	0.15	0.42	0.88	0.27	0.48	0.09	0.78	54	113	1.1	III	0.57	left shoulder on S2
5070	1545.34	71.0	426	0.27	0.49	0.79	0.35	0.62	0.10	0.87	56	91	0.5	III	0.39	left shoulder on S2
5100	1554.48	70.6	445	0.09	0.53	0.69	0.14	0.77	0.08	0.76	70	91	0.8	III	0.94	narrow S2
5120	1560.58	70.8	428	0.14	0.33	0.81	0.30	0.41	0.08	0.75	44	108	0.8	III	0.47	left shoulder on S2
5170	1575.82	70.9	428	0.20	0.48	0.69	0.29	0.70	0.09	0.84	57	82	1.1	III	0.47	large left shoulder on S2
5190	1581.91	70.0	433	0.14	0.32	0.69	0.30	0.46	0.07	0.80	40	86	0.5	III	0.63	left shoulder on S2
5210	1588.01	70.2	433	0.14	0.44	0.62	0.25	0.71	0.08	0.86	51	72	0.8	III	0.63	small left shoulder on S2
5250	1600.20	70.0	432	0.06	0.23	0.53	0.20	0.43	0.05	0.61	38	87	0.2	III	0.60	asymmetrical S2
5270	1606.30	70.3	436	0.07	0.42	0.76	0.14	0.55	0.08	0.92	46	83	0.5	III	0.72	right shoulder on S2
5300	1615.44	70.9	434	0.05	0.26	0.74	0.17	0.35	0.06	0.74	35	100	0.9	III	0.66	slightly asymmetrical S2
5340	1627.63	70.3	432	0.13	0.57	0.80	0.19	0.71	0.09	0.84	68	95	0.7	III	0.60	left shoulder on S2
5370	1636.78	70.2	436	0.14	0.70	0.83	0.17	0.84	0.10	0.99	71	84	0.5	III	0.72	small left shoulder on S2
5410	1648.97	71.1	433	0.14	0.70	0.71	0.17	0.99	0.10	0.98	71	72	0.4	III	0.63	S1 90% recovery, large left shoulder on S2
5430	1655.06	71.2	435	0.13	0.53	0.90	0.19	0.59	0.09	0.87	61	103	0.5	III	0.69	small left shoulder on S2
5470	1667.26	70.6	433	0.09	0.38	0.61	0.19	0.62	0.06	0.82	46	74	0.6	III	0.63	
5490	1673.35	70.8	436	0.12	0.51	0.69	0.19	0.74	0.09	0.88	58	78	0.6	III	0.72	small left shoulder on S2
5520	1682.50	70.2	414	0.29	1.67	0.55	0.15	3.04	0.19	1.17	143	47	0.3	III		S1 80% recovery, large left shoulder on S2
5550	1691.64	69.8	436	0.08	0.63	0.59	0.12	1.07	0.08	1.00	63	59	0.4	III	0.72	right shoulder on S2

Depth (ftKB)	Depth (mKB)	Qty (mg)	Tmax	S1	S2	S3	PI	S2/S3	PC (%)	TOC (%)	HI	OI	MINC (%)	Organic Type	%Roeq	Comments
5580	1700.78	70.8	434	0.15	0.78	0.72	0.16	1.08	0.11	1.06	74	68	0.3	III	0.66	S1 80% recovery, large left shoulder on S2
5610	1709.93	70.4	436	0.08	0.64	0.73	0.11	0.88	0.09	1.04	62	70	0.3	III	0.72	small left shoulder and a right shoulder on S2
5640	1719.07	70.4	416	0.12	0.96	0.67	0.11	1.43	0.12	1.00	96	67	0.7	III		S1 80% recovery, left shoulder on S2; dead oil
5670	1728.22	70.8	435	0.13	0.46	0.52	0.22	0.88	0.08	0.88	52	59	0.4	III	0.69	small left shoulder on S2
5700	1737.36	70.4	434	0.07	0.39	0.43	0.15	0.91	0.06	0.71	55	61	0.9	III	0.66	small left and right shoulder on S2
5730	1746.50	70.4	436	0.13	0.67	0.97	0.17	0.69	0.13	1.00	67	97	0.5	III	0.72	small left and right shoulder on S2
5750	1752.60	70.3	436	0.16	0.92	0.83	0.15	1.11	0.13	1.37	67	61	0.5	III	0.72	small left shoulder and a right shoulder on S2
5780	1761.74	70.7	423	0.20	1.44	0.71	0.12	2.03	0.18	1.17	123	61	0.5	III	0.27	S1 80% recovery, asymmetrical S2
5830	1776.98	70.8	427	0.38	0.60	0.56	0.39	1.07	0.10	0.62	97	90	1.0	III	0.43	large left shoulder on S2; trace dead oil
5850	1783.08	70.9	436	0.11	0.57	0.82	0.16	0.70	0.09	0.91	63	90	0.7	III	0.72	right shoulder on S2
5880	1792.22	70.1	435	0.12	0.52	0.61	0.18	0.85	0.08	0.88	59	69	0.7	III	0.69	right shoulder on S2
5910	1801.37	70.4	436	0.13	0.74	0.64	0.15	1.16	0.10	1.04	71	62	0.5	III	0.72	small left and right shoulder on S2
5940	1810.51	70.5	436	0.22	0.75	0.54	0.23	1.39	0.11	0.94	80	57	0.3	III	0.72	large left shoulder on S2; trace dead oil
5960	1816.61	70.0	435	0.16	0.65	0.57	0.19	1.14	0.10	0.90	72	63	0.6	III	0.69	small left and right shoulder on S2
6000	1828.80	70.9	438	0.12	0.54	0.61	0.19	0.89	0.10	0.85	64	72	0.8	III	0.78	small left shoulder and a right shoulder on S2
6030	1837.94	70.7	437	0.10	0.57	0.81	0.15	0.70	0.11	0.94	61	86	0.6	III	0.75	right shoulder on S2
6060	1847.09	70.3	438	0.08	0.52	0.62	0.14	0.84	0.08	0.94	55	66	0.4	III	0.78	right shoulder on S2
6090	1856.23	70.6	434	0.28	0.85	0.48	0.25	1.77	0.12	0.82	104	59	0.9	III	0.66	large left shoulder on S2
6120	1865.38	70.4	436	0.13	0.60	0.76	0.18	0.79	0.10	0.88	68	86	0.5	III	0.72	small left and right shoulder on S2
Ave			429.7													all values (85)
SD			6.7													
Ave			**435.7**													selected values (13)
SD			**3.0**													
													Smok. Hills/B.C			
6140	1871.47	70.0	427	0.63	0.96	0.64	0.40	1.50	0.17	0.87	110	74	0.5	II	0.40	large left peak on S2; dead oil
6180	1883.66	70.1	437	0.11	0.66	0.66	0.14	1.00	0.08	0.90	73	73	0.3	II	0.66	small left and right shoulder on S2
6210	1892.81	70.7	436	0.11	0.61	0.61	0.16	1.00	0.09	0.84	73	73	0.4	II	0.64	S1 90% recovery, small left and right shoulder on S2
6240	1901.95	70.4	429	0.26	1.25	1.86	0.17	0.67	0.21	1.28	98	145	1.1	II	0.47	
6270	1911.10	70.8	428	0.21	1.69	1.25	0.11	1.35	0.21	1.58	107	79	0.6	II	0.43	
6310	1923.29	69.7	431	0.22	1.00	1.01	0.18	0.99	0.15	1.11	90	91	0.8	II	0.53	small left shoulder on S2
6330	1929.38	70.4	431	0.18	0.93	0.68	0.17	1.37	0.13	1.19	78	57	0.5	II	0.53	
6360	1938.53	71.2	430	0.31	1.90	1.22	0.14	1.56	0.23	1.54	123	79	0.4	II	0.50	
6380	1944.62	70.7	429	0.21	1.47	1.11	0.12	1.32	0.20	1.52	97	73	0.7	II	0.47	small left shoulder on S2
6420	1956.82	71.0	429	0.20	1.99	0.58	0.09	3.43	0.22	1.66	120	35	0.6	II	0.47	
6450	1965.96	70.0	431	0.13	0.85	0.41	0.13	2.07	0.11	1.10	77	37	0.3	II	0.53	
6480	1975.10	70.5	429	0.14	0.63	0.66	0.19	0.95	0.10	1.01	62	65	0.5	II	0.47	small right shoulder on S2
6510	1984.25	71.1	416	0.21	1.26	1.11	0.14	1.14	0.18	1.20	105	93	1.4	II		bitumen, dead oil stain?
6540	1993.39	70.9	432	0.21	1.56	0.45	0.12	3.47	0.18	1.43	109	31	0.3	II	0.55	narrow S2
6570	2002.54	70.4	432	0.17	1.26	1.22	0.12	1.03	0.17	1.37	92	89	0.5	II	0.55	
6610	2014.73	70.2	428	0.31	1.59	0.78	0.16	2.04	0.21	1.40	114	56	1.0	II	0.43	
6650	2026.92	70.5	429	0.36	2.48	0.91	0.13	2.73	0.28	1.71	145	53	0.5	II	0.47	
6670	2033.02	70.0	429	0.21	0.99	0.59	0.17	1.68	0.13	1.13	88	52	0.5	II	0.47	small left shoulder on S2
6690	2039.11	70.3	430	0.20	1.57	0.60	0.11	2.62	0.19	1.50	105	40	0.7	II	0.50	

Depth (ftKB)	Depth (mKB)	Qty (mg)	Tmax	S1	S2	S3	PI	S2/S3	PC (%)	TOC (%)	HI	OI	MINC (%)	Organic Type	%Roeq	Comments
6720	2048.26	70.9	428	0.29	1.97	0.57	0.13	3.46	0.21	1.47	134	39	0.4	II	0.43	
6740	2054.35	70.5	432	0.18	1.28	0.65	0.12	1.97	0.15	1.30	98	50	0.7	II	0.55	
6780	2066.54	70.6	432	0.22	1.68	0.52	0.12	3.23	0.19	1.38	122	38	0.3	II	0.55	
6810	2075.69	70.0	427	0.20	1.01	0.70	0.17	1.44	0.14	1.31	77	53	0.5	II	0.40	
6840	2084.83	70.1	433	0.12	0.89	0.63	0.12	1.41	0.13	1.20	74	53	0.7	II	0.58	small right shoulder on S2
6870	2093.98	70.3	431	0.10	0.61	0.56	0.14	1.09	0.09	0.94	65	60	0.8	II	0.53	right shoulder on S2
6900	2103.12	70.2	430	0.45	1.54	0.62	0.23	2.48	0.21	1.29	119	48	0.7	II	0.50	small left shoulder on S2
6920	2109.22	70.5	430	0.29	1.38	0.51	0.17	2.71	0.18	1.41	98	36	0.4	II	0.50	
6960	2121.41	70.5	424	0.23	1.62	0.54	0.12	3.00	0.19	1.83	89	30	0.3	II	0.26	narrow S2
6980	2127.50	70.4	423	0.29	2.67	0.68	0.10	3.93	0.30	2.41	111	28	0.3	II	0.21	
7020	2139.70	70.4	430	0.16	0.89	0.67	0.15	1.33	0.12	1.09	82	61	1.1	II	0.50	
7050	2148.84	70.2	423	0.29	3.56	0.63	0.07	5.65	0.36	2.77	129	23	0.5	II	0.21	dead oil stain
7090	2161.03	70.8	428	0.13	1.32	0.63	0.09	2.10	0.16	1.81	73	35	0.6	II	0.43	
7150	2179.32	70.4	439	0.08	0.51	1.73	0.14	0.29	0.14	1.00	51	173	1.6	II	0.70	right shoulder on S2
7170	2185.42	69.8	437	0.17	0.71	1.07	0.19	0.66	0.17	1.14	62	94	2.1	II	0.66	small right shoulder on S2
7200	2194.56	70.1	435	0.16	1.15	1.21	0.12	0.95	0.18	1.70	68	71	1.1	II	0.62	small right shoulder on S2
7230	2203.70	70.2	434	0.26	1.41	0.74	0.16	1.91	0.18	1.73	82	43	0.6	II	0.60	
7260	2212.85	70.5	438	0.14	0.65	2.19	0.18	0.30	0.25	1.14	57	192	2.0	II	0.68	small right shoulder on S2
7290	2221.99	70.9	435	0.12	0.71	1.36	0.15	0.52	0.16	1.04	68	131	1.9	II	0.62	small right shoulder on S2
7320	2231.14	70.7	439	0.07	0.57	0.88	0.11	0.65	0.12	1.05	54	84	1.4	II	0.70	right shoulder on S2
7350	2240.28	71.0	440	0.12	0.87	0.87	0.12	1.00	0.13	1.30	67	67	0.8	II	0.72	right shoulder on S2
7380	2249.42	70.0	433	0.18	1.25	0.55	0.13	2.27	0.15	1.46	86	38	0.7	II	0.58	
7410	2258.57	70.7	436	0.11	0.98	4.21	0.10	0.23	0.26	1.43	69	294	0.9	II	0.64	small right shoulder on S2
7440	2267.71	70.4	438	0.16	0.75	1.75	0.18	0.43	0.19	1.34	56	131	1.4	II	0.68	right shoulder on S2
7470	2276.86	70.6	440	0.09	0.65	0.91	0.13	0.71	0.11	1.20	54	76	0.8	II	0.72	small right shoulder on S2
7500	2286.00	70.7	434	0.12	1.04	1.10	0.10	0.95	0.21	1.37	76	80	2.0	II	0.60	small right shoulder on S2
7530	2295.14	70.2	437	0.25	1.02	1.12	0.20	0.91	0.21	1.26	81	89	1.2	II	0.66	small left and right shoulders on S2
7560	2304.29	70.3	438	0.13	0.76	1.00	0.14	0.76	0.13	1.11	68	90	1.0	II	0.68	small right shoulder on S2
7590	2313.43	70.0	440	0.08	0.56	0.63	0.12	0.89	0.09	0.94	60	67	0.4	II	0.72	right shoulder on S2
7610	2319.53	70.4	434	0.11	1.41	1.82	0.07	0.77	0.22	1.71	82	106	1.0	II	0.60	left peak on S2; solid bitumen
7650	2331.72	70.9	439	0.10	0.93	0.52	0.10	1.79	0.12	1.42	65	37	0.5	II	0.70	right shoulder on S2
7680	2340.86	70.5	439	0.09	0.94	0.61	0.08	1.54	0.13	1.39	68	44	0.8	II	0.70	right shoulder on S2
7710	2350.01	69.9	439	0.07	0.70	0.69	0.09	1.01	0.15	1.13	62	61	1.6	II	0.70	right shoulder on S2
7740	2359.15	70.3	442	0.07	0.80	0.87	0.08	0.92	0.12	1.24	65	70	0.8	II	0.76	large right shoulder on S2
7770	2368.30	70.1	432	0.07	0.86	0.92	0.08	0.93	0.16	1.35	64	68	1.7	II	0.55	
7800	2377.44	70.8	440	0.07	0.68	0.77	0.09	0.88	0.12	1.16	59	66	1.2	II	0.72	right shoulder on S2
7830	2386.58	70.6	442	0.06	0.63	0.96	0.09	0.66	0.14	1.07	59	90	1.7	II	0.76	right shoulder on S2
7860	2395.73	70.7	446	0.07	0.51	1.30	0.13	0.39	0.16	1.02	50	127	1.7	II	0.86	right shoulder on S2
7890	2404.87	70.0	442	0.08	0.74	0.95	0.10	0.78	0.14	1.32	56	72	1.5	II	0.76	right shoulder on S2
8010	2441.45	70.5	442	0.07	0.56	0.79	0.11	0.71	0.11	1.05	53	75	1.6	II	0.76	right shoulder on S2
8040	2450.59	69.8	438	0.09	1.00	0.63	0.08	1.59	0.13	1.38	72	46	1.5	II	0.68	
8070	2459.74	70.2	433	0.20	1.67	0.73	0.11	2.29	0.22	1.54	108	47	1.5	II	0.58	
8100	2468.88	70.3	444	0.17	0.54	1.33	0.24	0.41	0.14	1.05	51	127	1.8	II	0.80	small right shoulder on S2

Depth (ftKB)	Depth (mKB)	Qty (mg)	Tmax	S1	S2	S3	PI	S2/S3	PC (%)	TOC (%)	HI	OI	MINC (%)	Organic Type	%Roeq	Comments
8130	2478.02	70.7	442	0.06	0.45	0.54	0.11	0.83	0.06	0.70	64	77	0.5	II	0.76	large right shoulder on S2
8160	2487.17	70.4	434	0.32	1.56	0.60	0.17	2.60	0.20	1.54	101	39	1.5	II	0.60	
8190	2496.31	69.9	437	0.29	1.80	0.84	0.14	2.14	0.24	1.86	97	45	1.4	II	0.66	
8220	2505.46	70.4	439	0.12	1.01	0.66	0.10	1.53	0.14	1.45	70	46	1.2	II	0.70	small right shoulder on S2
8250	2514.60	70.5	432	0.10	0.96	0.66	0.09	1.45	0.14	1.29	74	51	2.1	II	0.55	small right shoulder on S2
8280	2523.74	70.9	436	0.28	1.38	0.70	0.17	1.97	0.19	1.65	84	42	1.4	II	0.64	
8318	2535.33	70.5	439	0.30	3.71	0.20	0.08	18.55	0.34	1.99	186	10		II	0.70	**core;** bitumen
8340	2542.03	70.4	428	0.39	4.21	0.51	0.08	8.25	0.42	2.73	154	19	0.2	II	0.43	
8370	2551.18	70.2	439	0.13	0.82	0.78	0.14	1.05	0.14	1.01	81	77	2.4	II	0.70	small right shoulder on S2
8400	2560.32	69.9	436	0.19	1.05	1.00	0.15	1.05	0.21	1.28	82	78	2.1	II	0.64	small right shoulder on S2
8430	2569.46	70.5	429	0.20	1.19	0.64	0.15	1.86	0.16	1.50	79	43	1.0	II	0.47	small right shoulder on S2
8460	2578.61	70.2	438	0.14	1.02	0.80	0.12	1.28	0.14	1.65	62	48	1.2	II	0.68	small right shoulder on S2; oil stain
8490	2587.75	70.8	438	0.11	0.86	0.59	0.11	1.46	0.12	1.74	49	34	2.4	II	0.68	small right shoulder on S2; oil stain
Ave			433.9													all values (75)
SD			5.6													
Ave			**432.1**													selected values (55)
SD			**4.9**													
													Arctic Red			
8520	2596.90	70.0	437	0.22	1.30	0.49	0.15	2.65	0.16	1.43	91	34	0.7	II	0.66	
8550	2606.04	70.1	437	0.32	2.41	0.42	0.12	5.74	0.25	1.66	145	25	0.4	II	0.66	
8580	2615.18	71.0	440	0.26	1.96	0.49	0.12	4.00	0.21	1.63	120	30	0.7	II	0.72	small right shoulder on S2
8610	2624.33	70.4	436	0.38	2.18	0.44	0.15	4.95	0.24	1.61	135	27	0.6	II	0.64	
8640	2633.47	70.9	437	0.17	1.80	0.67	0.09	2.69	0.21	1.68	107	40	1.1	II	0.66	small right shoulder on S2
8670	2642.62	69.8	438	0.33	2.18	0.74	0.13	2.95	0.27	1.98	110	37	1.0	II	0.68	trace oil stain
8700	2651.76	70.0	440	0.23	1.78	0.43	0.12	4.14	0.19	1.49	119	29	0.3	II	0.72	small right shoulder on S2
8730	2660.90	70.4	437	0.29	1.94	0.64	0.13	3.03	0.23	1.80	108	36	0.5	II	0.66	
8760	2670.05	71.1	438	0.36	1.68	0.46	0.18	3.65	0.23	1.43	117	32	1.1	II	0.68	trace oil stain
8790	2679.19	70.5	441	0.37	2.34	0.25	0.14	9.36	0.24	1.54	152	16	0.2	II	0.74	
8820	2688.34	70.6	441	0.32	1.43	0.47	0.18	3.04	0.17	1.53	93	31	0.4	II	0.74	dead oil stain
8850	2697.48	70.8	439	0.39	3.05	0.30	0.11	10.17	0.30	1.88	162	16	0.3	II	0.70	
8880	2706.62	70.3	440	0.52	2.10	0.31	0.20	6.77	0.24	1.50	140	21	0.3	II	0.72	small left shoulder on S2
8910	2715.77	70.7	443	0.26	1.03	0.31	0.20	3.32	0.13	0.94	110	33	0.2	II	0.78	small right shoulder on S2
8940	2724.91	70.8	439	0.22	1.17	0.65	0.16	1.80	0.21	1.10	106	59	1.5	II	0.70	small right shoulder on S2
8970	2734.06	70.1	440	0.44	2.89	0.52	0.13	5.56	0.31	1.76	164	30	0.4	II	0.72	small left shoulder on S2; solid bitumen
9000	2743.20	71.0	444	0.25	1.32	0.43	0.16	3.07	0.16	1.17	113	37	0.2	II	0.80	small right shoulder on S2
9030	2752.34	70.4	440	0.33	1.72	0.66	0.16	2.61	0.22	1.31	131	50	1.0	II	0.72	small right shoulder on S2; trace oil
9060	2761.49	70.8	441	0.28	1.37	0.94	0.17	1.46	0.19	1.33	103	71	1.0	II	0.74	small right shoulder on S2
9090	2770.63	70.7	441	0.34	1.52	1.21	0.18	1.26	0.21	1.58	96	77	0.7	II	0.74	small right shoulder on S2
9120	2779.78	71.0	440	0.30	1.12	1.34	0.21	0.84	0.21	1.17	96	115	1.8	II	0.72	small left and right shoulder on S2
9150	2788.92	70.5	442	0.25	1.20	0.43	0.17	2.79	0.14	1.15	104	37	0.6	II	0.76	small left and right shoulder on S2
9180	2798.06	70.0	440	0.55	2.34	0.08	0.19	29.25	0.25	1.58	148	5	0.3	II	0.72	small left shoulder on S2
9210	2807.21	70.2	440	0.41	1.18	0.71	0.26	1.66	0.19	1.20	98	59	1.5	II	0.72	small left and right shoulder on S2
9255	2820.92	70.2	447	0.21	1.16	0.30	0.15	3.87	0.13	1.21	96	25	0.4	II	0.89	**core**, small left and right shoulder on S2; solid bitumen

Depth (ftKB)	Depth (mKB)	Qty (mg)	Tmax	S1	S2	S3	PI	S2/S3	PC (%)	TOC (%)	HI	OI	MINC (%)	Organic Type	%Roeq	Comments
9270	2825.50	70.6	440	0.48	1.33	0.52	0.27	2.56	0.20	1.29	103	40	1.3	II	0.72	
9300	2834.64	70.7	442	0.23	0.79	1.37	0.22	0.58	0.23	1.03	77	133	2.6	II	0.76	small right shoulder on S2
9320	2840.74	70.6	444	0.37	1.34	0.71	0.22	1.89	0.19	1.45	92	49	0.8	II	0.80	small right shoulder on S2
9360	2852.93	70.4	448	0.16	0.71	1.75	0.18	0.41	0.16	1.03	69	170	1.0	II	0.92	right shoulder on S2
9380	2859.02	70.1	434	0.33	0.89	0.61	0.27	1.46	0.13	1.31	68	47	0.5	II	0.60	
9420	2871.22	70.9	447	0.22	0.99	0.65	0.18	1.52	0.14	1.13	88	58	0.8	II	0.89	left and right shoulder on S2
9450	2880.36	70.0	443	0.32	1.08	1.26	0.23	0.86	0.21	1.36	79	93	1.7	II	0.78	small left and right shoulder on S2
9480	2889.50	70.8	445	0.32	1.15	0.55	0.21	2.09	0.15	1.29	89	43	0.9	II	0.83	left and right shoulder on S2
9510	2898.65	70.1	446	0.20	0.90	0.75	0.18	1.20	0.12	1.18	76	64	0.6	II	0.86	right shoulder on S2
9540	2907.79	70.6	447	0.20	0.73	0.72	0.21	1.01	0.16	1.09	67	66	2.0	II	0.89	right shoulder on S2
9570	2916.94	70.5	444	0.30	1.05	0.49	0.22	2.14	0.15	1.15	91	43	1.0	II	0.80	left and right shoulder on S2
9600	2926.08	70.9	447	0.15	0.73	0.59	0.17	1.24	0.13	1.09	67	54	2.1	II	0.89	right shoulder on S2
9630	2935.22	70.8	448	0.18	0.69	0.84	0.21	0.82	0.16	1.05	66	80	2.2	II	0.92	right shoulder on S2
9660	2944.37	70.1	444	0.30	0.92	0.77	0.25	1.19	0.16	1.18	78	65	1.6	II	0.80	right shoulder on S2
9690	2953.51	70.7	441	0.26	1.18	0.58	0.18	2.03	0.16	1.37	86	42	1.2	II	0.74	right shoulder on S2; solid bitumen
9810	2990.09	70.6	444	0.23	1.04	0.88	0.18	1.18	0.18	1.36	76	65	1.5	II	0.80	right shoulder on S2
9840	2999.23	70.9	444	0.20	0.65	0.53	0.24	1.23	0.10	1.02	64	52	0.5	II	0.80	left and right shoulder on S2
9870	3008.38	70.3	447	0.20	0.96	0.52	0.17	1.85	0.12	1.23	78	42	0.6	II	0.89	right shoulder on S2
9900	3017.52	71.1	450	0.21	0.83	0.77	0.20	1.08	0.13	1.16	72	66	0.8	II	1.00	right shoulder on S2
9930	3026.66	70.8	450	0.21	0.91	1.13	0.19	0.81	0.17	1.29	71	88	0.4	II	1.00	right shoulder on S2
9960	3035.81	71.1	447	0.41	1.24	0.46	0.25	2.70	0.16	1.35	92	34	0.4	II	0.89	small left peak and right shoulder on S2
9990	3044.95	70.1	450	0.27	0.89	0.58	0.23	1.53	0.13	1.28	70	45	0.7	II	1.00	right shoulder on S2
10020	3054.10	70.4	450	0.37	1.38	0.48	0.21	2.88	0.17	1.53	90	31	0.5	II	1.00	left peak and right shoulder on S2
10060	3066.29	69.8	449	0.34	1.12	0.33	0.23	3.39	0.14	1.24	90	27	0.6	II	0.96	left peak and right shoulder on S2
10080	3072.38	70.7	450	0.28	0.75	0.48	0.27	1.56	0.13	0.86	87	56	1.5	II	1.00	small left peak and right shoulder on S2
10110	3081.53	70.0	449	0.27	0.94	0.34	0.22	2.76	0.12	1.17	80	29	0.7	II	0.96	left peak and right shoulder on S2
10140	3090.67	70.7	447	0.24	0.93	0.95	0.21	0.98	0.14	1.19	78	80	0.8	II	0.89	right shoulder on S2
10170	3099.82	71.2	454	0.18	0.74	0.44	0.19	1.68	0.11	1.25	59	35	0.8	II	1.21	large right shoulder on S2
10200	3108.96	70.2	452	0.26	0.78	0.57	0.25	1.37	0.11	1.11	70	51	0.9	II	1.09	small left peak and right shoulder on S2
10230	3118.10	70.0	452	0.36	1.02	0.38	0.26	2.68	0.13	1.15	89	33	1.1	II	1.09	large left peak and small right shoulder on S2
10254	3125.42	70.9	454	0.37	1.09	0.28	0.25	3.89	0.14	1.31	83	21	0.3	II	1.21	**core**, small left peak and right shoulder on S2; solid bitumen
10260	3127.25	70.3	449	0.25	0.88	0.40	0.22	2.20	0.14	1.17	75	34	1.3	II	0.96	right shoulder on S2
10290	3136.39	70.4	454	0.34	0.98	0.24	0.26	4.08	0.13	1.10	89	22	0.5	II	1.21	left peak and right shoulder on S2
10320	3145.54	70.8	453	0.19	0.77	0.35	0.20	2.20	0.11	1.09	71	32	1.2	II	1.15	left peak and right shoulder on S2
10350	3154.68	70.0	455	0.19	0.76	0.26	0.20	2.92	0.10	1.08	70	24	0.6	II	1.27	left peak and right shoulder on S2
10380	3163.82	70.8	455	0.13	0.50	0.99	0.21	0.51	0.18	0.92	54	108	2.8	II	1.27	large right shoulder on S2
10410	3172.97	70.6	452	0.34	0.85	0.52	0.28	1.63	0.12	1.14	75	46	1.1	II	1.09	left and right shoulder on S2
10440	3182.11	70.3	451	0.27	0.68	0.43	0.28	1.58	0.11	1.01	67	43	2.2	II	1.04	left peak and right shoulder on S2
10470	3191.26	70.4	453	0.26	0.73	0.45	0.26	1.62	0.11	1.05	70	43	0.8	II	1.15	left peak and large right shoulder on S2
10530	3209.54	70.8	451	0.24	0.74	0.45	0.24	1.64	0.11	1.03	72	44	0.7	II	1.04	left peak and right shoulder on S2
10500	3200.40	70.4	447	0.40	1.02	0.56	0.28	1.82	0.15	1.10	93	51	1.0	II	0.89	large left peak and a right shoulder on S2
10560	3218.69	70.5	448	0.43	1.23	0.43	0.26	2.86	0.16	1.27	97	34	0.6	II	0.92	left peak and right shoulder on S2
10590	3227.83	70.0	452	0.31	0.84	0.57	0.27	1.47	0.14	1.09	77	52	1.0	II	1.09	left and right shoulder on S2

Depth (ftKB)	Depth (mKB)	Qty (mg)	Tmax	S1	S2	S3	PI	S2/S3	PC (%)	TOC (%)	HI	OI	MINC (%)	Organic Type	%Roeq	Comments
10620	3236.98	70.8	444	0.51	1.24	0.55	0.29	2.25	0.18	1.34	93	41	1.0	II	0.80	left peak and small right shoulder on S2
10650	3246.12	70.5	452	0.25	0.82	0.34	0.23	2.41	0.10	1.11	74	31	0.6	II	1.09	left and right shoulder on S2
10680	3255.26	70.9	453	0.23	0.70	0.72	0.25	0.97	0.13	1.01	69	71	1.7	II	1.15	left peak and right shoulder on S2
10710	3264.41	69.9	453	0.29	0.96	0.21	0.23	4.57	0.12	1.24	77	17	0.4	II	1.15	left peak and right shoulder on S2
10740	3273.55	70.3	448	0.39	0.84	0.42	0.32	2.00	0.13	1.09	77	39	0.7	II	0.92	left peak on S2
10770	3282.70	70.8	451	0.32	0.86	0.53	0.27	1.62	0.14	1.17	74	45	1.2	II	1.04	left peak and right shoulder on S2
10800	3291.84	70.2	449	0.39	0.97	0.52	0.29	1.87	0.14	1.15	84	45	0.8	II	0.96	left peak and small right shoulder on S2
10840	3304.03	70.0	452	0.37	0.91	0.65	0.29	1.40	0.14	1.21	75	54	0.9	II	1.09	left peak and right shoulder on S2
10860	3310.13	70.4	450	0.57	1.05	0.70	0.35	1.50	0.19	1.30	81	54	1.4	II	1.00	left and small right shoulder on S2
10890	3319.27	70.8	448	0.36	1.01	0.52	0.26	1.94	0.15	1.17	86	44	1.0	II	0.92	left peak and right shoulder on S2
10920	3328.42	70.7	453	0.20	0.41	0.50	0.33	0.82	0.09	0.86	48	58	1.2	II	1.15	small left and right shoulder on S2
10940	3334.51	70.4	452	0.25	0.95	0.26	0.21	3.65	0.12	1.30	73	20	0.6	II	1.09	small left peak and a right shoulder on S2
10980	3346.70	70.6	454	0.23	0.82	0.45	0.22	1.82	0.12	1.11	74	41	0.8	II	1.21	left peak and right shoulder on S2
11000	3352.80	69.7	456	0.22	0.69	0.60	0.24	1.15	0.12	0.96	72	63	1.4	II	1.34	left peak and right shoulder on S2
11023	3359.81	70.4	462	0.16	0.60	0.23	0.21	2.61	0.07	1.07	56	21	0.4	II	1.89	**core**, small left peak and large right shoulder on S2; solid bitumen
11040	3364.99	69.9	449	0.24	0.83	0.52	0.23	1.60	0.12	1.02	81	51	1.1	II	0.96	large left peak and right shoulder on S2
11070	3374.14	70.2	455	0.19	0.72	0.29	0.21	2.48	0.09	1.07	67	27	0.6	II	1.27	left shoulder and large right shoulder on S2
11100	3383.28	70.9	455	0.27	0.89	0.40	0.23	2.23	0.12	1.16	77	34	0.9	II	1.27	left peak and right shoulder on S2
11130	3392.42	70.1	455	0.28	0.79	0.36	0.26	2.19	0.12	1.09	72	33	0.7	II	1.27	left peak and right shoulder on S2
11160	3401.57	70.1	456	0.20	0.64	0.38	0.24	1.68	0.11	0.97	66	39	1.1	II	1.34	small left peak and a right shoulder on S2
11190	3410.71	70.0	453	0.26	0.76	0.38	0.26	2.00	0.12	1.16	66	33	1.2	II	1.15	small left peak and right shoulder on S2
11220	3419.86	70.2	456	0.21	0.78	0.31	0.21	2.52	0.10	1.14	68	27	0.6	II	1.34	left peak and right shoulder on S2
11250	3429.00	70.3	452	0.23	0.79	0.39	0.22	2.03	0.10	1.20	66	33	1.2	II	1.09	right shoulder on S2
11280	3438.14	70.8	462	0.24	1.00	0.34	0.19	2.94	0.12	1.57	64	22	0.5	II	1.89	small left peak and a large right shoulder on S2
11310	3447.29	70.6	457	0.20	0.68	0.42	0.23	1.62	0.10	0.99	69	42	1.5	II	1.41	small left peak and a right shoulder on S2
11315	3448.81	70.7	463	0.20	1.03	0.24	0.17	4.29	0.13	1.61	64	15	0.4	II	2.01	**core**, small left peak and large right shoulder on S2; solid bitumen
11340	3456.43	70.4	457	0.23	0.71	0.28	0.25	2.54	0.10	1.05	68	27	1.7	II	1.41	small left peak and a right shoulder on S2
11370	3465.58	70.5	456	0.23	0.65	0.43	0.26	1.51	0.10	1.01	64	43	1.3	II	1.34	small left peak and a right shoulder on S2
11400	3474.72	70.9	453	0.33	0.62	0.39	0.35	1.59	0.11	0.80	78	49	3.0	II	1.15	left peak on S2
11430	3483.86	70.1	457	0.17	0.43	0.29	0.28	1.48	0.07	0.67	64	43	3.2	II	1.41	small left peak and a right shoulder on S2
11460	3493.01	69.8	449	0.20	0.54	0.29	0.27	1.86	0.08	0.75	72	39	3.7	II	0.96	small left peak and right shoulder on S2
11480	3499.10	70.8	453	0.20	0.35	0.34	0.36	1.03	0.07	0.56	62	61	3.8	II	1.15	left peak on S2
11520	3511.30	70.8	407	0.05	0.07	0.30	0.43	0.23	0.02	0.08	88	375	1.5	II		large left shoulder on S2
11550	3520.44	70.5	453	0.79	0.92	0.39	0.46	2.36	0.16	1.03	89	38	2.5	II	1.15	left peak on S2
11580	3529.58	70.2	449	0.42	0.64	0.26	0.40	2.46	0.10	0.70	91	37	2.3	II	0.96	left peak on S2
11586	3531.41	70.2	306	0.72	1.09	0.23	0.40	4.74	0.17	0.51	214	45	0.5	II		**core**, S1 70% recovery, asymmetrical S2, solid bitumen
11606	3537.51	69.9	428	0.25	0.19	0.20	0.57	0.95	0.04	0.25	76	80	0.2	II	0.43	**core**, irregular S2
11616	3540.56	70.0	338	0.12	0.30	0.13	0.29	2.31	0.04	0.20	150	65	0.1	II		**core**, broad S2
11700	3566.16	49.8	385	3.63	6.31	2.93	0.37	2.15	0.95	2.37	266	124	0.9	II		large left shoulder on S2
11712	3569.82	70.4	457	0.37	0.90	0.29	0.29	3.10	0.12	1.17	77	25	0.1	II	1.41	**core**, S1 80% recovery, bimodal S2, solid bitumen
11720	3572.26	70.8	347	2.03	6.29	1.20	0.24	5.24	0.74	2.10	300	57	0.9	II		S1 90% recovery; low Tmax, diesel
11760	3584.45	70.2	378	2.45	3.54	0.62	0.41	5.71	0.52	1.45	244	43	1.1	II		large left shoulder on S2; diesel
11790	3593.59	70.4	442	1.56	1.82	0.83	0.46	2.19	0.32	1.52	120	55	0.6	II	0.76	bimodal S2

Depth (ftKB)	Depth (mKB)	Qty (mg)	Tmax	S1	S2	S3	PI	S2/S3	PC (%)	TOC (%)	HI	OI	MINC (%)	Organic Type	%Roeq	Comments
11820	3602.74	70.1	320	2.07	2.25	0.53	0.48	4.25	0.39	1.67	135	32	0.3	II		irregular S2
11860	3614.93	70.9	452	0.95	1.42	0.43	0.40	3.30	0.22	1.61	88	27	0.4	II	1.09	bimodal S2
11870	3617.98	70.8	452	0.82	1.32	0.40	0.38	3.30	0.20	1.56	85	26	0.5	II	1.09	bimodal S2
11920	3633.22	69.8	446	0.76	1.54	0.40	0.33	3.85	0.21	1.60	96	25	0.5	II	0.86	S1 90% recovery, bimodal S2
11930	3636.26	69.9	463	0.34	1.10	0.26	0.24	4.23	0.14	2.17	51	12	0.4	II	2.01	left peak and a large right shoulder on S2; solid bitumen
11970	3648.46	70.5	460	0.32	0.85	0.10	0.27	8.50	0.10	1.72	49	6	0.4	II	1.68	left peak and right shoulder on S2
12000	3657.60	70.2	459	0.39	1.13	0.34	0.26	3.32	0.14	1.86	61	18	0.3	II	1.58	large left peak and a right shoulder on S2
12030	3666.74	70.7	464	0.39	0.94	0.27	0.29	3.48	0.12	1.88	50	14	0.4	II	2.13	left peak and right shoulder on S2
12060	3675.89	70.3	462	0.44	1.03	0.32	0.30	3.22	0.14	1.82	57	18	0.4	II	1.89	large left peak and a right shoulder on S2
12090	3685.03	70.1	458	0.42	1.19	0.42	0.26	2.83	0.16	1.96	61	21	0.3	II	1.49	large left peak and a right shoulder on S2
12169	3709.11	70.0	470	0.37	0.98	0.34	0.28	2.88	0.14	1.98	49	17	0.5	II	3.08	**core**, small left peak and a right shoulder on S2, solid bitumen
Ave			443.3													all values (122)
SD			24.5													
Ave			**440.0**													selected values (30)
SD			**2.7**													

Table 5. Cuttings samples from Reindeer D-27 for geochemical analysis

Sample ID	Depth (m)	Formation/ Sequence	Amount (g)	Rock-Eval TOC (%)	Pr/Ph ratio from GC extract analysis
X11364	822.96	Taglu	2.5	23.67	1.25
X11365	1133.86	Taglu	3.85	34.7	1.21
X11366	1392.94	Taglu	2.94	17.09	1.93
X11367	1722.12	Aklak	1.53	1.26	1.01
X11368	2761.49	Aklak	3.40	1.39	1.49
X11369	3550.92	Arctic Red	2.95	1.55	1.26
X11370	3706.37	Arctic Red	3.51	1.43	2.33

Table 6: Rock-Eval results for shale or coal samples from cored intervals from the Reindeer D-27 and Tununuk K-10 wells.

GSC Lab ID	GSC Sample ID	Well name	Depth (m)	Sequence/ Formation	TOC (wt%)	Tmax (°C)	S1	S2	S3	PI	HI	OI	MINC (%)	PC (%TOC)	RC (%TOC)	%Ro*
X11570	C-560352	Reindeer D-27	1129.3	Taglu	52.59	415	1.15	32.26	67.24	0.03	61	128	1.76	5.93	46.66	0.46
X11571	C-560353		2021	Aklak	2.15	431	0.17	2.29	5.76	0.07	107	268	0.67	0.39	1.76	0.54
X11572	C-560354		2723.5	Aklak	1.71	434	0.16	1.25	4.11	0.11	73	240	0.49	0.25	1.46	0.61
X11601	C-560355		3157	Aklak	0.98	443	0.06	0.58	0.56	0.10	59	57	0.62	0.08	0.90	0.69
X11573	C-560356		3313.62	Arctic Red	2.14	434	0.13	3.53	0.50	0.03	165	23	0.40	0.34	1.80	0.69
X11574	C-560357		3481.5	Arctic Red	1.47	443	0.19	2.02	0.04	0.08	137	3	0.23	0.19	1.28	0.75
X11616	C-560358		3623.35	Arctic Red	1.41	445	0.17	1.17	0.04	0.13	83	3	0.27	0.12	1.29	0.79
X11575	C-560359		3798.5	Arctic Red	1.12	447	0.36	0.76	0.12	0.32	68	11	0.18	0.11	1.01	0.79
X11510	C-560389	Tununuk K-10	898.53	Aklak	0.84	435	0.02	0.28	0.18	0.07	33	21	0.04	0.04	0.80	0.59
X11511	C-560390		2824.42	Arctic Red	1.31	450	0.15	1.09	0.19	0.12	83	15	0.48	0.11	1.20	0.86
X11512	C-560391		3357.6	Arctic Red	1.00	463	0.07	0.41	0.00	0.16	41	0	0.29	0.04	0.96	1.07
X11513	C-560392		3708.5	Arctic Red	2.01	470	0.22	0.86	0.11	0.20	43	5	0.51	0.10	1.91	1.30

S1: mg HC/g Rock; S2: mg HC/g Rock; S3: mg CO2/g Rock; PI: S1/(S1+S2); HI: mg HC/g TOC; OI: mg CO2/g TOC; %Ro*: Vitrinite reflectance measured previously on a separate set of core and cuttings samples of similar depth.

Table 7. Selected depositional environment and maturation related biomarker parameters for the core samples from Reindeer D-27 and Tununuk K-10 wells.

GSC Lab ID	GSC Sample ID	Well	Depth (m)	Formation	Pr/Ph	DBT/ Phen	Cadal/ TeMN	Retene/ Phen	Simoneil/ Phen	Peryl/ Phen	Peryl/ BFls	Sterane Distribution (%)			C_{29} St S/(S+R)	C_{32} Hop S/(S+R)
												C_{27}	C_{28}	C_{29}		
X11570	C-560352	Reindeer D-27	1129.3	Taglu	0.51	0.31	3.88	3.70	21.61	2.32	7.54	<10	<10	>90	n.a.	n.a.
X11571	C-560353		2021	Aklak	1.45	0.03	1.88	1.48	0.61	0.71	3.41	10.6	27.0	62.4	0.17	0.29
X11572	C-560354		2723.5	Aklak	2.06	0.05	1.41	0.35	0.49	0.69	1.31	16.4	24.1	59.6	0.14	0.45
X11601	C-560355		3157	Aklak	2.94	0.04	0.60	0.09	0.04	0.90	1.33	17.4	22.6	59.9	0.28	0.57
X11573	C-560356		3313.62	Arctic Red	2.51	0.03	0.06	0.05	0.00	0.01	0.04	29.1	37.9	33.0	0.37	0.59
X11574	C-560357		3481.5	Arctic Red	1.43	0.03	0.03	0.05	0.00	0.00	0.01	33.2	27.8	39.0	0.51	0.59
X11616	C-560358		3623.35	Arctic Red	2.22	0.03	0.02	0.01	0.00	0.00	0.00	31.5	26.4	42.1	0.57	0.60
X11575	C-560359		3798.5	Arctic Red	2.05	0.06	0.21	0.02	0.00	0.00	0.01	34.2	24.3	41.5	0.61	0.59
X11510	C-560389	Tununuk K-10	898.53	Aklak	1.5	0.08	0.28	0.11	0.01	2.19	4.45	25.6	17.4	57.0	0.10	0.27
X05132	C-012560		2535.94	Smoking Hills/ Boundary Creek	2.83	0.09	0.02	0.07	0.00	0.00	0.01	35.6	30.4	34.0	0.57	0.58
X05133	C-551828		2822.45	Arctic Red	2.57	0.08	0.03	0.03	0.00	0.00	0.01	30.7	26.7	42.6	0.66	0.57
X11511	C-560390		2824.42	Arctic Red	2.28	0.04	0.05	0.02	0.00	0.01	0.04	27.1	28.5	44.4	0.60	0.60
X05134	C-551829		3122.37	Arctic Red	2.18	0.10	0.03	0.01	0.00	0.00	0.00	31.5	27.6	40.9	0.56	0.65
X11512	C-560391		3357.60	Arctic Red	2.33	0.05	0.05	0.00	0.00	0.00	0.01	30.5	31.5	37.9	0.50	0.55
X05136	C-544003		3540.56	Arctic Red	1.47	0.08	0.03	0.07	0.01	0.01	0.00	38.4	30.7	30.8	0.56	0.56
X11513	C-560392		3708.50	Arctic Red	2.15	0.03	0.05	0.00	0.00	0.00	0.01	36.0	27.9	36.1	0.57	0.63

Pr/Ph: ratio of pristane over phytane; DBT/Phen: ratio of dibenzothiophene over phenanthrene; Cadal/TeMN: ratio of cadalene over the sum of tetramethyl naphthalenes; Retene/Phen: ratio of retene over phenanthrene; Simoneil/Phen: ratio of simoneillite over phenanthrene; Peryl/Phen: ratio of perylene over phenanthrene; Peryl/BFls: ratio of perylene over benzofluoranthenes and benzopyrenes; C_{29} St S/(S+R): C_{29} $\alpha\alpha\alpha$ steranes 20S/(20S+20R); C_{32} Hop S/(S+R): C_{32} homohopanes 22S/(22S+22R).